SOURCES OF Ga, In, Zr and Hf TO THE COASTAL WATERS OF THE CALIFORNIA CURRENT SYSTEM

By

Kira Lanthier

B.Sc. (Hons.), The University of Sherbrooke, 1996

A THESIS SUBMITTED IN PARTIAL FULFILMENT OF
THE REQUIREMENTS FOR THE DEGREE OF
MASTER OF SCIENCE

in

THE FACULTY OF GRADUATE STUDIES

(Department of Chemistry)

We accept this thesis as confirming
to the required standard.

THE UNIVERSITY OF BRITISH COLUMBIA
October 1999

In presenting this thesis in partial fulfilment of the requirements for an advanced degree at the University of British Columbia, I agree that the Library shall make it freely available for reference and study. I further agree that permission for extensive copying of this thesis for scholarly purposes may be granted by the head of my department or by his or her representatives. It is understood that copying or publication of this thesis for financial gain shall not be allowed without my written permission.

Department of Chemistry

The University of British Columbia
Vancouver, Canada

Date November 9th, 1999

DE-6 (2/88)

Abstract

A method developed for the determination of picomolar levels of Ga, In, Zr and Hf in seawater is used to study the sources of these hydrolysis-dominated elements to the coastal surface waters of the California Current System (CCS), focussing mainly on the Columbia River and upwelling regions along the western coast of the United States. This thesis provides the first detailed measurements of Ga, In, Zr and Hf in the CCS.

A resin extraction/preconcentration step featuring Chelex-100 was used to achieve ~1000-fold concentration factors. Metals were quantified by flow injection-ICP/MS following addition of a Rh internal standard. Metal recoveries for Ga, In, Zr and Hf were 89, 97, 38 and 36%, respectively. Detection limits for one liter samples were 0.24, 0.012, 6 and 0.25pmol/kg, respectively, Ga, Zr and Hf being blank-limited while In is limited by sensitivity. Although this procedure was well suited for In, the data acquired was not usable as mass-115 was not corrected for isobaric Sn interferences, which were found to be significant.

Results from this study revealed that the Columbia River is a significant source of Ga, Zr and Hf to CCS surface waters, with maximum values ([Ga]=49pM; [Zr]=86pM; [Hf]=6pM) corresponding to the lowest salinity waters sampled (S=21). Ga and Zr traces were still detectable as far south as the Oregon-California border ([Ga]~30pM; [Zr]~50pM) therefore these two metals are good tracers of the Columbia River effluent. Dissolved metal/salinity plots of Ga and Zr show evidence of removal in these coastal waters, with ~30 and 50%, respectively, of the dissolved Ga and Zr in the plume core (S~21) being removed in the region sampled. Estimated minimum river concentrations for Ga (150±30pM) and Zr (240±150pM) were comparable to other previously reported rivers ([Ga]=68-250pM; [Zr]=300-1834pM).

Upwelling of deeper waters is also a moderate source of Ga (7-14pM), Zr (24-65pM) and Hf (0.6-1.5pM) to the background levels of the CCS ([Ga]=5-8pM; [Zr]=16-34pM; [Hf]=0.3-0.6pM). Particularly for Ga and possibly also for Zr, concentrations in the upwelled waters were highest in areas overlying wider (>10km) continental shelves, revealing shelf sediments as a significant source of metals to these bottom waters. Zr/Hf molar ratios of all samples from this study (Zr/Hf~44±40) indicate that the previously-observed marine fractionation between these two elements (Zr/Hf~100-300) does not arise from processes originating in coastal environments.

Table of Contents

Abstract		ii
Table of Contents		iii
List of Tables		vii
List of Figures		viii
Glossary		x
Acknowledgement		xii
CHAPTER 1. INTRODUCTION		
1.1	Trace Metal Marine Biogeochemistry	1
	1.1.1 Background	1
	1.1.2 Oceanic Sources and Sinks of Trace Metals	1
	1.1.3 Trace Metal Distributions	2
1.2	Physical Characteristics of the West Coast of North America	4
	1.2.1 The California Current System	4
	1.2.2 River Systems	4
	1.2.3 Coastline and Bathymetry	5
1.3	The Marine Geochemistries of Ga, In, Zr and Hf	7
	1.3.1 Hydrolysis-dominated Elements	7
	1.3.2 Gallium	7
	1.3.3 Indium	8
	1.3.4 Zirconium and Hafnium	9
1.4	Inductively Coupled Plasma Mass Spectrometry	11
1.5	Aims of Present Study	12
1.6	References	13
CHAPTER 2. EXPERIMENTAL		
2.1	Background	16
2.2	Instrumentation, Material and Reagents	17

2.2.1 ICP/MS 17
2.2.2 GFAAS 17
2.2.3 Pumps 18
2.2.4 Distilled Deionized Water (DDW) 19
2.2.5 Acids 19
2.2.6 Metal Standards 19
2.2.7 Resins 19
2.2.8 Reagents 20
2.2.9 Laboratory Material 20
2.3 Methods 21
2.3.1 Seawater Collection and Storage 21
2.3.2 Salinity, Temperature, Nutrient and Chlorophyll a Measurements 21
2.3.3 Acid Cleaning 21
2.3.4 Seawater Sample Processing 22
2.3.5 Recovery Tests 23
2.4 Study area 23
2.5 Analytical Technique Development 24
2.5.1 Volume of Sample 24
2.5.2 Resins 24
2.5.3 Flow Rates 25
2.5.4 Evaporation 26
2.5.5 Matrix Effects 27
2.5.5.1 Isotope Dilution Analysis 28
2.5.5.2 Standard Additions 29
2.5.5.3 Internal Standardization 29
2.5.6 Alternative resins 30
2.5.6.1 AG-Chelate-650M 30
2.5.6.2 8-Hydroxyquinoline Resins 32
2.5.7 Batch Method 33
2.5.8 HF Experiment 35
2.5.9 Titanium Determination 38
2.5.10 Spectral Interferences 40

2.5.10.1 Gallium 42
2.5.10.2 Indium 43
2.5.10.3 Zirconium 43
2.5.10.4 Hafnium 44
2.5.11 Analytical Figures of Merit 45
2.5.11.1 Detection Limits and Procedural Blanks 45
2.5.11.2 Precision 46
2.5.11.3 Accuracy 47
2.6 Summary 50
2.7 References 52

CHAPTER 3. THE COLUMBIA RIVER AS A SOURCE OF Ga, In, Zr AND Hf TO THE CALIFORNIA CURRENT SYSTEM
3.1 Introduction 55
3.1.1 Rivers and Estuaries as Sources of Trace Metals 55
3.1.2 Metal/Salinity Diagrams 56
3.2 Results and Discussion 58
3.2.1 Temperature and Salinity 58
3.2.2 Nutrients and Chlorophyll a 61
3.2.3 Trace Metals 64
3.2.4 Metal/Salinity Diagrams 69
3.3 The San Francisco Bay Effluent 77
3.4 Summary 81
3.5 References 82

CHAPTER 4. UPWELLING AS A SOURCE OF Ga, In, Zr and Hf TO THE CALIFORNIA CURRENT SYSTEM
4.1 Introduction 84
4.2 Results and Discussion 88
4.2.1 Upwelling Events along the West Coast of North America during

Summer 1997 88
4.2.2 Trace Metal Content of Upwelled Waters vs. Oceanic Waters 97
4.2.3 The Continental Shelf and Sediments 105
4.2.4 Zirconium and Hafnium Fractionation 108
4.3 Summary 110
4.4 References 111

CHAPTER 5. CONCLUSIONS 113

APPENDIX 1: RAW DATA TABLES 116
APPENDIX 2: CTD PROFILES 119

List of Tables

		Page
Table 2.2.1.1	ICP/MS operating conditions.	18
Table 2.5.3.1	Extraction step metal recoveries of spiked standards as a function of flow rate.	25
Table 2.5.4.1	Evaporation step metal recoveries of spiked standards.	26
Table 2.5.7.1	Metal recoveries for batch experiment.	34
Table 2.5.8.1	HF experiment results.	36
Table 2.5.8.2	Effect of standing time on the metal recoveries of spiked standards.	37
Table 2.5.10.1	Potential spectral interferences for Ga, In, Zr and Hf.	41
Table 2.5.10.1.1	Response (in cps) for Ga and Ba in seawater samples obtained from different transects.	42
Table 2.5.10.2.1	Response (in cps) for In and Sn in seawater samples obtained from different transects.	43
Table 2.5.10.4.1	Response (in cps) for Dy, Er and Hf in seawater samples obtained from different transects.	44
Table 2.5.11.1.1	Blanks and detection limits.	45
Table 2.5.11.2.1	Relative standard deviations of the analytical method.	46

List of Figures

		Page
Figure 1.1.3.1	The distributions of conservative and nutrient-type elements in North Pacific waters.	2
Figure 1.1.3.2	The distributions of Pb and Al in North Pacific waters.	3
Figure 1.2.3.1	The bathymetry off the west coast of the United States of America.	6
Figure 2.5.6.1.1	Metal recoveries of spiked standards using AG-Chelate-650M at various flow rates and pH's.	31
Figure 2.5.8.1	Effect of standing time of spiked standards on the metal recoveries.	37
Figure 2.5.11.3.1	Ga and In distributions at a) Station-P and b) AVHS-10.	48
Figure 2.5.11.3.2	Zr and Hf distributions at a) Station-P and b) AVHS-10.	49
Figure 3.1.2.1	Study area depicting transects influenced by the Columbia River effluent.	57
Figure 3.2.1.1	Temperature and salinity data for a)WCSST#09 b)#08 and c)#07.	59
Figure 3.2.1.2	Temperature and salinity data for WCSST#10.	60
Figure 3.2.2.1	Nutrient data for a) WCSST#09 b) #08 and c) #07.	62
Figure 3.2.2.2	Chlorophyll a data for a) WCSST#09 b) #08 and c) #07.	63
Figure 3.2.3.1	In data for a) WCSST#09 b) #08 and c) #07.	66
Figure 3.2.3.2	Ga and Zr data for a) WCSST#09 b) #08 and c) #07.	67
Figure 3.2.3.3	Hf data for a) WCSST#09 b) #08 and c) #07.	68
Figure 3.2.4.1	Silicic acid vs. salinity plot for transects WCSST#09, #08 and #07.	69
Figure 3.2.4.2	a) Gallium and b) Zirconium vs. salinity plots for transects WCSST#09, #08 and #07.	71
Figure 3.2.4.3	Silicic acid vs. salinity plot of data from transects WCSST#09, #08 and #07 used to extrapolate the original and effective silicic acid river concentrations of the Columbia River.	73
Figure 3.2.4.4	Gallium vs. salinity plot of data from transects WCSST#09, #08 and #07 used to extrapolate the original and effective silicic acid river concentrations of the Columbia River.	74
Figure 3.2.4.5	Zirconium vs. salinity plot of data from transects WCSST#09,	

	#08 and #07 used to extrapolate the original and effective silicic acid river concentrations of the Columbia River.	75
Figure 3.3.1	a) Temperature and salinity b) nutrient and c) chlorophyll a data for WCSST#03.	78
Figure 3.3.2	a) Ga b) Zr and c) In and Hf data for WCSST#03.	80
Figure 4.1.1	Sea surface temperature (SST) satellite image of the waters off California on June 23rd, 1997.	85
Figure 4.1.2	Study area depicting transects affected by upwelling.	87
Figure 4.2.1.1	Temperature, salinity, nutrients and chlorophyll a data for WCSST#01.	90
Figure 4.2.1.2	Temperature, salinity, nutrients and chlorophyll a data for WCSST#02.	91
Figure 4.2.1.3	Temperature, salinity, nutrients and chlorophyll a data for WCSST#03.	92
Figure 4.2.1.4	Temperature, salinity, nutrients and chlorophyll a data for WCSST#04.	93
Figure 4.2.1.5	Temperature, salinity, nutrients and chlorophyll a data for WCSST#05.	94
Figure 4.2.1.6	Temperature, salinity, nutrients and chlorophyll a data for WCSST#06.	95
Figure 4.2.1.7	Temperature, salinity, nutrients and chlorophyll a data for WCSST#08.	96
Figure 4.2.2.1	Trace metal data for WCSST#01.	98
Figure 4.2.2.2	Trace metal data for WCSST#02.	99
Figure 4.2.2.3	Trace metal data for WCSST#03.	100
Figure 4.2.2.4	Trace metal data for WCSST#04.	101
Figure 4.2.2.5	Trace metal data for WCSST#05.	102
Figure 4.2.2.6	Trace metal data for WCSST#06.	103
Figure 4.2.2.7	Trace metal data for WCSST#08.	104
Figure 4.2.4.1	Zr/Hf molar ratios of samples taken from all transects.	109

Glossary

Å	angstrom
CC	California Current
CCS	California Current System
Chl a	chlorophyll a
cm	centimeter
cps	counts per second
CUC	California Undercurrent
CTD	Conductivity-Temperature-Depth
DC	Davidson Current
DDW	distilled deionized water
FEP	fluorinated ethylene propylene
GFAAS	graphite furnace atomic absorption spectrometry
HEPA	high efficiency pure air
HDPE	high density polyethylene
HNLC	high nitrate low chlorophyll
hrs	hours
ICP/OES	inductively coupled plasma atomic emission spectrometry
ICP/MS	inductively coupled plasma mass spectrometry
IDA	isotope dilution analysis
ID/ICP/MS	isotope dilution inductively coupled plasma mass spectrometry
ISTD	internal standard
kg	kilogram
km	kilometer
kW	kilowatt
L	liter
m	meter
M	molarity
MDX	membrane desolvator
mg	milligram

min	minute
mL	milliliter
mm	millimeter
MΩ	megaohm
ms	milliseconds
m/z	mass to charge ratio
N	normality
ng	nanogram
nM	nanomolar
NOAA	National Oceanic and Atmospheric Administration
pm	picometer
pM	picomolar
ppb	parts per billion
PTFE	poly(tetrafluoroethylene)
REEs	rare earth elements
RF	radio frequency
RSD	relative standard deviation
s	second
S	salinity[1]
T	temperature
μL	microliter
μm	micrometer
μM	micromolar
μmol	micromole
USN	ultrasonic nebulizer
W	watt
yrs	years
τ	residence time

[1] According to the Practical Salinity scale, salinity is dimensionless.

Acknowledgment

I would never have made it through the past two years, nor would I have been able to write this thesis without the help of many great people. First and foremost, I would like to thank Kristin Orians for providing guidance and direction throughout the course of these studies. I would also like to acknowledge Ken Bruland and Geoffrey Smith for their warm welcome and friendly demeanor during my visit to California. They provided the nutrient, temperature, salinity data and sea surface temperature satellite images as well as helpful advice concerning data handling and interpretation for which I am most grateful.

I am indebted to Bert Mueller, an invaluable source of information both in and out of the lab, who has taught me so much more about the ICP/MS than he realizes. Thanks to him, I leave here with tremendous interest and respect for yet another instrument.

I thank my officemates Stephanie Kienast and David Timothy for allowing me to distract them from their work for many trivial questions. To my friends Claire Merrin, Stephanie and Markus Kienast, Cristian Harrison and Diana Walhorn: thank you for lifting my spirits and for your kind words of encouragement; I greatly appreciated them.

I am grateful for financial assistance provided to me by a scholarship sponsored by the Fonds pour la Formation de Chercheurs et l'Aide à la Recherche (Fonds FCAR).

Last but not least, I reserve my most heartfelt thanks for Alain-Sébastien Caillé, without whose unending support, patience and encouragement I would never have made it through the last six months. ☺

Chapter 1: Introduction

1.1 Trace Metal Marine Biogeochemistry

1.1.1 Background

Most of the naturally occurring elements of the periodic table are present in seawater, in concentrations varying from femtomolar to molar levels. Trace elements, the majority of which are metals, are by definition those present in concentrations less than 0.05μmol/kg.

Much of our understanding of the marine chemistry of trace metals stems from research carried out during the last two decades. It is generally agreed that any trace metal determinations performed on seawater prior to 1975 are questionable, principally due to contamination during sampling and analysis which leads to artificially high results. Today the elimination, or at least the control, of contamination during sampling, storage and analysis is achieved by practicing 'clean' handling techniques[1,2]. In addition, major advances in areas of spectroscopy, mass spectrometry, chromatography and electrochemistry have created analytical instruments which keep lowering the detection limits. In sum, these two factors have resulted in our ability to 1) measure trace metal concentrations in seawater orders of magnitude lower than those previously accepted and 2) obtain oceanographically-consistent datasets which permit the elucidation of the behavior of these elements in the oceans.

1.1.2 Oceanic Sources and Sinks of Trace Metals

The concentrations of dissolved trace metals in seawater are determined by their relative rates of supply and removal. Trace metals are supplied to the oceans by three external sources: rivers, the atmosphere (via transport by winds or rain) and hydrothermal vents. Internal sources include diagenic remobilization, regeneration from sinking particles and advection. Removal can occur via adsorption onto sinking particles (also known as scavenging), incorporation into biogenic material, and/or during interaction with hot basalt in hydrothermal systems.

The residence time of an element can be described as the amount of time spent in the ocean before being permanently removed (usually to sediments) and is given by

$$\tau = \frac{\text{Total amount dissolved in the ocean}}{\text{Rate of supply (or removal)}}$$

The only condition being that the ocean is in a long-term steady state.

1.1.3 Trace Metal Distributions

Trace metals, to a first approximation, may be divided into three behavioral categories based on their vertical distributions in the ocean.

1) Conservative-type Behavior

Elements whose concentrations in seawater are altered only by physical processes (i.e. mixing of different water masses, atmospheric precipitation, evaporation) are said to behave conservatively. This type of conduct leads to very long residence times in the ocean (10^5-10^7 years) and concentrations which are high relative to their crustal abundance. Mo and W are examples of elements that behave conservatively (figure 1.1.3.1).

2) Nutrient-type Behavior

Nutrient-type elements, like the major nutrients NO_3^-, HPO_4^{-2} and H_4SiO_4, exhibit surface depletion as a result of biological uptake and increase with depth as sinking biological matter is oxidized following death. Nutrient-type elements possess intermediate oceanic residence times (10^3-10^5 years). Zn and Ni are two such examples (figure 1.1.3.1).

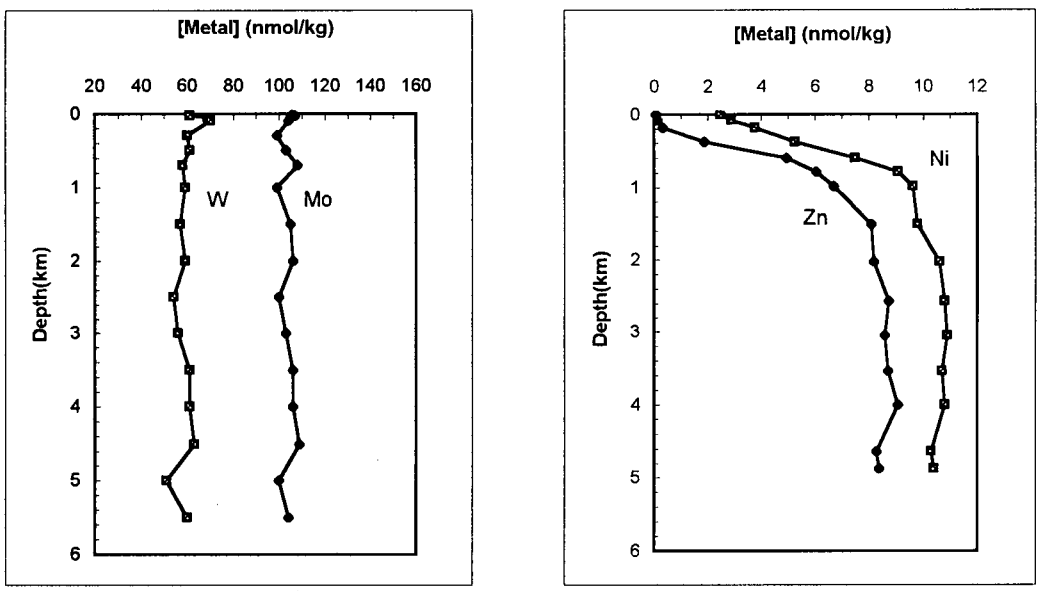

Figure 1.1.3.1 The distributions of conservative (Sohrin et al.[3]) and nutrient-type (Bruland[4]) elements in North Pacific waters.

3) Scavenged-type Behavior

Scavenged metals are rapidly removed from the water column, primarily by adsorption onto sinking particles. This behavior results in extremely short residence times ($<10^3$ years) and low concentrations in seawater relative to their crustal abundances. Trace metals which exhibit scavenged-type behavior strongly reflect their sources as their concentrations decrease rapidly with distance from that source, resulting in considerable spatial and temporal variability. This, in turn, makes them valuable tracers of transport and mixing mechanisms in the ocean. Vertical profiles generally exhibit surface enrichments along with depletion at depth although many variations which reflect complex biogeochemical controls have also been observed. For example, profiles for Pb and Al (figure 1.1.3.2) indicate an atmospheric source for both elements, scavenging throughout the water column and, in the case of Al, a bottom source possibly due to surface sediment remineralization or sediment diagenesis.

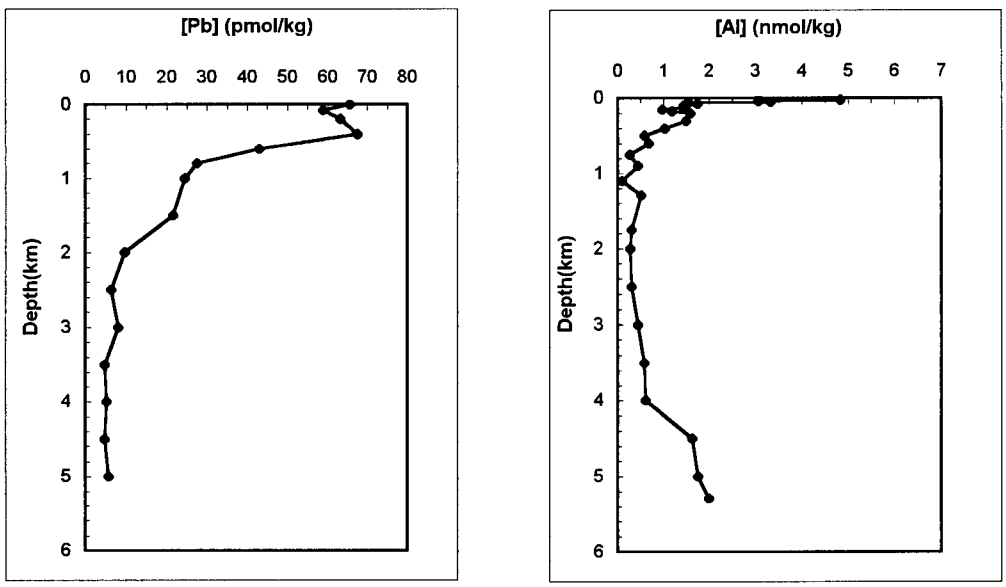

Figure 1.1.3.2 The distributions of Pb (Schaule and Patterson[5]) and Al (Orians and Bruland[6]) in North Pacific waters.

1.2 Physical Characteristics of the West Coast of North America

1.2.1 The California Current System

Waters off the west coast of North America from the Strait of Juan de Fuca to the tip of Baja California are part of an eastern boundary current system known as the California Current System (CCS). The CCS is traditionally described in terms of three major components namely the California Current (CC), the Davidson Current (DC) and the California Undercurrent (CUC). The California Current is a broad (~1000km) relatively slow (~10-30cm/s) equatorward surface flow which extends to ~500m depth. The Davidson Current and the California Undercurrent are poleward flows. While the CUC is confined to the continental slope, the DC is thought to be the result of the surfacing in wintertime of the CUC.

The water masses associated with the CCS are quite distinctive. The CC brings low temperature, low salinity, high oxygen and high nutrient subarctic-type water from high to low latitudes. The CUC and DC both bring warmer, saltier, low oxygen, high nutrient equatorial-type water from low to high latitudes[7].

1.2.2 River Systems

Water masses in the Northeast Pacific are modified by precipitation and run-off. Most river plumes on the coast between the Strait of Juan de Fuca and the tip of Baja California are relatively small and their effects are confined to within a few kilometers of the mouth of the river or estuary. The two exceptions are the Columbia River which forms part of the boundary between the states of Washington and Oregon and the Sacramento/San Joaquin river system which flows through the San Francisco Bay in Central California.

The Columbia River is the second largest river in North America. It is responsible for 77% of the total drainage into the Pacific between the Strait of Juan de Fuca and San Francisco Bay. The Columbia River estuary is partially mixed as a result of a high river discharge averaging 7300 m^3/s (or 9800m^3/s for the total April through August discharge), which peaks annually in June. The outflowing upper layer forms a plume of relatively low salinity water, which can be distinguished over a large area of the adjacent ocean. The behavior of the effluent, which varies in thickness between 5 and 20m, depends largely on the wind and wind-driven currents and shows a seasonal variation. In winter, the plume flows northward along the Washington coast and is

confined primarily to the shelf (bottom depths <200m). In summer, the plume flows southward with an Ekman component in the offshore direction. Because of wind-induced upwelling off the coast of Oregon, the plume is often separated from the coast by a band of colder, more saline water. Although the greatest effect of the Columbia River plume is felt within 50km of the river mouth, the effluent can spread seaward for several hundred kilometers. Occasionally, it has been traced as far south as Cape Mendocino (41.5°N) in the summer season, a distance of over 400km south of the river mouth[8].

The San Francisco Bay/Sacramento-San Joaquin delta estuary is the largest estuary on the west coast of the Americas and drains over 40% of the water in California. The combined mean monthly discharges from these two rivers into San Francisco Bay is approximately $1800m^3$/sec (one quarter that of the Columbia River). The estuary is relatively shallow (mean depth of 6m) and has a large tidal range of up to 1.7m at its mouth.

San Francisco Bay is a highly urbanized estuary today; with more than 7.5 million people presently living in the greater Bay area, the bay is the ultimate receptacle for municipal and industrial wastes.

1.2.3 Coastline and Bathymetry

The coastline and bathymetry of the CCS (figure 1.2.3.1) are oriented in a north/south direction from the Strait of Juan de Fuca to Cape Mendocino and in a northwest/southeast direction from Cape Mendocino to the tip of Baja California. The continental shelf is relatively narrow and deep along the entire coast. The average width to the 200m isobath is 25km as opposed to 200km on the east coast of the United States. More specifically, the shelf adjacent to Washington and Oregon varies in width between 25 and 60km with a shelf break depth of 150 to 200m. Off California, the continental shelf is generally even narrower being no more than 6-8km in many places. Plus, in some areas north and south of Point Sur, the shelf is non-existent: the distance to the 100m isobath is typically less than 3-4km. By contrast, the shelf widens to almost 50 km in the Gulf of Farallones (off San Francisco Bay)[9,10].

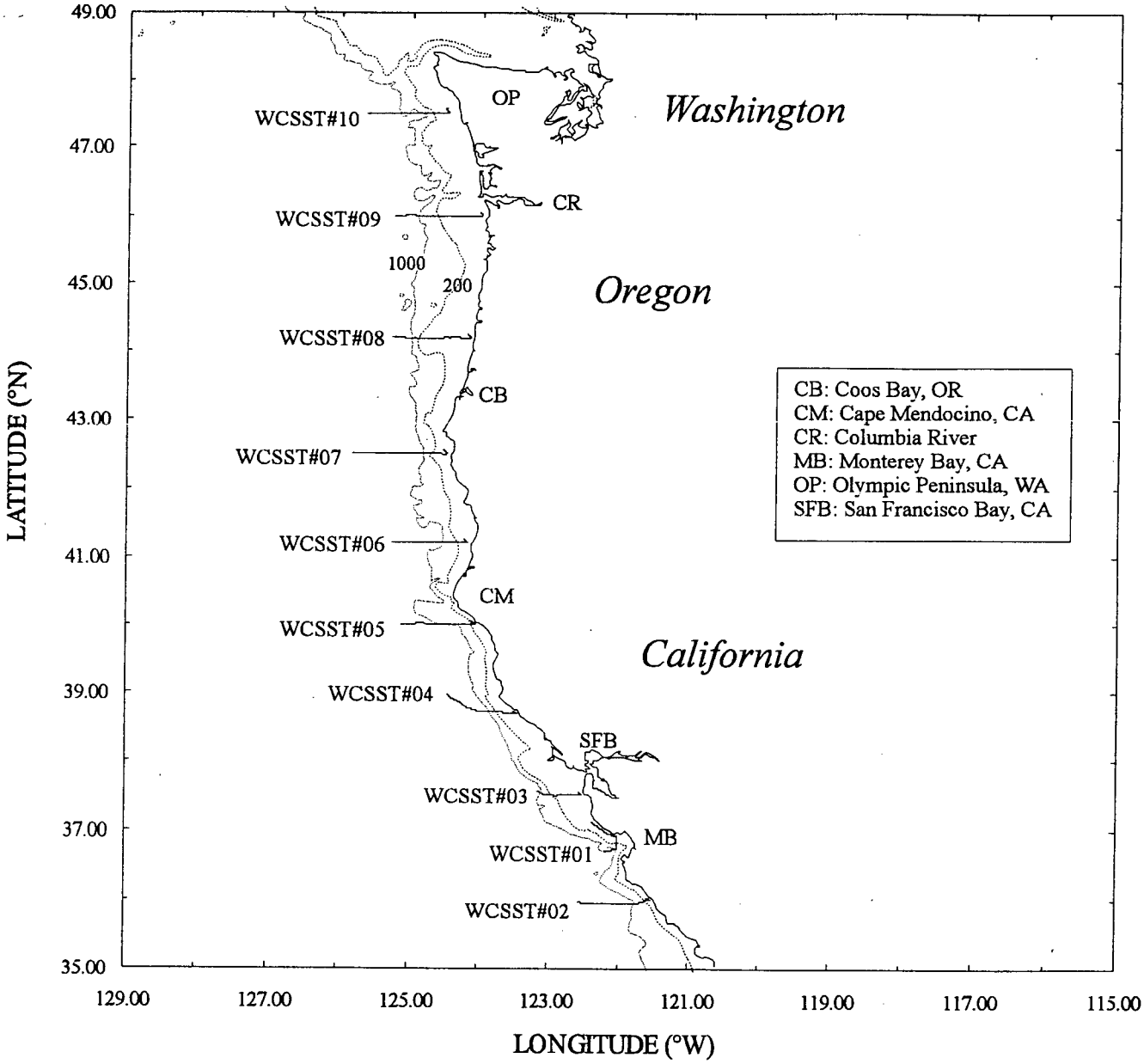

Figure 1.2.3.1 The bathymetry off the west coast of the United States of America. (Isobaths are in meters). Also shown are the 9 transects from which seawater samples were collected.

1.3 The Marine Geochemistries of Ga, In, Zr and Hf

1.3.1 Hydrolysis-dominated Elements

The elements of interest in this study, Ga, In, Zr and Hf are all characterized by their strong tendency to undergo hydrolysis in aqueous media. At the pH of seawater (7.5-8.2), the thermodynamically predicted states of these elements are $Ga(OH)_4^-$, $In(OH)_3$, $Zr(OH)_5^-$ and $Hf(OH)_5^-$[ref.11]. Elements that are dominated by their hydroxide speciation in seawater are known to be extremely particle-reactive, resulting in relatively short residence times. This feature makes them valuable tracers of chemical and physical processes occurring within the oceans.

1.3.2 Gallium

The interest in Ga initially stemmed from its position under Al in the periodic table and its potential to act as an analog for Al. Recently though, it has been suggested that Ga is the only element that can significantly compete with Fe for siderophores and transport into cells[12], possibly as a result of their similar ionic radii (Fe^{+3}=64.5pm; Ga^{+3}=62pm).

Previous work in both the Atlantic and Pacific oceans has provided a better understanding of the many geochemical processes that control Ga distributions in seawater. Horizontal surface transects from both oceans have shown that aeolian input is the main source of Ga to surface waters of the open ocean. Concentrations are highest closer to the major dust sources (Saharan and Asian deserts) then decrease markedly in coastal and/or productive waters as a result of intense scavenging. Very little or no fluvial input to the open ocean was observed in either ocean indicating that any potential coastal sources are efficiently removed in estuaries or highly productive coastal regions[13-15].

In the Pacific, vertical distributions are characterized by intermediate concentrations at the surface (2-17pM), a subsurface maximum between 150-300m (6-20pM), a broad minimum from 500 to 1000m (4-10pM) followed by increasing concentrations with depth below 1000m to a maximum in bottom waters (14-30pM)[13,14].

Surface concentrations are governed mainly by the flux of atmospheric dust and the extent of dissolution of Ga from aeolian particles. The subsurface maximum and intermediate minimum are thought to originate from reversible exchange processes involving sinking particles, followed by scavenging throughout the water column. Sediment diagenesis or surface sediment remineralization are the most likely sources of Ga to the deep waters of the Pacific.

Atlantic profiles show some differences from their Pacific counterparts. Surface values, naturally higher in the Atlantic due to the greater atmospheric flux, are highest in the Sargasso Sea (>40pM) where an additional anthropogenic source (from coal burning) is suspected. In the southern Atlantic bottom waters, Ga seems to behave conservatively whereas in the northern Atlantic, resuspended sediments are believed to cause the increasing concentrations with depth. The subsurface maximum present in the Pacific is not observed in the Atlantic. It is possible this feature is obscured by intermediate low Ga-containing waters of the Atlantic, which are advective features. In fact, in the younger waters of the Atlantic, Ga vertical distributions seem to reflect mainly the advective features of the water masses which they intersect rather than vertical biogeochemical processes[15].

In summary, it is clear that additional work needs to be carried out on Ga before its marine biogeochemistry is completely and confidently understood.

1.3.3 Indium

Indium belongs to the same group as Al, Ga and Tl, a group which has received a growing amount of interest these past two decades. However up until very recently, little was known about the behavior of In in aqueous environments nor its oceanic distribution due to its low concentrations. Al and Ga exhibit scavenged-type distributions, being mainly controlled by aeolian and bottom sediment sources, as well as considerable interocean fractionation[14]. In contrast, Tl (which exists primarily in the +1 oxidation state rather than +3 like Al and Ga) appears to behave conservatively regardless of location and depth[16]. Obviously, In may be important in achieving a better understanding of the comparative marine geochemistries of the 3B group elements.

In the first reports on In concentrations in seawater, Chow and Snyder[17] measured 17-52pM In in Pacific waters while Riley and Taylor[18] obtained values ranging from 0.9 to 2.7pM in the Atlantic. More recently, Orians and Boyle[19] developed a method for determining In in natural waters which Chan[20] applied to samples from the Central Pacific gyre. This study revealed the behaviour of In was similar to that of Ga, with intermediate surface values (~0.3pM), a subsurface maximum at ~500m (0.45pM), a mid-depth minimum at ~1500m (0.16pM) and a slight increase in concentration with depth to 0.3pM in deep waters.

Recently, Amakawa et al[21] presented more data from the western North Pacific. In their studies, vertical distributions exhibited surface and intermediate (1000-1500m) maxima (~0.10pM), scavenging throughout the water column (~0.06pM) and slight increase with depth (~0.08pM). Alibo et al[22] also measured In in rivers and estuaries, subsequently revealing that the In load supplied by rivers is largely removed by scavenging in the estuarine mixing zone therefore concluding fluvial input to the ocean is minimal.

Finally, results from the eastern North Atlantic and Mediterranean Sea[23] reveal considerable interocean fractionation, similar to that observed for Al and Ga, which is attributed to the large difference in continentally-derived dust input between the Atlantic and Pacific oceans. In the North Atlantic, concentrations increase with depth whereas the vertical distribution is featureless in the Mediterranean sea. Between 40 and 60% of the dissolved In in the latter was in particulate form, demonstrating this element's high reactivity for particles.

1.3.4 Zirconium and Hafnium

Due to the virtually identical atomic (Zr=145pm; Hf=144pm) and ionic radii (Zr^{+4}=74pm; Hf^{+4}=75pm), Zr and Hf have extremely similar chemical properties and are very closely associated, which is why they are often studied, and thus discussed concurrently in this section.

The earliest data on Zr and Hf in marine environments were mainly restricted to single elemental measurements[24-26]. In contrast, Boswell and Elderfield[27] studied Zr/Hf ratios in rivers, estuaries and open ocean settings. Although these elements are expected to behave similarly, Boswell and Elderfield[27] confirmed the occurrence of significant fractionation of Zr and Hf in the marine environment. The reasons behind this fractionation remain as yet unknown, as do many of the processes that control Zr and Hf distributions in seawater.

Much of what we do know about the biogeochemistries of Zr and Hf can be attributed to the works of McKelvey and Orians[28], McKelvey[29], and Godfrey et al[30]. These studies, conducted in the North Pacific and North Atlantic, have revealed the following facts. Vertical distributions of dissolved Zr and Hf exhibit large dynamic ranges and strong depth gradients. Minimum concentrations in surface waters and maximum concentrations in bottom waters result from removal by particle scavenging throughout the water column and regeneration at depth. A benthic source was observed for both elements in the North Pacific[28,29] while removal of Hf[30] was observed in the North Atlantic. Horizontal surface transects in both oceans indicate a strong coastal source

of dissolved Zr and Hf, possibly from riverine input and/or a flux from reducing shelf sediments. McKelvey[29] determined that reducing shelf sediments are a major source of dissolved Zr and Hf to the oceans whereas hydrothermal fluids are not.

Despite their chemical similarities, there is general agreement among scientists that fractionation between Zr and Hf occurs in the marine environment, although the extent of fractionation and its causes warrant further investigation. Boswell and Elderfield[27] found little fractionation took place in the Tamar river and estuary in comparison to the Indian and Atlantic oceans where Zr/Hf ratios (<10) indicated a Zr depletion and/or Hf enrichment. Fractionation between these two elements was also observed in the deep waters of the North Pacific (Zr/Hf ratios ~350)[28] and throughout the water column in the North Atlantic (Zr/Hf ratios varying from 164-250)[30], although in these cases the ratios were indicative of Zr enrichment and/or Hf removal. A horizontal transect along the Northern Pacific[29] revealed minimal fractionation in surface waters.

Deep water scavenging residence times (Zr=1000yrs; Hf=750yrs in the North Pacific[29] and 5000,1500yrs in the North Atlantic[30]) reveal Hf to be more reactive towards particle scavenging than Zr.

1.4 Inductively Coupled Plasma Mass Spectrometry

In a relatively short period of time, inductively coupled plasma mass spectrometry (ICP/MS) has matured into one of the most powerful techniques for elemental analysis. Since its introduction in the early eighties, ICP/MS has been used to measure trace elements in such complex matrices as human serum, urine, crude oils, sediments, lake water, river water and seawater.

The basic operation of ICP/MS is as follows. The plasma consists of a partially ionized gas (usually Ar, less than 1% ionized) which is generated in a quartz torch using a 1-2,5kW radiofrequency power supply. Samples are typically converted to an aerosol and transported into the plasma where the desolvation-vaporization-atomization-excitation-ionization processes take place. A two- or three-stage differentially pumped interface containing both a sampler and a skimmer cone is used to extract ions from the atmospheric pressure plasma into the low pressure ($\sim 10^{-5}$-10^{-6} Torr) mass spectrometer. Ion optics, typically cylinders held at appropriate voltages, are used to focus and transmit the ions into a mass analyzer. Detection of ions based on their mass-to-charge ratio is achieved by either an ion counting or an analogue detector.

Currently, the majority of commercial ICP/MS instruments use quadrupole-based mass analyzers because of their relative simplicity, low cost and good performance. Quadrupoles do suffer from one major limitation which is their low resolution (typically one mass unit).

The rapid development and wide acceptance of ICP/MS is attributed mainly to its low detection limits, wide linear dynamic range, multi-element capabilities and the capacity to perform isotope dilution analysis of solutions. Unfortunately, no method is ever perfect and ICP/MS is not without its share of interferences. Spectral interferences, although not as prevalent as in ICP/OES, do occur and can be quite serious. Non-spectral interferences (matrix effects), particularly those attributable to differences in solvent composition, tend to be more severe in ICP/MS than in ICP/OES or GFAAS.

1.5 Aims of Present Study

Although we are beginning to gain a better understanding of the biogeochemistries of Ga, In, Zr and Hf in open ocean settings, very little is known about these elements in coastal environments. As the link between the continents and the oceans, coastal waters are important geochemical reactors in which many trace metals are supplied, removed and transformed. River runoff, estuarine mixing, continental shelf sediment resuspension and diagenesis, coastal upwelling events and their ensuing phytoplankton blooms all contribute to the dynamic cycling of trace metals in near shore environments.

Off the west coast of North America, oceanic surface waters of the CCS are modified by freshwater river runoff (of which the Columbia River is by far the major contributor) and by upwelling: both potential sources of trace metals. Questions which will be addressed in this thesis are as follows. Is the Columbia River a significant source of Ga, In, Zr and Hf to the coastal waters of Washington and Oregon? How do the metals behave as the river plume moves offshore and mixes with seawater? Similarly, is coastal upwelling a considerable source of these metals to surface waters? If so, what is the effect of the continental shelf width on the trace metal content of the upwelled waters? Can the source of Zr/Hf fractionation be unraveled? It is hoped that surface samples obtained from waters off the west coast of the United States of America will help answer some of these questions.

To this effect, chapter 2 will present a detailed description of the development of the analytical technique employed to measure Ga, In, Zr and Hf in the seawater samples. Results obtained using this method will be presented and discussed in chapters 3 and 4. Chapter 3 will concentrate on the Columbia River samples whereas chapter 4 will focus on those affected by upwelling events. Finally, conclusions resulting from the whole body of this work will be detailed in chapter 5.

1.6 References

1) K.W. Bruland, R.P. Franks (1979) Sampling and analytical methods for the determination of copper, cadmium, zinc, and nickel at the nanogram per liter level in sea water, *Analytica Chimica Acta*, **105**, 233-245.

2) A.G. Howard, P.J. Statham (1983) Inorganic Trace Analysis: Philosophy and Practice, John Wiley and Sons LTD, England, 182 pages.

3) Y. Sohrin, K. Isshiki, T. Kuwamoto (1987) Tungsten in North Pacific waters, *Marine Chemistry*, **22**, 95-103.

4) K.W. Bruland (1980) Oceanographic distributions of cadmium, zinc, nickel, and copper in the North Pacific, *Earth and Planetary Science Letters*, **47**, 176-198.

5) B.K. Schaule, C.C. Patterson (1981) Lead concentrations in the Northeast Pacific: evidence for global anthropogenic perturbations, *Earth and Planetary Science Letters*, **54**, 97-116.

6) K.J. Orians, K.W. Bruland (1986) The biogeochemistry of aluminum in the Pacific ocean, *Earth and Planetary Science Letters*, **78**, 397-410 .

7) B.M. Hickey (1979) The California current system- hypotheses and facts, *Progress in Oceanography*, **8**, 191-279.

8) A.T. Pruter, D.L. Alverson (1972) The Columbia River estuary and adjacent waters, University of Washington Press, Seattle, 868 pages.

9) J.M. Steger, C.A. Collins, F.B. Schwing, M. Noble, N. Garfield, M.T. Steiner (1998) An empirical model of the tidal currents in the Gulf of the Farallones, *Deep-Sea Research II*, **45**, 1471-1505.

10) S.R. Ramp, C.L. Abbott (1998) The vertical structure of currents over the Continental Shelf off Point Sur, CA, during spring 1990, *Deep-Sea Research II*, **45**, 1411-1442.

11) D.R. Turner, M. Whitfield, A.G. Dickson (1981) Equilibrium speciation of dissolved components in freshwater and seawater at 25°C and 1atm pressure, *Geochimica et Cosmochimica Acta*, **45**, 855-881.

12) T. Emery, P.B. Hoffer (1980) Siderophore-mediated mechanism of gallium uptake demonstrated in the microorganism *Ustilago sphaerogena*, *Journal of Nuclear Medicine*, **21**, 935-939.

13) K.J. Orians, K.W. Bruland (1988) Dissolved gallium in the open ocean, *Nature*, **332**, 717-719.

14) K.J. Orians, K.W. Bruland (1988) The marine geochemistry of dissolved gallium: A comparison with dissolved aluminum, *Geochimica et Cosmochimica Acta*, **52**, 2955-2962.

15) A.M. Shiller (1998) Dissolved gallium in the Atlantic ocean, *Marine Chemistry*, **61**, 87-99.

16) A.R. Flegal, C.C. Patterson (1985) Thallium concentrations in seawater, *Marine Chemistry*, **15**, 327-331.

17) T.J. Chow, C.B. Snyder (1969) Indium content of sea water, *Earth and Planetary Science Letters*, **7**, 221-223.

18) A.D. Mathews, J.P. Riley (1970) The determination of indium in seawater, *Analytica Chimica Acta*, **51**, 287-294.

19) K.J. Orians, E.A. Boyle (1993) Determination of picomolar concentrations of titanium, gallium and indium in sea water by inductively coupled plasma mass spectrometry following an 8-hydroxyquinoline chelating resin preconcentration, *Analytica Chimica Acta*, **282**, 63-74.

20) S. Chan (1993) Evaluation of electrothermal vapourization as a method of sample introduction for the ICP-MS and determination of trace levels of titanium, gallium and indium in the Central Pacific gyre, M.Sc. Thesis, University of British Columbia.

21) H. Amakawa, D.S. Alibo, Y. Nozaki (1996) Indium concentration in Pacific seawater, *Geophysical Research Letters*, **23**, 2473-2476.

22) D.S. Alibo, H. Amakawa, Y. Nozaki (1998) Determination of indium in natural waters by flow injection inductively coupled plasma mass spectrometry, *submitted to Earth and Planetary Sciences...*

23) D.S. Alibo, Y. Nozaki, C. Jeandel (1999) Indium and yttrium in North Atlantic and Mediterranean waters: comparison to the Pacific data, *submitted to Geochimica et Cosmochimica Acta...*

24) T. Shigematsu, Y. Nishikawa, K. Hiraki, H. Nakagawa (1964) Zirconium in seawater, *Nippon Kagaku Zasshi*, **85**, 490-492.

25) D.F. Shutz, K.K. Turekian (1965) The investigation of the geographical and vertical distribution of several trace elements in seawater using neutron activation analysis, *Geochimica et Cosmochimica Acta*, **29**, 259-313.

26) V.N. Sastry, T.M. Krishnamoorthy, T.P. Sarma (1969) Microdetermination of zirconium in the marine environment, *Current Science*, **38**, 279-281.

27) S.M. Boswell, H. Elderfield (1988) The determination of Zr and Hf in natural waters using isotope dilution mass spectrometry, *Marine Chemistry*, **25**, 197-210.

28) B.A. McKelvey, K.J. Orians (1993) Dissolved zirconium in the North Pacific ocean, *Geochimica et Cosmochimica Acta*, **57**, 3801-3805.

29) B.A. McKelvey (1993) The marine geochemistry of zirconium and hafnium, Ph.D. Thesis, University of British Columbia.

30) L.V. Godfrey, W.M. White, V.J.M. Salters (1996) Dissolved zirconium and hafnium distributions across a shelf break in the northeastern Atlantic ocean, *Geochimica et Cosmochimica Acta*, **60**, 3995-4006.

Chapter 2: Experimental

2.1 Background

Under ideal conditions, the analysis of trace elements would not require any initial concentration or separation stage. However, even with recent developments in selectivity and sensitivity, direct instrumental analysis is often impossible because the concentrations of analytes are below the detection limits of the method or the matrix provides an interference which must be removed. When both problems are encountered simultaneously, a separation/preconcentration step is essential. The determination of Ga, In, Zr and Hf in seawater using ICP/MS is such an example. The most attractive features of ICP/MS are its high sensitivity and capability of simultaneous multi-elemental analysis. However, there are some drawbacks when the sample contains large amounts of salts. High dissolved solids can cause clogging of the sampler and skimmer cones as well as certain nebulizers. Also, highly concentrated matrix ions such as the alkaline and alkaline-earth metals present in seawater can cause signal suppression, space charge effects and spectral interferences. Moreover, since the concentrations of Ga, In, Zr and Hf in the open ocean (anywhere from 0.1 to 300×10^{-12}M)[1-5] are much lower than instrumental detection limits ($\sim 10^{-10}$M), selective enrichment of these elements is indispensable prior to ICP/MS analysis.

Preconcentration techniques that have been applied to the determination of trace metals in seawater include coprecipitation[6,7], liquid-liquid extraction[8,9], sorption[10] and chelating ion-exchange resins[11,12]. Depending on the anticipated enrichment factor, most of these isolation methods require large volumes of chemicals that can lead to high blanks. On the other hand, chelating ion-exchange resins are simple to use and yield surprisingly low analytical blanks while allowing much higher preconcentration factors to be attained.

In this chapter, a method is presented which uses a chelating resin as a means of concentrating and separating Ga, In, Zr and Hf from their salt-water matrix.

2.2 Instrumentation, Material and Reagents

2.2.1 ICP/MS

The ICP/MS system used in this study consisted of VG Elemental's 'PlasmaQuad Turbo Plus' (Surrey, UK) which is equipped with a SX300 quadrupole mass analyzer and Galileo 4870-V channel electron multiplier. Liquid Ar (>99% pure), obtained from Praxair (Vancouver, Canada) served as the nebulizer, auxiliary and cooling gas.

A flow injection system proved essential to accommodate the small sample volumes generated by this method. A peristaltic pump, a 6-way Rheodyne valve (Mandel Scientific, Guelph, Canada) equipped with a 100μL loop was used to introduce the sample into the plasma. A V-groove or de Galan nebulizer and double-pass spray chamber cooled to 5°C ensured the delivery of fine, reproducibly-sized droplets to the plasma thus minimizing water loading and noise due to flickering.

The operating conditions of the system are summarized in table 2.2.1.1. Torch positioning and electrostatic lens settings were optimized daily using a 10ppb Be, Mg, Co, In, Ce, Pb, Bi, U solution. To obtain maximum sensitivity, the instrument was tuned on Be-9. This procedure was found to ensure greater instrumental stability throughout the course of the day.

External standards were used to build calibration curves from which the concentrations of Ga, In, Zr and Hf in the seawater samples were determined. Rhodium was used as an internal standard (ISTD) to correct for plasma instabilities or sensitivity changes during the course of the analysis. The isotopes chosen for ICP/MS analyses were Ga-69, Ga-71, Zr-90, Zr-91, In-115, Hf-177, Hf-178 and Rh-103.

A 2N HNO_3 blank was run between each sample to ensure memory effects due to the more refractory elements were negligible.

2.2.2 GFAAS

A Varian Spectra AA300 graphite furnace atomic absorption spectrometer was used to measure Ca in seawater sample eluates. External standards were used to build linear calibration curves from which the metal concentrations were derived. Instrumental parameters used were those suggested by the manufacturer.

ICP-MS Spectrometer	
RF Power (W)	1350
Ar gas flow rate (L/min)	
- Nebulizer gas	1.1
- Auxiliary gas	0.6
- Cooling gas	13.8
Sampler cone/orifice (mm)	Al / 1
Skimmer cone/orifice (mm)	Ni / 0.4
Data acquisition	
Scan mode	Peak jumping
Dwell times (ms)	
- In-115, Hf-177, Hf-178	20
- Ga-69, Ga-71	10
- Zr-90, Zr-91, Rh-103	5
Points (per spectral peak)	3
Total acquisition (s)	30

Table 2.2.1.1 ICP/MS operating conditions.

2.2.3 Pumps

A Masterflex L/S Multi-Channel Cartridge pump (Cole-Palmer Instrument Co.; Chicago, USA) equipped with an 8-channel, 3-roller pump head was used to pump the samples through the resin during the preconcentration step. "C-Flex" (a fluoro-elastomer) and FEP tubing (Labcor; Anjou, Canada) completed the pumping circuit. This setup allowed for 8 samples to be pumped simultaneously. Flow rates were determined by weighing the amount of DDW pumped through the columns over a 10-minute period.

2.2.4 Distilled Deionized Water (DDW)

High purity distilled, deionized water (18MΩ) was obtained by passing distilled water (Barnstead/Thermolyne; Dubuque, USA) through a "Milli-Q" water system (Millipore; Mississauga, Canada).

2.2.5 Acids

Ultra clean acids (Q-HNO_3, Q-HCl) used for sample analysis were purified by sub-boiling distillation in a quartz or Teflon still and provided by Seastar Chemicals (Sidney, Canada). For plasticware cleaning purposes, the use of ultra-clean acids was not essential therefore reagent-grade (UBC Chemistry Stores; Vancouver, Canada) and environmental-grade acids (Anachemia; Vancouver, Canada) were used to minimize costs.

2.2.6 Metal Standards

Multi-element standard solutions of Ga, In, Zr, Hf and Rh in the μg/L range were prepared by serial dilutions of 1000mg/L single-element certified atomic absorption standards (Delta Scientific; Mississauga, Canada) using 2N Q-HNO_3.

2.2.7 Resins

Analytical Grade Chelex-100 resin (100-200 mesh), a polystyrene/divinyl benzene copolymer containing an iminodiacetate functional group, was purchased from Bio-Rad Laboratories (Mississauga, Canada).

Toyopearl HW-40EC, HW-75F (two ethylene glycol/methacrylate copolymer-based resins) as well as AF-Chelate-650M and AF-Epoxy-650M (same backbone as previous resins but with iminodiacetate and epoxy functional groups attached, respectively) were purchased from TosoHaas (Montgomeryville, USA).

Resins used for preconcentration purposes were initially cleaned by 5 consecutive 3-day batch extractions of environmental grade 2N HNO_3, with 3 DDW rinses in between. In addition, the resin was further cleaned once loaded in columns by the passage of 30mL 2N Q-HNO_3.

2.2.8 Reagents

NaCl, $MgCl_2$ and KHP (potassium hydrogen phthalate) were all obtained from BDH Chemicals (Vancouver, Canada). These reagents were used in solution to rinse the resin of Ca following the passage of seawater samples. The solutions were initially cleaned of any trace metal impurities by passing them twice through 2mL of Chelex-100.

2.2.9 Laboratory Material

All solutions were stored in high-density polyethylene bottles (VWR Canlab; Mississauga, Canada). Evaporations were conducted in Teflon PFA beakers (Nalgene; Edmonton, Canada). Polyprep disposable chromatography columns (0.8cm diameter X 4cm) were obtained from Bio-Rad Laboratories (Richmond, USA). Equipped with a porous polymer bed support which holds the resin in place, these columns can hold up to 2mL of resin as well as 10mL of eluant or sample in an integral reservoir.

2.3 Methods

2.3.1 Seawater Collection and Storage

Following clean sampling procedures developed by Bruland et al.[13], seawater samples were collected using a trace metal-clean all-teflon pump system. The intake tubing, attached to a plastic encased weight (or 'fish'), was towed off the bow of the ship at 1-2m depth. The pumped seawater was filtered through acid-cleaned 0.45μm polypropylene cartridge filters, transferred to 1L acid-cleaned HDPE bottles, then acidified to pH2 using Q-HCl. All shipboard sample handling was carried out in either a trace metal clean portalab or in a clean area built inside the ship's dry lab from polyethylene sheets and supplied with filtered air from a portable high efficiency pure air (HEPA) unit. Doubly-bagged samples were stored away from any light source, at pH2, for 1.5 years awaiting processing and analysis.

2.3.2 Salinity, Temperature, Nutrient and Chlorophyll a Measurements

All measurements were performed by personnel from the Institute of Marine Sciences, University of California at Santa Cruz. Seawater salinity and temperature were determined using the ship's flowthrough SAIL loop system. Preliminary nutrient (NO_3^- and H_4SiO_4) measurements were monitored at sea with an autoanalyzer on seawater obtained from the flowthrough system described in section 2.4.1. Simultaneously, seawater samples were collected, frozen and brought back to the laboratory in Santa Cruz for analysis and confirmation but only the flowthrough data are used in this study. Chlorophyll a was measured at sea fluorometrically on samples vacuum-filtered on to polycarbonate filters and extracted in 90% acetone according to methods by Parsons et al[14].

2.3.3 Acid Cleaning

All new and previously used plasticware was subjected to rigorous acid cleanings in order to minimize contamination. The procedure found to be most effective involved soaking in 4N reagent grade HCl at 60°C for 2 days, rinsing 3 times with DDW, followed by soaking in 0.1N environmental grade HNO_3 for a minimum of one week. In addition, new plasticware had to be

rinsed with acetone prior to the acid soakings in order to remove any oils or greases leftover from the manufacturing process.

To avoid memory effects due to the refractory nature of Zr and Hf, sample bottles, columns and resin were never re-used. Because of their higher cost, teflon beakers were re-used but 0.5% HF was added to the 0.1N HNO_3 during the second acid soaking to remove refractory Zr and Hf.

2.3.4 Seawater Sample Processing

The analytical procedure used to determine Ga, In, Zr and Hf throughout this study was modified from two existing methods and adapted for the simultaneous determination of all four metals. In the first method, Ga and In in seawater were measured by standard addition using ICP/MS following preconcentration on an 8-HQ (8-hydroxyquinoline) chelating ion exchange resin (TSK-8HQ)[11]. The second method used ID/ICP/MS following preconcentration by Chelex-100 in order to measure Zr and Hf[12]. Experimental conditions in each procedure were considerably different from the other, therefore neither one could be applied to the analysis of all four elements without undergoing modifications. The final procedure is presented in this section although the method developments, main features and modifications of the original methods will be discussed further in section 2.5.

Approximately 1.5mL of Chelex-100 (hydrogen form, pH2) was loaded into each column. A final pre-cleaning of the resin was carried out by the passage of 30mL of 2N Q-HNO_3 through the columns. This extra cleaning step was found to be effective for minimizing the 10ml 2N Q-HNO_3 column blanks, which were collected next. Next, 30mL of pH2 adjusted DDW was passed through the columns to pH adjust the resins prior to the passage of the seawater samples.

Acidified seawater samples (1L) were pumped through the columns at a flow rate of 0.2mL/min, followed by resuspension of the resin using 5mL of pH2 DDW and rinsing with 20mL of pH2 DDW to wash the resin free of residual seawater and possibly weakly-bound calcium and magnesium. The chelated metals were then eluted into Teflon beakers using 10mL 2N Q-HNO_3 (gravity flow). The eluates were then slowly evaporated down to near dryness on a hot plate. Finally, the residual concentrated drops were taken up into 1000µL of 2N Q-HNO_3 to which 50µL of 10ppb Rh was added. The solutions were then stored in 4mL acid cleaned HDPE bottles until analysis.

2.3.5 Recovery Tests

Recovery tests were performed by spiking known amounts of Ga, In, Zr and Hf into seawater samples and subjecting them to the preconcentration procedures described previously in section 2.3.4. Tests conducted in order to study varying experimental conditions were subjected only to the extraction step of this procedure whereas recovery tests conducted alongside actual seawater samples were subjected to the full procedure (extraction and evaporation steps). The recoveries were calculated from the difference between spiked and unspiked seawater samples.

2.4 Study area

Seawater samples used in this study were collected on board the RV Point Sur during the summer of 1997 from 9 horizontal transects which covered most of the west coast of North America, from the Olympic Peninsula (Washington) extending down to central California (figure 1.2.3.1). For most transects, the ship initially traveled alongshore south and east ('dog leg') then changed direction and headed offshore for the remainder of the transect. Even though no samples were collected from WCSST#10, references are made to this transect in ensuing chapters.

2.5 Analytical Technique Development

Even with the most sensitive detection instrumentation, measurements of trace metals are meaningless unless the background noise due to metal contamination in sample collecting, handling and analysis is significantly lower than the signal one wishes to detect. To achieve this, all sample preparations were performed in a "clean" laboratory equipped with laminar flow "clean" benches and fume cupboards, providing a class 100 working environment.

2.5.1 Volume of Sample

In order to be able to measure Ga, In, Zr and Hf accurately and precisely by ICP/MS, these metals needed to be concentrated by approximately 3 orders of magnitude. To achieve this, 1L seawater samples were subjected to column extractions, followed by elution of the trace metals and evaporation of the eluates down to 1mL. Yet, in spite of these 1000-fold enrichment factors, In and Hf were still limited by low signals. However for reasons which will be discussed later on, opting for larger sample volumes was not a practical possibility.

2.5.2 Resins

At the heart of the preconcentration procedure lies the chelating/ion-exchange resin. Ideally, the perfect resin should demonstrate great selectivity, high capacities, rapid-exchange kinetics, good mechanical strength and stability at various pH's. Of course, no resin ever fulfills all these criteria. Nonetheless, Chelex-100 was found to be the best choice for the extraction of Zr and Hf in seawater[12]. Ga and In were originally preconcentrated using TSK-8HQ (8-hydroxyquinoline bound to a vinyl polymer substrate) but for reasons which will be discussed in section 2.5.6, it was rejected in favor of Chelex-100.

Chelex-100 is the most commonly employed chelating resin for the removal and preconcentration of trace metals from saline solutions. Consisting of an iminodiacetate functional group immobilized onto a styrene/divinylbenzene substrate, its main advantages are its selectivity for polyvalent metals over commonly occurring monovalent cations such as Na^+ and K^+, high capacities and commercial availability. Unfortunately, it also has the disadvantage of undergoing shrinking and swelling as a function of the pH.

An extensive study by McKelvey and Orians[12] found that the highest recoveries for Zr and Hf using Chelex-100 were obtained at pH2 using a flow rate of 0.2mL/min. When Ga and In were tested under these conditions, near-quantitative recoveries were obtained (table 2.5.3.1.) indicating this resin was appropriate for the preconcentration of all four metals.

2.5.3 Flow Rates

Unfortunately, when applied to 1L samples, a 0.2mL/min flow rate results in a pumping time of 3.5 days. Attempts to use higher flow rates resulted in considerably lower recoveries for all elements except In (table 2.5.3.1). The exceedingly lengthy pumping procedure associated with Chelex-100 is the main drawback of this method. However, since the concentrations of these elements (In and Hf in particular) in seawater are so low, it was necessary to do whatever possible to maximize their signals. Consequently, a flow rate of 0.2mL/min was maintained throughout the entire study.

Element	Recoveries (%)	
	0.2mL/min	0.6mL/min
Ga	90 ± 2	84 ± 6
In	98 ± 4	96 ± 3
Zr	88 ± 3	64 ± 4
Hf	93 ± 7	79 ± 4

Table 2.5.3.1 Extraction step metal recoveries of spiked standards as a function of flow rate. Errors represent one standard deviation. All measurements are based on 6 replicates.

2.5.4 Evaporation

The column extraction step of the preconcentration procedure results in a 100-fold concentration. To obtain higher enrichment factors which are necessary to detect picomolar concentrations of Ga, In, Zr and Hf, the 10mL column eluates were concentrated further by evaporation. It was discovered however, that when evaporated to complete dryness, a silver residue was left behind which would not always go back into solution. In these instances, losses occurred for all metals and recoveries were especially erratic for Zr and Hf. Instead, when 2N Q-HNO_3 spiked with 10 ng Ga, In, Zr and Hf was evaporated to near-dryness, quantitative recoveries were obtained for all elements (figure 2.5.4.1). In addition, recoveries for Zr and Hf were found to be more consistent. Hence, care was taken to ensure the eluates were never evaporated to complete dryness.

Thus, sample eluates were slowly heated (~6hrs) on a hot plate and removed when a tiny concentrated drop (~10μL) remained. To this drop, 1mL of 2N Q-HNO_3 and 50μL of 10ppb Rh ISTD were added which resulted in overall concentration factors of 900-1000x depending on the amount of sample initially available.

Element	Recoveries (%)	
	Dryness	Near-dryness
Ga	89 ± 4	97 ± 4
In	86 ± 3	100 ± 4
Zr	88 ± 13	102 ± 8
Hf	71 ± 13	96 ± 8

Table 2.5.4.1 Evaporation step metal recoveries of spiked standards. Errors represent one standard deviation. All measurements are based on 8 replicates.

Note that although recovery studies for both the extraction and evaporation steps were performed separately and each provided acceptable recovered metal amounts, when the entire procedure was performed on spiked seawater standards, recoveries for Zr and Hf were considerably less and would tend to vary somewhat. It is not known where this behaviour stems from. Numerous attempts were made to determine where the metals were lost: from repeating all experiments to studying such parameters as the effect of the volume of the resin or the presence of HF in the cleaning acid on the metal recoveries, but to no avail. It might be that, as the volume decreases during the evaporation step, metals precipitate out of solution to varying degrees. In the evaporation recovery studies, only the metals of interest are present in a 2N Q-HNO_3 matrix. When real seawater samples are involved, it is possible the eluates contain other species besides Ga, In, Zr and Hf that may interfere in some way, altering these elements' chemistries and causing them to precipitate. In any case, not much could be done about this except to conduct as many recovery tests as possible in order to be certain of how much is lost and to correct the results appropriately for these losses. Final metal recoveries were 89% ± 4% (Ga), 97% ± 3% (In), 38% ± 8% (Zr) and 36% ± 7% (Hf), based on 51 measurements.

2.5.5 Matrix Effects

ICP/MS is considerably prone to matrix effects, i.e. changes in analyte sensitivity caused by variable concentrations of matrix elements. Matrix ions generated in the plasma deposit on the interface cones, cause changes in the ionization potential of the plasma and reduce the extraction and transport efficiency of the analyte ions in the ion lens region due to space charge effects. In any case, signal suppression occurs. Generally, matrix effects are most severe when the analyte is light and the matrix is heavy. For practical analysis, the matrix effect is minimized by using fairly dilute solutions, with total dissolved solid levels typically 0.1% or less. Even these matrix concentrations however can cause significant signal suppression.

The matrix elements most likely to cause analyte suppression in these samples are Ca and Mg (monovalent ions such as Na and K are not retained by Chelex-100). Even though one of the purposes of the preconcentration step was to separate the trace metals from most of the matrix, it is possible that residual Ca and Mg in the eluates may still pose a problem. Thus compensation by isotope dilution analysis (IDA), standard additions or internal standardization is required.

2.5.5.1 Isotope Dilution Analysis

IDA coupled to mass spectrometry is one of the most accurate methods of trace analysis[15,16]. It is capable of a high degree of accuracy and provides a means whereby the analyte in question serves as its own internal standard. The method is based on the addition of a known quantity of an isotopically enriched solution (or 'spike') to a sample. After equilibration of the spiked isotope with the natural element in the sample, mass spectrometry is used to measure the altered isotopic ratio of the mixture, which in turn is used to calculate the concentration of the element in the original sample. IDA corrects for all non-spectroscopic interferences (i.e. all factors affecting sample transport, plasma ionization, ion extraction, instrumental drift) because both isotopes are affected equally during these processes. Since it cannot correct for spectral interferences, it requires that two isotopes be free of any isobaric interferences.

McKelvey and Orians[12] used IDA to determine Zr and Hf in seawater. The main advantage of IDA is that chemical separation or isolation of an element from its matrix need not be quantitative. Once equilibration is achieved between the sample and the spike, the isotopic ratio defines the elemental concentration and any subsequent loss of substance during the isolation procedure has no effect on the analytical result. This feature, which contributes to the high precision and accuracy of the method, is what makes IDA perfectly suited to the analysis of Zr and Hf. At least one week at 70°C is required for these two elements to reach equilibrium, mainly because the spiked isotopes are equilibrating with Zr and Hf adsorbed to the container walls.

One difficulty associated with IDA is that the best measurements require an optimum mixture of the spike and sample. Based on error propagation, greater accuracy is obtained when the measured isotope ratio is equal to the square root of the product of the ratios of the spike and natural isotopes, while greater precision is achieved for ratios near unity. Consequently, analyte concentrations must be estimated beforehand. This poses a problem if there are no means by which to estimate how much metal is present or if one expects large variabilities in the concentrations, as was the case in this study. Ideally, if duplicate samples are available, one can use results from a first run to optimize the spike added to a second sample. This was not possible in this study as only one sample was collected per site and the entire volume (1L) was necessary to achieve the high preconcentration factors required to detect these low-level elements.

Many practice attempts were made to repeat Zr and Hf results from open ocean seawater samples using IDA but were not successful. Whereas Zr occasionally gave adequate results, Hf results were extremely erratic. Since these samples were collected in 1992, it is possible their

concentrations changed significantly over the course of the years (contamination due to improper storage and handling, evaporation, metals adsorbing onto bottle walls) which could have made it more difficult to achieve the optimum spiking ratio. These discouraging attempts, plus the fact that no estimates could be made of the concentrations of Ga, In, Zr and Hf present in the coastal samples, resulted in the method of IDA being abandoned.

Adsorption of Zr and Hf onto bottle walls will be discussed further in section 2.5.8.

2.5.5.2 Standard Additions

The method of standard additions is extremely useful when the sample composition is unknown or complex and affects the analytical signal. Orians and Boyle[11] used standard additions to measure Ga and In. This method could have been applied to the determination of Ga, In, Zr and Hf, although with the small sample volumes generated by this preconcentration procedure, multi-point calibrations and replicate measurements would require the use of smaller sample loops. Orians and Boyle could afford to use smaller sample volumes as their samples were concentrated 3000x. In this procedure, 100μL was barely enough to obtain In and Hf signals above blank levels. Consequently, the method of standard additions was not considered.

2.5.5.3 Internal Standardization

Internal standardization has been shown to be an extremely effective means of compensating for matrix effects, providing that an ISTD of similar mass and ionization energy to the analyte is chosen. Furthermore the routine use of an ISTD is recommended for even the simplest matrices in order to compensate for instrumental drift.

Only one ISTD (Rh) was chosen to correct for all four elements studied. Rh was picked because of its low abundance in seawater and also because it was not extracted by Chelex-100 at the chosen conditions. In addition, it is situated in the middle of the mass range of the analytes of interest, a compromise position for any mass effects. If matrix effects happened to be considerable in these samples, the elements farthest in mass from Rh should be the most affected (i.e. the most incorrectly accounted for). The use of Re as a second ISTD to correct for Hf was tested at one point. However, it was rapidly abandoned as Re is significantly extracted by the resin at these

conditions. Ideally, if a second ISTD were found which was similar in mass and ionization energy to Hf and which was not extracted by the existing conditions, this might have improved Hf results.

To determine if space charge effects due to alkaline earth elements were indeed present, the responses for all five elements were studied in the presence of increasing amounts of Ca. No signal suppression was observed for any of the elements of interest up to 500ppb of added Ca (~12.5μM). The Ca content of the seawater eluates was measured by GFAAS and was found to vary from 200 to 400ppb. Mg was not measured, but since it is even lighter than Ca the amounts present in the eluates are not expected to have a significant effect in terms of space charge.

In conclusion, the use of Rh as ISTD in this study provides a rapid and simple means of quantification by external calibration using non-matrix matched standards.

2.5.6 Alternative resins

2.5.6.1 AG-Chelate-650M

In hopes of reducing the pumping time, other resins which could be used at higher flow rates were investigated. Since it was believed the hydrophobic nature of Chelex-100's styrene/divinylbenzene substrate was responsible for the low recoveries of Zr and Hf at higher flow rates, the search was on to find an iminodiacetate-containing resin with a hydrophilic substrate. One such possibility was BioRad's AG-Chelate-650M. This resin's matrix consists of semi-rigid beads synthesized by a copolymerization of ethylene glycol and methacrylate type polymers. The presence of ether and hydroxyl groups at its surface results in a resin that is highly hydrophilic in nature.

The recoveries of Ga, In, Zr and Hf using this resin were tested for a variety of flow rates and pH's (figure 2.5.6.1.1). The only element that undergoes significant change with varying flow rates is Ga. However the big surprise was In. Usually the most well behaved element with nearly 100% recovered material on any resin tested, recoveries in this case were barely 20% at pH2. Recoveries did increase but only up to 60% at pH6. Meanwhile, Zr and Hf recoveries had dropped considerably at this pH. Because In and Hf are the least abundant, it is important to maximize their responses. Since they increase in opposite directions, pH4 was the best tradeoff; in the mean time, Zr was nearly at its worst with less than 15% of the material recovered. In sum, AG-Chelate-650M was not really suitable for the simultaneous analysis of these four metals.

a)

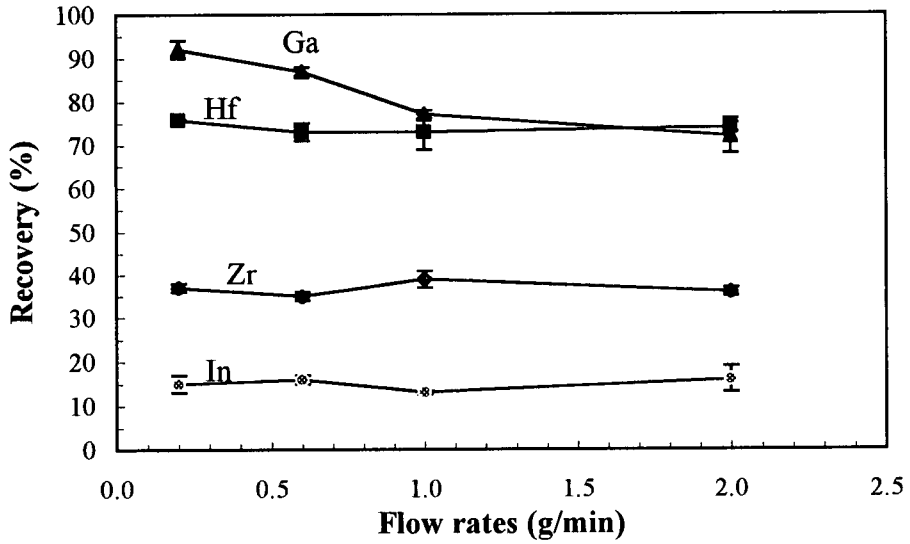

b)

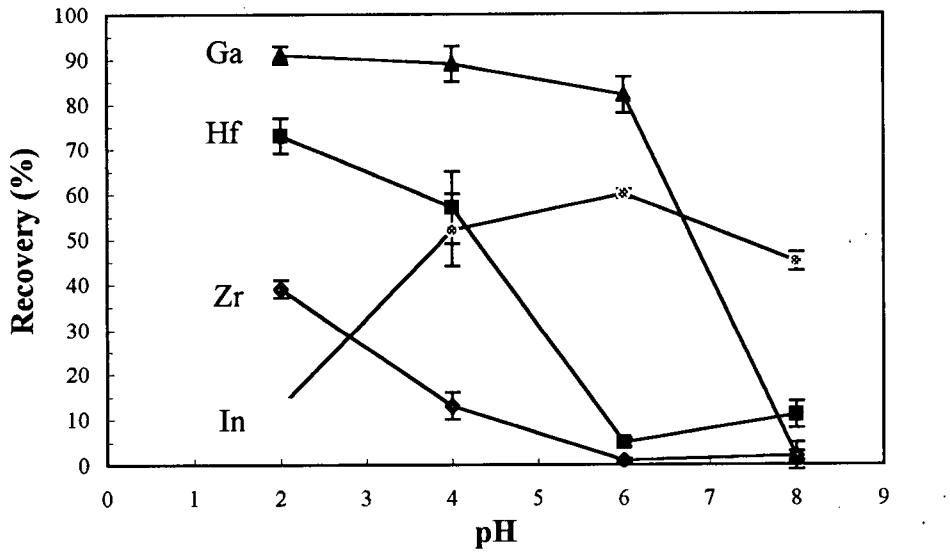

Figure 2.5.6.1.1 Metal recoveries of spiked standards using AG-Chelate-650M a) at various flow rates (pH=2) and b) pH's (flow rate=0.2mL/min). Error bars represent one standard deviation. All measurements are based on 3 replicates.

2.5.6.2 8-Hydroxyquinoline Resins

Iminodiacetic acid resins are not the only complexing resins that have been used for extracting trace metals in seawater. 8-HQ bound to either silica or a stable organic polymer matrix has been extensively used in the extraction of first row transition elements from aquatic samples[17,18]. One advantage of these 8HQ-based resins over the commercially available Chelex-100 is a greater difference in affinity between transition metals and alkaline earth elements. For example, Orians and Boyle[11] used TSK-8HQ to extract Ti, an element which is heavily interfered by calcium, from seawater.

Orians and Boyle[11] were using flow rates of 3-5mL to preconcentrate Ga and In using TSK-8HQ. The ability to be able to use higher flow rates would prove very beneficial to this procedure therefore tremendous effort was invested in this resin. Unfortunately, its synthesis is time-consuming and often fails for unknown reasons[19]. Many attempts were made to synthesize the resin, which only resulted in low capacities (3-4μmol Cu/g resin as opposed to 100μmol/g for Chelex-100). An alternative synthesis in which 8-HQ is covalently bonded via a secondary amino link to the polymer substrate resin was recently developed[20]. This greatly simplified one-step synthesis successfully produced a resin with a capacity exceeding 100μmol/g resin with respect to copper. Yet, regardless of this promising result, no recoveries were ever conducted for Ga, In, Zr and Hf since the polymer matrix and reagents used in this synthesis are extremely expensive. This resin would probably find greater uses in small-scale applications such as in the miniature columns found in on-line systems.

2.5.7 Batch Method

Chelating resins can be used in either column or batch mode. Columns have advantages because the resin material is well isolated. In batch methods, the resin must be added to the sample, mixed and recovered, the analytes then being eluted. These extra transfer and handling steps all have associated contamination potential. They can also be less efficient than columns in cases where partition coefficients are unfavorable. On the other hand, batch methods do not require the use of a pumping system which is definitely one aspect this procedure could benefit from.

Accordingly, a small-scale batch recovery study was set up in which eight 100mL seawater samples were spiked with 10ng of Ga, In, Zr and Hf. Approximately 1.5mL of Chelex-100 was added to each sample, which was then affixed to a mechanical shaker. Half the samples were left to shake 24 hours, the other half for 96 hours. Then, the entire solution was transferred to a column where the resin was recovered, rinsed and eluted. The results for this experiment were very promising (table 2.5.7.1). Recoveries were comparable, if not better, to those obtained by the column method.

Little was gained from shaking the samples any longer than 24hours. In fact, longer contact times resulted in lower recoveries, possibly because the metals were adsorbing onto the bottle walls. The improved recoveries associated with the batch method compared to the column method could be explained by the longer contact time between the metals and the resin beads. In a column of 0.4cm diameter, 1.5mL of resin is approximately 3cm high. At a flow rate of 0.2mL/min, any given parcel of seawater is in close contact with the resin for only 7.5 minutes after which it is evacuated to waste. In the batch method, the resin was left in contact with the seawater for 24 hours. Even though the same parcel of seawater is not in continuous contact with the resin, presumably the amount of time it does meet a resin bead adds up to more than 7.5 minutes. This confirms the extraction of Ga, In, Zr and Hf by Chelex-100 is kinetically limited.

These promising results led to a larger-scale experiment in which the same amount of metals and Chelex-100 were added to 1L seawater samples. Already this posed a greater challenge, as the mechanical shaker was not able to accommodate more than four samples at a time. Also, even on the highest shaking speed, it was not able to homogenize the resin throughout the entire 1L solution as effectively as for the 100mL solutions. Instead, the resin tended to stay close to the bottom and the seawater was sloshed around rather than being properly mixed.

Nevertheless, twelve samples were subjected to the same treatment as for the small-scale experiment, with contact times varying from 12 to 48 hours.

The results, which are also summarized in table 2.5.7.1, were very interesting although not as encouraging. Metal recoveries were considerably lower. Since the same amounts of material were used in both experiments, the larger volumes (and their associated mixing difficulties) are clearly the determining factor. Had the mixing been vigorous enough to properly homogenize the resin, recoveries probably would have resembled those obtained from the small-scale experiment.

This time, all elements benefited somewhat from increasing the contact time from 12 to 24hrs. Even longer mixing times might lead to higher recoveries up until the time when adsorption onto bottle walls intervenes. Beyond mixing times of 2 days, the gains in recovery are not worth the longer sample preparation time.

Increasing the amount of Chelex-100 could also lead to higher recoveries. But since the resin cannot be reused, increasing the amount of Chelex-100 would add considerably to the cost of sample analysis.

In conclusion, unless a more efficient way of thoroughly mixing 1L samples can be devised, the column method remains the better choice. On the other hand, for 100mL samples this method shows great potential.

Element (10ng)	Recoveries (%)			
	100mL		1L	
	24 hours	96 hours	12h	24h
Ga	82.7 ± 0.6	79 ± 1	66 ± 3	72 ± 3
In	94 ± 2	92 ± 1	51 ± 5	58 ± 7
Zr	88 ± 2	75 ± 5	33 ± 4	40 ± 4
Hf	98 ± 1	81 ± 4	20 ± 4	24 ± 3

Table 2.5.7.1 Metal recoveries for batch experiment using 1.5mL of Chelex-100 for 100mL and 1L samples. Errors represent one standard deviation. All measurements are based on 3 replicates.

2.5.8 HF Experiment

One important aspect about Zr and Hf in solution is that they are known to adhere to bottle walls at working pH's above 3, possibly even lower[21]. The method of isotope dilution can account for the loss of analyte in solution if the spiked isotopes are allowed enough time to equilibrate with the metals adsorbed to the container walls. The method of internal standard on the other hand cannot, therefore whatever metals are adsorbed to bottle walls are lost and contribute to a systematic error. A 2-part experiment was set up in order to verify if these metals could be leached off the bottle walls using a ligand that shows some affinity for them. Since HF acid is commonly added to certified metal standards of elements like Zr and Hf to stabilize them, adding a slight amount to seawater samples might prevent these metals from adsorbing to surfaces. In the first part of the experiment, a normal recovery test was carried out in which four 100mL seawater samples were spiked with 10ng of Ga, In, Zr and Hf. Approximately 0.1% HF was added to two of the samples. The goal was to subject these solutions to the entire preconcentration procedure 7 days after they were prepared, then quantify the loss of metals due to adsorption from the samples that did not contain HF by comparing them to the samples that did.

In the second part of the experiment, eight spiked seawater samples were prepared on one day and 0.1% HF was added to all one week later. Then two by two, the samples were subjected to the preconcentration procedure 1,3,7 and 14 days after the HF addition. This test would hopefully indicate how rapidly the adsorbed metals could be leached back into solution.

The results of this experiment are shown in tables 2.5.8.1. Unfortunately, adding HF had the opposite effect of what was anticipated. While the recoveries for In are identical for both types of sample in Part I, Ga, Zr and Hf recoveries decreased by as much as 68%. Virtually no Zr or Hf was retained by the columns. Apparently, the fluoride has such a strong affinity for these metals that the Chelex-100 is unable to compete successfully for the metals. These results were very similar to those obtained by Yang et al[22], who developed a method in which Zr and Hf were separated by extraction chromatography using liquid anionic exchangers. They observed that no separation was achieved when small amounts of HF acid were present in solution. This comes as no surprise once one realizes Zr-fluoride complexes are the most stable fluorocomplexes known[23].

The time study results are therefore non-conclusive since they are practically identical to those solutions in Part I that contained HF. The challenge lies in finding a ligand strong enough to pull Zr and Hf off the bottle walls, but weak compared to iminodiacetic acids. Consequently, addition of HF was abandoned.

a)

Element	Recoveries (%)	
	HF	No HF
Ga	36.5 ± 0.6	89 ± 2
In	95.8 ± 0.4	97.8 ± 0.4
Zr	0	69 ± 1
Hf	0	56.8 ± 0.05

b)

Element	Recoveries (%)			
	1 day	3 days	7 days	14 days
Ga	39 ± 1	38.00 ± 0.05	42 ± 2	43 ± 2
In	93 ± 2	95.5 ± 0.6	95 ± 4	100 ± 4
Zr	2.5 ± 0.6	2	3	3
Hf	1	1	1	1

Table 2.5.8.1 HF experiment results. a) The effect of the presence of HF on metal recoveries b) Metal recoveries as a function of the number of days after the addition of HF. Errors represent one standard deviation.

In another attempt to quantify adsorption to bottle walls, additional recovery tests were conducted on 8 spiked seawater standards a range of times after addition of the metal spikes to the seawater matrices. Recoveries were very similar for all metals whether the solutions were extracted on the same day they were prepared or anywhere from 1 to 6 days after (figure 2.5.8.1). Consequently, if adsorption to bottle walls does occur, it is not significantly noticeable, at least for the higher levels used in these recovery tests (~10^{-9}M). In actual seawater samples, where concentrations are three orders of magnitude lower, adsorption onto surfaces is likely quite significant.

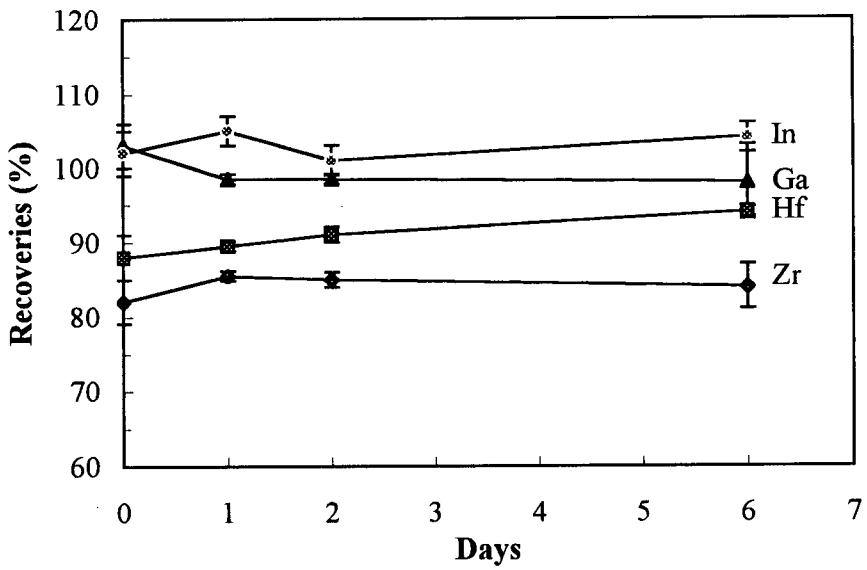

Figure 2.5.8.2 Effect of standing time on the metal recoveries of spiked standards. Errors represent one standard deviation.

2.5.9 Titanium Determination

Originally, the studies performed on these coastal seawater samples were to include Ti. Ti, which is situated above Zr and Hf in the periodic table, is also dominated by hydroxide speciation in seawater. The high concentration gradients observed in seawater of the North Central Pacific (from 4-8pM in the surface to ~300pM at 4000m)[24] indicate that Ti may provide a valuable tracer of chemical transport processes.

Although recovery studies using Chelex-100 showed promise, Ti proved to be the most troublesome of all the elements. The major difficulty associated with Ti is the high number of possible isobaric interferences at every isotope. While sulphate and phosphate interferences are cause for concern, Ca and $^{14}N^{18}O^{16}O^{+}$(ref.11) at mass 48 (Ti's most abundant isotope) are the real problem. Extra precautions need to be taken in order to rid the resin of as much Ca as possible prior to eluting the metals. The nitrogen oxide species originates from the nitric acid matrix and not much can be done to reduce it except by optimizing instrumental parameters so as to minimize oxide formation.

In this experiment, numerous rinse solutions (KHP, $MgCl_2$ and NaCl in various concentrations) aimed at removing the Ca from the resin were investigated. Although they seemed effective at removing the Ca (<50ppb Ca present as opposed to ~400ppb without these rinses), the background at mass 48 remained high, which left $^{14}N^{18}O^{16}O^{+}$ as the main culprit.

The use of an ultrasonic nebulizer (USN)-membrane desolvator (MDX) was sought to attempt to remove this interference. The USN improves detection limits (typically by one order of magnitude) by enhancing analyte transport efficiency and reducing solvent loading to the plasma. Some solvent loading still occurs when the USN is used alone therefore an MDX is usually employed in conjunction. In this unit, solvent vapor is removed through a microporous PTFE tubular membrane while the analyte continues through the tube and on to the plasma. This preserves the high sample transport efficiency of the USN and greatly reduces solvent loading into the ICP. It was hoped the USN-MDX might serve two purposes: 1) removing the $^{14}N^{18}O^{16}O^{+}$ background (via removal of the matrix) and 2) increasing the Ti signal (via increased transport efficiency).

Sadly, of the five elements investigated, only Ti did not benefit from improved signals. Ga, In, Zr and Hf signals were increased 2,4,5 and 16-fold, respectively while Ti signals were the same with the USN-MDX as with a pneumatic nebulizer. This sensitivity increase with increasing mass is probably due to non-spectroscopic interferences. The improved transport efficiency of USN-MDX (20%) compared to a pneumatic nebulizer (1%) means more ions are actually reaching the plasma, thus generating greater space charge effects in the sampling and ion lens regions. Since lighter ions are repelled to a greater extent than heavier elements, Ti and Ga benefit from lesser sensitivity gains than Zr, In and Hf.

As far as $^{14}N^{18}O^{16}O^{+}$ was concerned, backgrounds were lower at mass 48 but not enough that signal-to-noise ratios were greatly improved compared to pneumatic nebulizers. In conclusion, the complications associated with the USN-MDX system outweighed the benefits for Ti, therefore its use was discontinued.

Another complication in analyzing Ti occurred during the drying stage. As the eluant volume decreased, Ti would precipitate out of solution and could not be resolubilized without the use of HF. As a result, of the 10mL eluant, 1mL was analyzed directly after extraction for Ti while the other 9mL was further evaporated and used to determine Ga, In, Zr and Hf. Unfortunately, since IDA was originally used to quantify Ti, the low concentration factor (100x) sometimes resulted in signals at mass 49 that were limited by instrumental noise. In sum, the high background at mass 48 and the noise-limited signal at mass 49 led to erratic results. It was concluded that the simultaneous analysis of Ti along with the other four elements was not feasible.

2.5.10 Spectral Interferences

Spectral interferences are not as prevalent in ICP/MS as in ICP/OES but they are still important. These types of interferences are caused by atomic or molecular ions having the same nominal mass as the analyte isotope of interest. They may be subdivided into three categories: 1) isobaric atomic ions 2) multiply charged ions and 3) polyatomic ions of various origins.

The potential spectral interferences for Ga, In, Zr and Hf are listed in table 2.5.10.1. Except for ^{115}In, all other isotopes are free of isobaric interferences (first column of table 2.5.10.1). Many of the potential doubly-charged and polyatomic interfering species may be discounted on the basis that their presence in significant numbers in the sample or the plasma is not likely. To determine the magnitude of a potential interference, one has to consider the concentration of the interfering species, the abundance of the interfering isotope and the degree of formation (in the case of doubly charged species and polyatomics). A plasma is a very efficient ion source; it produces a high yield of singly charged ions and little else. The formation of doubly charged ions is negligible for most elements except those that possess low second ionization potentials (e.g. Ba and La). Also, polyatomic formation such as oxides and hydroxides are usually kept to a minimum by optimizing certain operating conditions such as the nebulizer gas flow rate, the RF power and the geometric design (sampling depth) of the interface. Yet regardless of these facts, when analyte concentrations are lower than most matrix elements, even low-abundance non-favored species may cause significant interferences. As this is the case, all species present in table 2.5.10.1 must be considered seriously.

	ISOBARIC	DOUBLY-CHARGED	POLYATOMICS
^{69}Ga (60.1)		$^{138}Ba^{++}$ (71.7) $^{138}La^{++}$ (0.09) $^{138}Ce^{++}$ (0.25)	$^{53}Cr^{16}O^{+}$ (9.50) $^{52}Cr^{16}OH^{+}$ (83.8)
^{71}Ga (39.9)		$^{142}Ce^{++}$ (11.1) $^{142}Nd^{++}$ (27.1)	$^{55}Mn^{16}O^{+}$ (100) $^{54}Cr^{16}OH^{+}$ (2.37) $^{54}Fe^{16}OH^{+}$ (5.8)
^{90}Zr (51.5)		$^{180}Hf^{++}$ (35.1) $^{180}Ta^{++}$ (0.01) $^{180}W^{++}$ (0.13)	$^{74}Ge^{16}O^{+}$ (36.5) $^{74}Se^{16}O^{+}$ (0.9) $^{73}Ge^{16}OH^{+}$ (7.8)
^{91}Zr (11.2)		$^{182}W^{++}$ (26.3)	$^{75}As^{16}O^{+}$ (100)
^{115}In (95.7)	$^{115}Sn^{+}$ (0.36)		$^{99}Ru^{16}O^{+}$ (12.7)
^{177}Hf (18.6)			$^{161}Dy^{16}O^{+}$ (18.9) $^{160}Gd^{16}OH^{+}$ (21.9) $^{160}Dy^{16}OH^{+}$ (2.34)
^{178}Hf (27.3)			$^{162}Dy^{16}O^{+}$ (25.5) $^{162}Er^{16}O^{+}$ (0.14) $^{161}Dy^{16}OH^{+}$ (18.9)

Table 2.5.10.1 Potential spectral interferences for Ga, In, Zr and Hf. Numbers in parentheses represent the isotopic abundance of the metal.

2.5.10.1 Gallium

The lower mass elements tend to have more spectral interferences than the higher mass elements as can be seen here with gallium. Interferences for Ga arise from Ba, La, Ce and Nd, which have a strong tendency to form doubly charged ions as well as oxide and hydroxide species. Since seawater levels of La, Ce and Nd[25,26] are comparable to Ga levels, these elements should not pose a problem. Likely, manganese oxides can be disregarded since many studies have shown that Mn is not extracted by Chelex-100 at low pH (pH<4)[27,28].

On the other hand, nanomolar seawater levels of Ba and Cr are cause for concern, therefore these two interferences were further investigated. A scan of a 10ppb Ba and 10ppb Cr standard showed that chromium oxide formation is negligible (<1%) whereas doubly charged Ba formation is ~3-3.5% (of total Ba), a considerable potential interference. To get an idea of the Ba concentrations in our sampling region, eight 120mL seawater samples from WCSST#09 (Columbia River plume) were mixed together and carried through the entire preconcentration procedure. The resulting eluate was monitored at masses 69(Ga) and 138(Ba). This procedure was also repeated on 8 samples from WCSST#01 and #03 (Southern California). The results (table 2.5.10.1.1) showed that even assuming a maximal 4% formation of doubly-charged Ba would result in no more than 1% interference for ^{69}Ga.

In addition, a good indication that Ga is devoid of any spectral interferences is that both isotopes were used to calculate elemental concentrations and the two results always agreed very closely with one another (RSD<2%). This would not be the case if one or both isotopes suffered from interferences since it would be very unlikely that both isotopes were interfered identically.

Isotope	Blank	WCSST#01&#03	WCSST#09
$^{69}Ga_{(60.1)}$	180	34168	76456
$^{138}Ba_{(71.7)}$	543	7440	19634

Table 2.5.10.1.1 Response (in cps) for Ga and Ba in seawater samples obtained from different transects. Isotopic abundances are shown in parentheses.

2.5.10.2 Indium

$^{99}Ru^{16}O^{+}$ is not a real concern since the concentrations of Ru in seawater are much lower (<0.05pM) than indium[29]. On the other hand, $^{115}Sn^{+}$ is a notable problem as ~70% of it is retained by the resin at these conditions. Even though the isotopic abundance at mass 115 is low, concentrations of inorganic tin in surface waters of the North Atlantic vary from 1 to 40pM[30,31]. No data was found for the North Pacific. Since sources of tin to the ocean are mainly anthropogenic however, coastal samples (and especially the river plume samples) are likely to be high. A scan of two seawater eluates (see section 2.5.10.1) confirmed what was feared (table 2.5.10.2.1). Significant amounts of tin contribute up to 50% of the signal observed at mass 115. Unfortunately, the tin interference was not discovered until after the samples had all been processed and analyzed. If duplicate samples had been available, this problem could have easily been resolved by monitoring a second isotope of tin along with mass 115, thus applying the right corrections. As this was not the case, no appropriate corrective measures were taken.

Isotope	Blank	WCSST#01&#03	WCSST#09
$^{115}In_{(95.7)}$ $^{115}Sn_{(0.36)}$	172	947	1370
$^{118}Sn_{(24.2)}$	468	26336	45596
$^{120}Sn_{(32.6)}$	635	24820	53872
$^{124}Sn_{(5.79)}$	206	-----	10463

Table 2.5.10.2.1 Response (in cps) for In and Sn in seawater samples obtained from different transects. Isotopic abundances are shown in parentheses.

2.5.10.3 Zirconium

Fortunately, Zr is present at higher pM levels; consequently, interferences with low isotopic abundances (Ta, Se) or low concentrations in seawater (Hf, Ge) are unlikely to be a problem. $^{182}W^{++}$ and $^{75}As^{16}O^{+}$ could be because of their high concentrations (high pM for W[34] and nM levels for inorganic As). A 10ppb W and 10ppb As standard revealed that doubly charged W and arsenic oxides were virtually nonexistent (<0.5%), therefore unlikely to interfere with Zr.

2.5.10.4 Hafnium

Species most likely to interfere with hafnium are oxides of the rare earth elements (REEs) Gd, Dy and Er. Despite their low seawater levels, these elements are still more abundant than Hf. Concentrations of Gd, Dy and Er[25,26] vary from less than 5pM in coastal/ocean margin/open ocean settings up to 20pM in estuaries or embayments. Since these elements do have a tendency to form oxides (high M-O bond strength), interferences with Hf are definitely a possibility and should be verified. A scan of the two coastal seawater eluates (see section 2.5.10.1) revealed REEs are extracted by this method (table 2.5.10.4.1). The difficulty is in evaluating the degree of oxide formation for these elements since no standards were available to measure them directly. Instead, a worst-case scenario was applied. The Ce oxide formation was measured and used to estimate DyO and ErO. As specified earlier, these elements do have a tendency to form oxides although not as readily as Ce. The CeO/Ce ratio was measured on many occasions and was found to vary from 4-6% although on one occasion it was as high as 10%. Assuming a 10% formation of DyO and ErO (at worst), this would still only contribute up to 3% of the signals at 177 and 178. This is well within the error of the technique.

The fact that two isotopes were used to determine Hf concentrations and yielded nearly identical results cannot be used to rule out possible interferences since both isotopes are affected by the same species.

Isotope	Blank	WCSST#01&#03	WCSST#09
$^{161}Dy_{(18.9)}$	59	140	402
$^{162}Dy_{(25.5)}$ $^{162}Er_{(0.14)}$	55	211	524
$^{177}Hf_{(18.6)}$	67	496	1019
$^{178}Hf_{(27.3)}$	75	795	1499

Table 2.5.10.4.1 Response (in cps) for Dy, Er and Hf in seawater samples obtained from different transects. Isotopic abundances are shown in parentheses.

2.5.11 Analytical Figures of Merit

2.5.11.1 Detection Limits and Procedural Blanks

The accurate determination of trace elements in seawater after preconcentration requires the achievement of low and reproducible blanks. Blanks were therefore carried through the preconcentration procedure described previously. This procedure was compared to column blanks involving only the acid elution of a cleaned column. Analysis of both blanks yielded nearly identical levels of all trace metals indicating that the resin was the most significant source of metal contamination.

Comparison of these blanks as well as the detection limits for each element are given in table 2.5.11.1.1. Detection limits were calculated based on three times the standard deviation of eight process blanks, and taking into account the non-quantitative recoveries of each element.

Element	Column blanks (ppb)	Procedural blanks (ppb)	Procedural blanks (pmol)	Detection limits (pmol/kg)
Ga	0.022	0.029	0.41 ± 0.07	0.24
In	0.0018	0.0020	0.026 ± 0.004	0.012
Zr	0.26	0.29	3.8 ± 0.8	6
Hf	0.010	0.013	0.09 ± 0.03	0.25

Table 2.5.11.1.1 Blanks and detection limits. All measurements are based on 8 replicates.

2.5.11.2 Precision

Since only one 1L sample was obtained at each location, sampling precision is unavailable. The analytical precision of this method however was determined by numerous spike recovery tests as well as by replicate analysis of seawater samples from other locations.

In the former case, an average of three recovery tests per batch of 8 was conducted alongside the seawater samples. The relative standard deviation (RSD) obtained is a measure of the batch-to-batch and column-to-column variability.

In the latter case, two 4L seawater samples from the North Pacific were mixed thoroughly in a 25L carboy and the resulting solution was re-divided into two 4L portions. Four 1L sub-samples were pumped directly from the two containers and subjected to the entire preconcentration procedure. This experiment was more representative of the low levels of metals that might be expected in the actual samples.

The RSD's for both experiments are shown in table 2.5.10.2.1. The analytical precision is clearly limited by the variability of the spiked metal recoveries since greater precision is obtained for Ga and In. Even though the variability of the metal recoveries of Zr and Hf are quite similar, the overall analytical precision is much worse for Hf because of the lower concentrations of this element.

Element	Recovery Tests	Seawater Samples
Ga	4%	5%
In	3%	9%
Zr	21%	13%
Hf	19%	38%

Table 2.5.11.2.1 Relative standard deviations of the analytical method. RSD's for recovery tests are based on 51 measurements. RSD's for seawater samples are based on 8 measurements

2.5.11.3 Accuracy

It is difficult to assess the accuracy of this method, as there are no certified reference materials for Ga, In, Zr and Hf in seawater. Instead, results obtained using this method can be compared to those of others who have tested the same samples for the same elements but using different methods.

For example, vertical profiles of these metals were obtained from two stations in the North Pacific (Station-P, 50°N, 145°W and AVHS-10, 47°N, 175°E). Results were compared to Orians and Boyle[11] who used TSK-8HQ to measure Ga and In at Station-P by standard additions as well as Chan[33] who used the same resin to determine Ga and In at AVHS-10 by ICP/MS. Zr and Hf results are compared to McKelvey[21] who measured these metals at both stations using ID/ICP/MS.

Gallium shows the best agreement of all elements, correlating perfectly at both stations (figure 2.5.11.3.1).

Indium is difficult to assess. Values obtained from this procedure are similar to those of Chan[33] even though the profiles are slightly different. Considering the age of the samples and also the fact that In may be contaminated by tin, Chan's results are likely more accurate.

Zirconium strangely shows good correlation at AVHS-10 and while the trend is similar at Station-P, absolute values are consistently lower suggesting possible loss due to adsorption onto bottle walls. Why the same is not observed at AVHS-10 is not known. The Station-P samples were analyzed eight years after collection. Since the coastal samples were analyzed two years after collection, it is possible some adsorption has taken place and results are underestimated (figure 2.5.11.3.1).

Hf shows the opposite trend as Zr. Even though vertical profiles are similar, absolute values are higher this time. Since isotope dilution which is supposed to be the most accurate quantitative method was used for the original data, then it is possible the current results are overcorrected (figure 2.5.11.3.2).

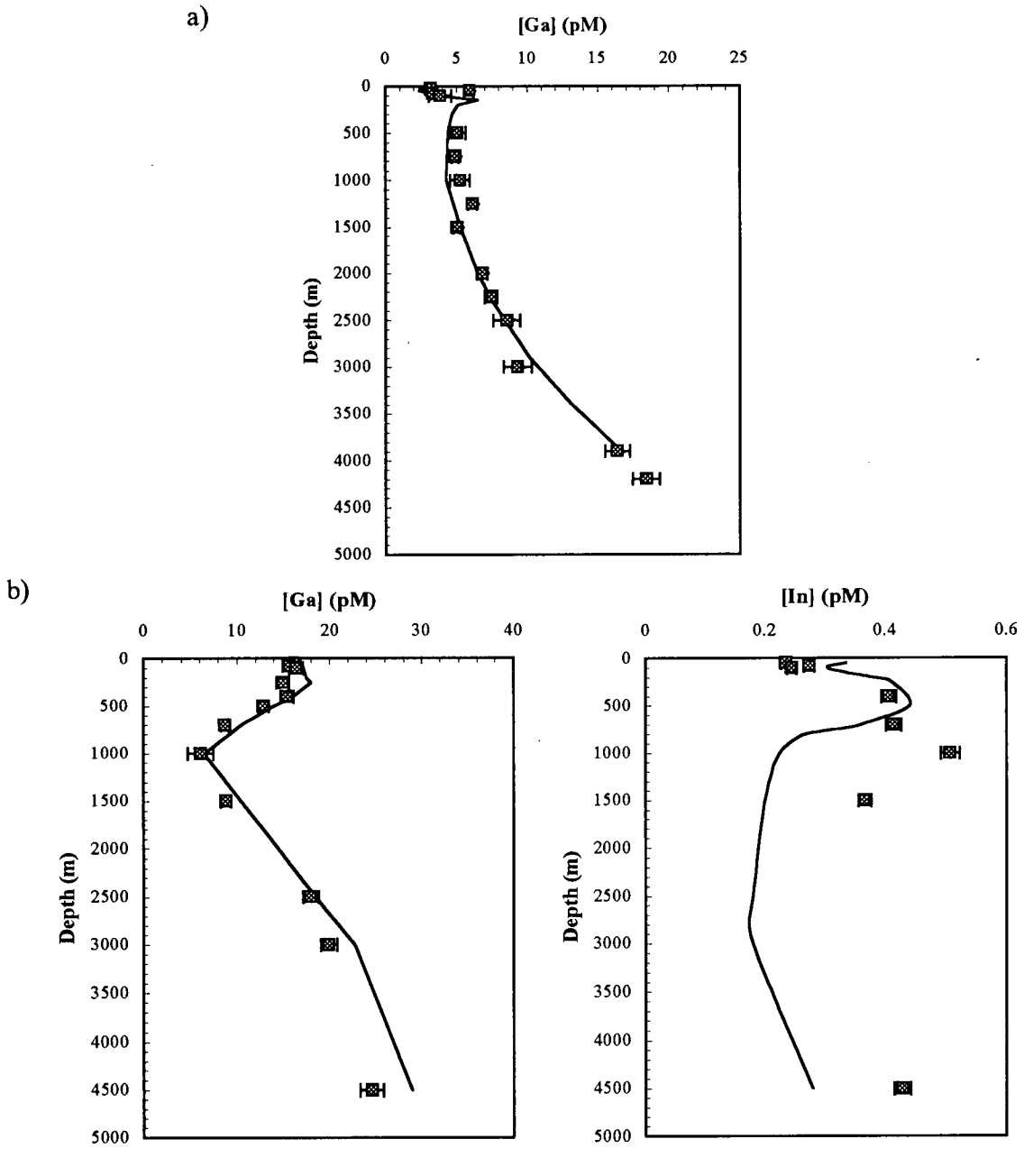

Figure 2.5.11.3.1 Ga and In distributions at a) Station-P and b) AVHS-10. (Legend: Line = a) Orians[11] data b) Chan[33] data; ■ = Data from this study).

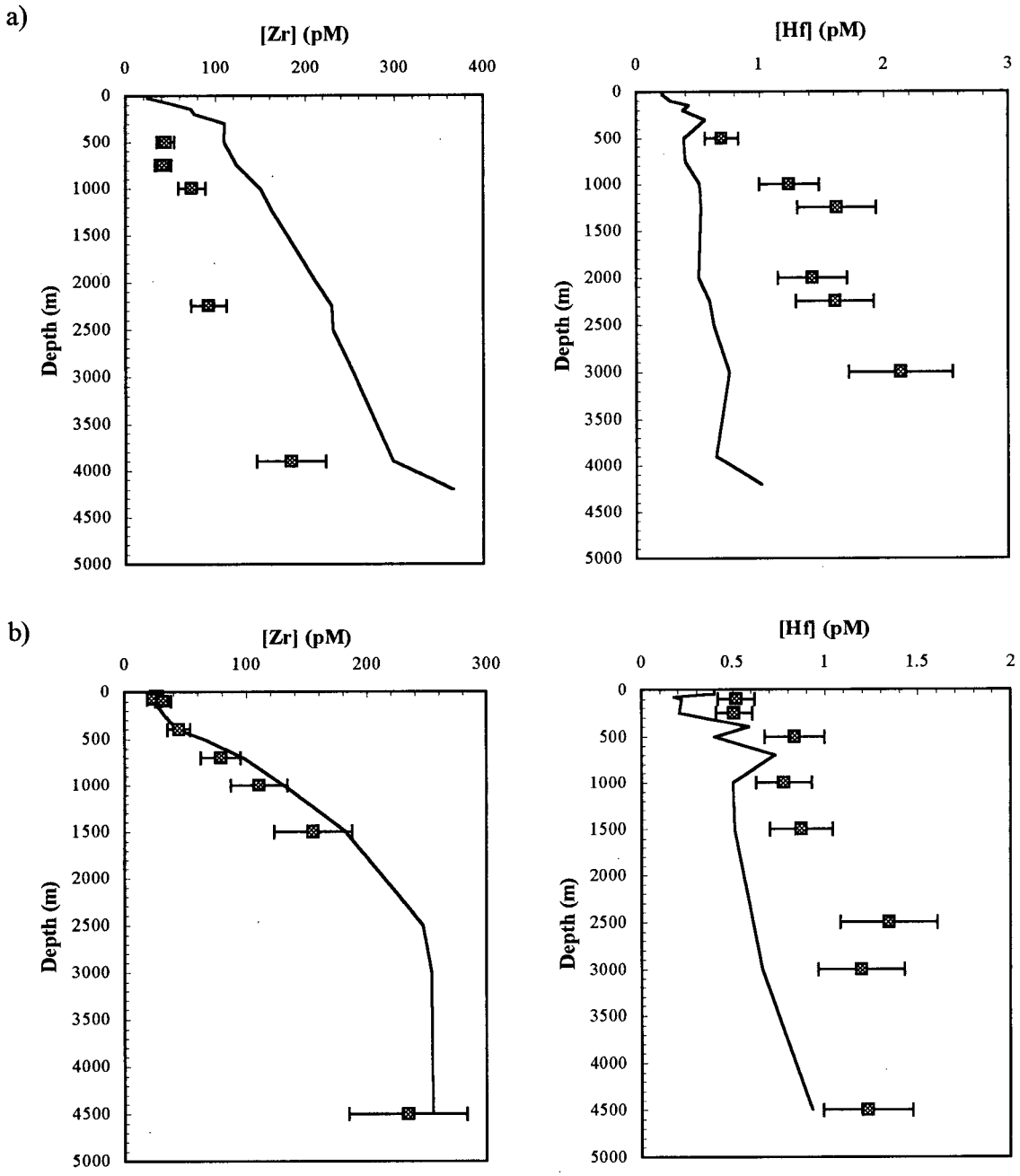

Figure 2.5.11.3.2 Zr and Hf distributions at a) Station-P and b) AVHS-10. (Legend: Line = McKelvey[21] data; ■ = Data from this study).

2.6 Summary

The analytical procedure used to determine Ga, In, Zr and Hf in seawater samples consists of an extraction/preconcentration step followed by detection and quantification using ICP/MS.

A 1L volume of pH2 adjusted seawater is pumped through 1.5mL of the chelating ion-exchange resin Chelex-100 (also pH2 adjusted) at a flow rate of 0.2mL/min. Trace metals are eluted using 10mL 2N Q-HNO_3 following extensive rinses of pH2 adjusted DDW and the eluate is evaporated down to near dryness. Evaporation to complete dryness resulted in low and erratic recoveries and therefore was avoided. The residual concentrate is taken up in 1mL of 2N Q-HNO_3 to which 50μL of 10ppb Rh ISTD is added, resulting in ~1000-fold concentration factors. Metal recoveries using this procedure are 89% ± 4% (Ga), 97% ± 3% (In), 38% ± 8% (Zr) and 36% ± 7% (Hf). Since recoveries for the extraction step only were much higher, it is thought that most of the metals are lost during the evaporation step, possibly as a result of seawater matrix interferences causing the metals to precipitate. Detection limits were 0.24 pmol/kg (Ga), 0.012 pmol/kg (In), 6 pmol/kg (Zr) and 0.25 pmol/kg (Hf).

The use of Rh as internal standard was deemed suitable for the analysis of Ga, In, Zr and Hf in the final matrix. Unfortunately, the method of internal standards is not able to account for losses of certain metals due to adsorption onto bottle walls. Even though samples were stored at pH2, adsorption is likely to have taken place over the course of their 1.5year storage period. Hence, the most susceptible elements, the refractive Zr and Hf, are possibly affected by systematic errors. IDA was considered as an alternative method for quantification, but the lack of duplicate samples made the task of estimating the optimum spiking ratio quite difficult.

Adding HF to seawater samples to 'resolubilize' the metals adsorbed onto the bottles is not possible. Instead, the fluoride binds the metals, preventing them from interacting with the resin. Metal recoveries were low for all elements save In when HF was present. Adsorption onto bottle walls was not noticeable in solutions containing 10^{-9}M metal levels. It is not known whether this is the case for real seawater samples which contain Ga, In, Zr and Hf levels closer to 10^{-12}M.

Alternative resins to Chelex-100 were also tested but none was able to match it in terms of analytical recovery and practicality. The low recoveries at high flow rates obtained using Chelex-100 are thought to result from the substrate's hydrophobicity. Yet surprisingly a hydrophilic iminodiacetate-containing resin did not yield the positive results anticipated. Only Ga and Hf showed promising recoveries with this resin.

The extraction of Ga, In, Zr and Hf from seawater using Chelex-100 was also investigated in a batch method. Metal recoveries were nearly quantitative when tested on 100mL samples. They decreased significantly, however, when 1L volumes were used instead. Inadequate mixing/resuspension of the resin in the 1L-seawater samples was thought to be the determining factor.

The determination of Ti using this method is quite problematic. Because it precipitated and could not be brought back into solution, Ti could not be concentrated by evaporation. Consequently, it had to be analyzed separately from the other four metals. Moreover, interferences by Ca and NO_2^+ caused high backgrounds at Ti-48. Ca was significantly reduced by appropriate rinses of the resin prior to elution. To reduce NO_2^+, samples were introduced into the plasma using an ultrasonic nebulizer-membrane desolvator. Ironically, Ti was the only element which did not benefit from enhanced signal-to-noise ratios. Ga, In, Zr and Hf signals were enhanced 2,4,5 and 16x. In the end, the resulting high backgrounds prevented Ti analysis.

No significant spectral interferences were detected for Ga, Zr and Hf. In is heavily interfered by Sn however, which is quantitatively extracted by Chelex-100 in this method. No appropriate measures were taken to correct for this interference and the lack of duplicate samples prevented the measurements from being repeated. Consequently, In results in ensuing chapters are questionable.

2.7 References

1) K.J. Orians, K.W. Bruland (1988) Dissolved gallium in the open ocean, *Nature*, **332**, 717-719.

2) K.J. Orians, K.W. Bruland (1988) The marine geochemistry of dissolved gallium: A comparison with dissolved aluminum, *Geochimica et Cosmochimica Acta*, **52**, 2955-2962.

3) A.M. Shiller (1998) Dissolved gallium in the Atlantic Ocean, *Marine Chemistry*, **61**, 87-99.

4) H. Amakawa, D.S. Alibo, Y. Nozaki (1996) Indium concentration in Pacific seawater, *Geophysical Research Letters*, **23**, 2473-2476.

5) B.A. McKelvey, K.J. Orians (1993) Dissolved zirconium in the North Pacific, *Geochimica et Cosmochimica Acta*, **57**, 3801-3805.

6) N. Belzile, H. Chen, J. Huang, Y-W. Chen (1997) Determination of trace metals in lake waters by x-ray fluorescence after a precipitation preconcentration, *Canadian Journal of Analytical Sciences and Spectroscopy,* **42**, 49-56.

7) L. Elçi, U. Sahin, S. Õztas (1997) Determination of trace amounts of some metals in samples with high salt content by atomic absorption spectrometry after cobalt-diethyldithiocarbamate coprecipitation, *Talanta*, **44**, 1017-1023.

8) M.B. Shabani, T. Akagi, H. Shimuzu, A. Masuda (1990) Determination of trace lanthanides and yttrium in seawater by inductively coupled plasma mass spectroscopy after preconcentration with solvent extraction and back-extraction, *Analytical Chemistry*, **62**, 2709-2714.

9) K.K. Namboothiri, N. Balasubramanian, T.V. Ramakrishna (1991) Spectrophotometric determination of thallium after its extraction as an ion-pair of the chloro-complex and pyronine G, *Talanta,* **8**, 945-949.

10) S.N. Willie, H. Tekgul, R.E. Sturgeon (1998) Immobilization of 8-hydroxyquinoline onto silicone tubing for the determination of trace elements in seawater using flow injection ICP-MS, *Talanta*, **47**, 439-445.

11) K.J. Orians, E.A. Boyle (1993) Determination of picomolar concentrations of titanium, gallium and indium in seawater by inductively coupled plasma mass spectrometry following an 8-hydroxyquinoline chelating resin preconcentration, *Analytica Chimica Acta*, **282**, 63-74.

12) B.A. McKelvey, K.J. Orians (1998) The determination of dissolved zirconium and hafnium from seawater using isotope dilution inductively coupled plasma mass spectrometry, *Marine Chemistry*, **60**, 245-255.

13) K.W. Bruland, R.P. Franks, G.A. Knauer, J. H. Martin (1979) Sampling and analytical methods for the determination of copper, cadmium, zinc and nickel at the nanogram per liter level in sea water, *Analytica Chimica Acta*, **105**, 233-245.

14) T.R. Parsons, Y. Maita, C.M. Lalli (1984) A manual of chemical and biological methods for seawater analysis. Pergamon Press, Oxford, 1-172.

15) J.D. Fassett, P.J. Paulsen (1989) Isotope dilution mass spectrometry for accurate elemental analysis, *Analytical Chemistry*, **61**, 643A-649A.

16) K.G. Heumann (1988) Isotope Dilution Mass Spectrometry, in *Inorganic Mass Spectrometry*, Chemical Analysis ed., Wiley, New York, 301-376.

17) K. Akatsuka, J.W. McLaren, J.W. Lam, S.S Berman (1992) Determination of iron and 10 other trace elements in the open ocean seawater reference material NASS-3 by inductively coupled plasma mass spectrometry, *Journal of Analytical Atomic Spectrometry*, **7**, 889-894.

18) A. Seubert, G. Petzold, J.W. McLaren (1995) Synthesis and application of an inert type of 8-hydroxyquinoline-based chelating ion exchanger for sea-water analysis using on-line inductively coupled plasma mass spectrometry detection, *Journal of Analytical Atomic Spectrometry*, **10**, 371-379.

19) W.M. Landing, C. Haraldsson, N. Praxéus (1986) Vinyl polymer agglomerate based transition metal cation chelating ion-exchange resin containing the 8-hydroxyquinoline functional group, *Analytical Chemistry*, **58**, 3031-3035.

20) H. Dierssen, W. Balzer, W.M. Landing (1999) Simplified synthesis of a chelating resin: Applications to trace metal profiles from Jelly Fish Lake, Palau, *submitted to Marine Chemistry*.

21) B.A. McKelvey (1993) The marine geochemistry of zirconium and hafnium, Ph.D. Thesis, University of British Columbia.

22) X.J. Yang, C. Pin, A.G. Fane (1999) Separation of hafnium from zirconium by extraction chromatography with liquid anionic exchangers, *Journal of Chromatographic Science*, 37, 171-178.

23) S.U. Aja, S.A. Wood, A.E. Williams-Jones (1995) The aqueous geochemistry of Zr and the solubility of some Zr-bearing minerals, *Applied Geochemistry*, **10**, 603-620.

24) K.J. Orians, E.A. Boyle, K.W. Bruland (1990) Dissolved titanium in the open ocean, *Nature*, **348**, 322-325.

25) J. Zhang, Y. Nozaki (1996) Rare earth elements and yttrium in seawater: ICP-MS determinations in the East Caroline, Coral Sea, and South Fiji basins of the western South Pacific Ocean, *Geochimica et Cosmochimica Acta*, **60**, 4631-4644.

26) J. Zhang, Y. Nozaki (1998) Behavior of rare earth elements in seawater at the ocean margin: A study along the slopes of the Sagami and Nankai troughs near Japan, *Geochimica et Cosmochimica Acta*, **62**, 1307-1317.

27) C.J. Cheng, T. Akagi, H. Haraguchi (1987) Simultaneous multi-element analysis for trace metals in sea water by inductively coupled plasma/atomic emission spectrometry after batch preconcentration on a chelating resin, *Analytica Chimica Acta*, **198**, 173-181.

28) L. Yang (1993) Dissolved trace metals in the Western North Pacific, M.Sc. Thesis, University of British Columbia.

29) M. Koide, M. Stallard, V.F. Hodge, E.D. Goldberg (1986) Preliminary studies on the marine chemistry of ruthenium, *Netherlands Journal of Sea Research*, **20**, 163-166.

30) J.T. Byrd, M.O. Andreae (1982) Tin and methyltin species in seawater: Concentrations and fluxes, *Science*, **218**, 565-569.

31) J.T. Byrd, M.O. Andreae (1986) Dissolved and particulate tin in North Atlantic seawater, *Marine Chemistry*, **19**, 193-200.

32) Y. Sohrin, K. Isshiki, T. Kuwamoto (1987) Tungsten in North Pacific waters, *Marine Chemistry*, **22**, 95-103.

33) S. Chan (1993) Evaluation of electrothermal vapourization as a method of sample introduction for the ICP-MS and determination of trace levels of titanium, gallium and indium in the Central Pacific gyre, M.Sc. Thesis, University of British Columbia.

Chapter 3: The Columbia River as a Source of Ga, In, Zr and Hf to the California Current System

3.1 Introduction

3.1.1 Rivers and Estuaries as Sources of Trace Metals

Rivers are major contributors of trace metals to the oceans. Yet, the amount of metals that do reach the oceans is only a very limited percentage of the river's original transported metal load. The mixing of freshwater with saline water is a drastic process. As a river discharges into the ocean, the increase in ionic strength from 0 to 0.7, together with the change in composition causes removal of many constituents and a change of dissolved forms of others[1]. Elements that form very strong anionic complexes are fully transported out of estuaries in dissolved form while others are removed to various extents. Some elements may undergo desorption or remineralization. A large percentage of other metals (in dissolved or particulate form) are incorporated into bottom sediments by processes of adsorption, flocculation or coprecipitation in association with humic acids, clay minerals, Fe and Mn oxyhydroxides. Estuarine bottom sediments therefore act as a sink for river-borne trace metals but represent a source of trace metals for the overlying water. Elements initially removed to particulate phases and to the sediments within the estuarine mixing zone may subsequently be recycled, re-transported and eventually re-deposited in the outer estuary or in regions on the shelf outside the estuary. In this manner, estuarine sediments act as additional indirect river sources of trace metals to the ocean. Thus on passing through an estuary, some metals are supplied, some removed and others are simply unaffected. These in-situ chemical, biological, geological and physical processes all combine to make estuaries dynamic geochemical reactors wherein output fluxes can be substantially different from input fluxes.

Yet estuaries are only a part, and geographically a small part, of the entire river-ocean boundary, hence it is not unreasonable to assume that the processes that govern trace metals and influence their behaviors in estuaries continue to a certain extent out into the coastal/continental shelf waters. In fact, for rivers of considerable discharge like the Mississippi and the Amazon, most of the initial mixing of freshwater with saline water occurs beyond the estuary over the continental shelf.

The Columbia River, with its annual freshwater discharge of $2.3x10^{11}m^3/yr$, is possibly the most influential coastal feature of the American West Coast. During periods of intense discharge (late spring-early summer), mixing occurs mostly in the lower estuary and extends out onto the shelf. The Columbia River estuary and coastal plume have been the subject of several large studies most of which are compiled in a work by Pruter and Alverson[2]. Within the estuary and a few tens of kilometers seaward from the river mouth, Columbia River water mixes with salt water of the adjacent Northeast Pacific Ocean. The effluent thus decreases the salinity of the ambient surface seawater but maintains its identity up to several hundred kilometers as it moves under the influence of local winds and ocean currents.

3.1.2 Metal/Salinity Diagrams

The extent of input of riverborne dissolved trace metals to the ocean depends largely on the chemical reactivity of an element in the estuary. A major tool used to study estuarine processes and thus determine which type of behavior applies to a particular element is a mixing plot in which the constituent of interest is plotted against a known chemically conservative property, generally salinity. If the plotted data fall on a straight line, then the constituent is said to mix conservatively (i.e. its concentration varies only as a result of physical dilution). If the relationship is non-linear, then either several end-members of different constituent concentrations are mixing or an internal source or sink is present. These conclusions are based on the assumption that the concentrations of the end-members are not variable over the time scale of mixing.

As will be seen from the ensuing temperature and salinity data, transects WCSST#07, #08 and #09 are heavily influenced by the Columbia River effluent. This chapter will concentrate mainly on these three transects (figure 3.1.2.1). Metal/salinity diagrams will be used to study the behavior of silicic acid, Ga and Zr in the river plume as it travels south along the coast of Washington and Oregon.

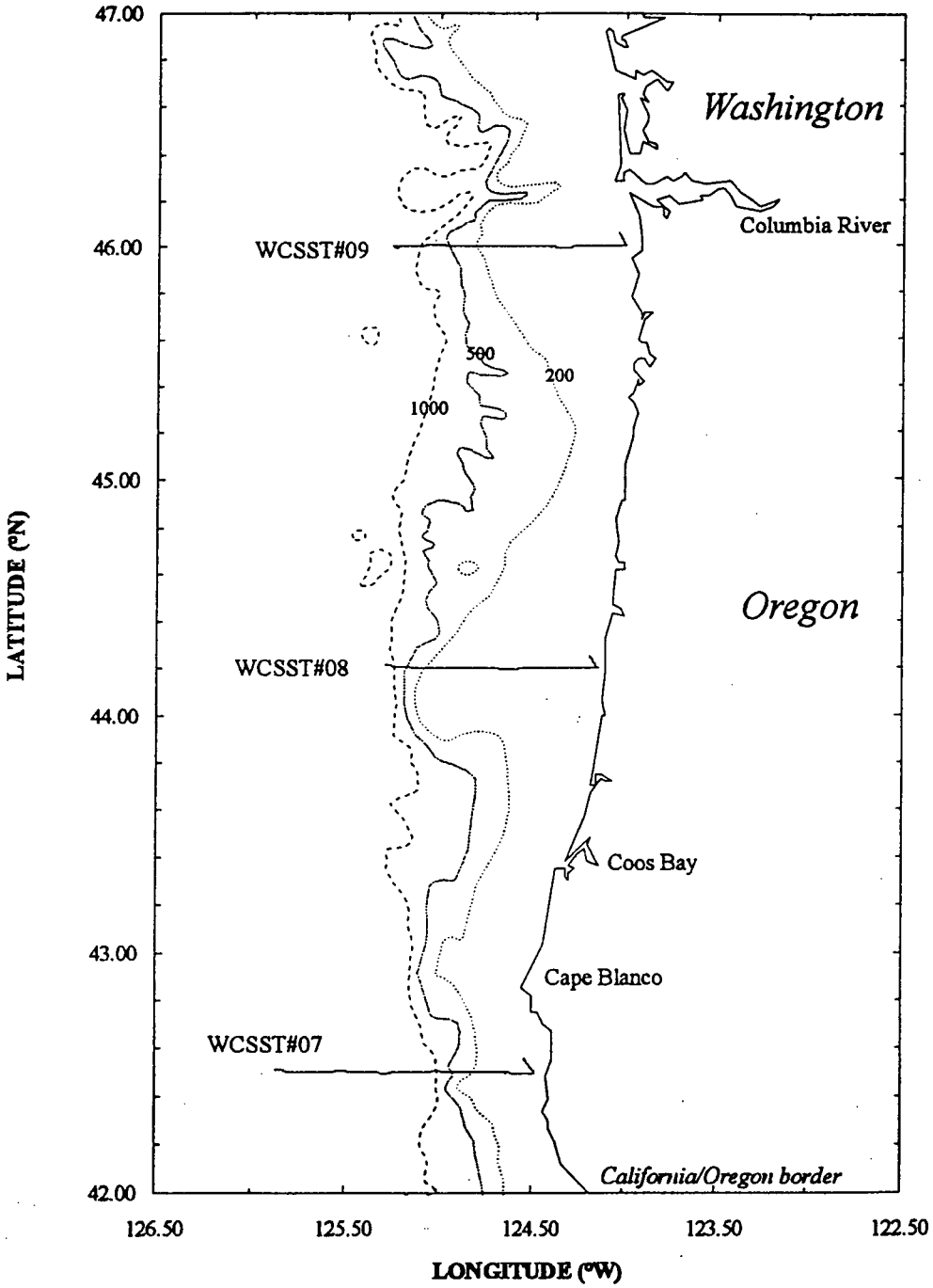

Figure 3.1.2.1 Study area depicting transects influenced by the Columbia River effluent. Isobaths are in meters.

3.2 Results and Discussion

Locations, temperature, salinity and trace metal data for transects WCSST#07, #08, #09 and #03 can be found in appendix 1.

3.2.1 Temperature and Salinity

The temperature and salinity data, presented in figure 3.2.1.1, clearly reveal the presence of the Columbia River plume in all three transects. The 'core' of the plume (i.e. water with the lowest salinity: S~21) is found, as expected, nearest to the estuary (WCSST#09). It can be easily followed, progressively mixing with surrounding water, as it travels south. At WCSST#08, the core is farther offshore and its salinity has increased to 27-28. By the time it has reached WCSST#07, the plume has diffused considerably and almost entirely spans the studied transect.

On the edges of the core, salinities increase to the low 30's. Historically, Columbia River plume water is defined as water with a salinity of less than 32.5[3]. According to this definition, with the exception of the high salinity-low temperature water mass closest to the coast at WCSST#08, what seems to be oceanic water in comparison to the core is still considered plume water, albeit measurably diluted. The high salinity-temperature signature of the near-shore water at WCSST#08 is characteristic of upwelled water and will be discussed in chapter 4.

Oddly enough, the plume at WCSST#07 is fresher (S~26) than the plume at WCSST#08 (S~27-28). There could be two possible explanations for this. Surface waters off southern Oregon (WCSST#07) may be affected by other tributaries, such as the Rogue or Umpqua rivers. It is questionable however whether the output from these rivers is large enough to significantly modify the characteristics of the waters they discharge into. Alternatively, strong local wind events or storms a few days prior to sampling could have mixed the plume at WCSST#08 more deeply with underlying water than at WCSST#07. If this were true, one would expect the temperatures to decrease as well. This is not the case here although surface temperatures may vary somewhat as a result of differences in local warming. In any case, CTD profiles obtained within the plume at both transects (appendix 2) do not support this hypothesis. For both transects, the mixed layer is very similar (~6-10 meters deep) therefore the plume did not appear to be mixing deeper at one transect than at the other. The only remaining explanation is that the plumes sampled at WCSST#08 and #07 acquired different salinities earlier on. Whether this occurred at the river's mouth or along the way remains unknown.

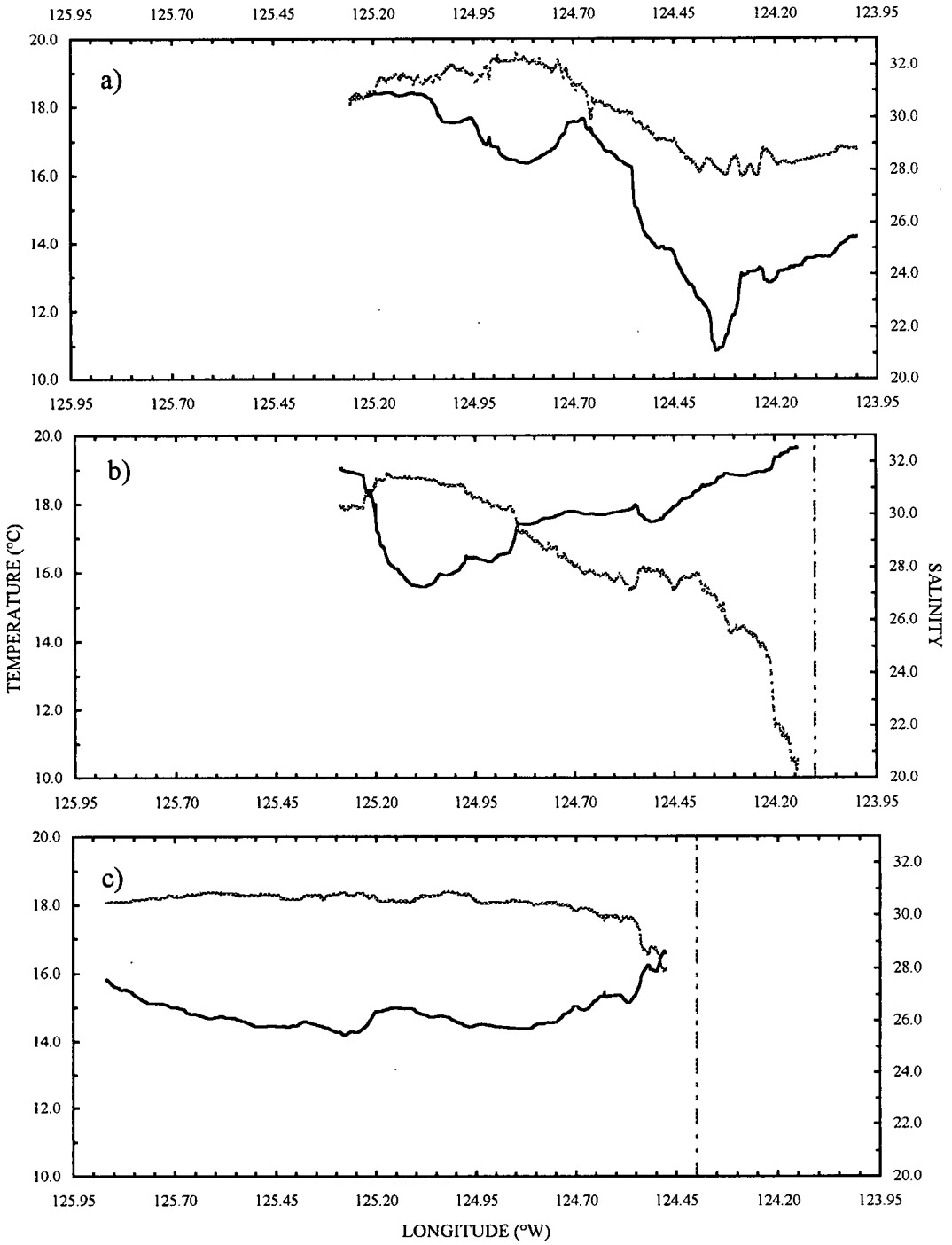

Figure 3.2.1.1 Temperature and salinity data for a) WCSST#09 b) #08 and c) #07. (Legend: Solid line = Salinity; Broken line = Temperature; Dashed line = coastline).

Temperature is not a conservative tracer in these three transects. As the river plume ages, i.e. as it travels southward, it warms up even though it is presumably mixing with colder oceanic water. This is due to the lack of winds during the summer in question. Calm seas inhibited vertical mixing of the surface waters resulting in a thin widely spread layer of fresher Columbia River effluent overlying denser oceanic water. This thin layer was subjected to considerable warming as it traveled hence salinity is a better indicator of what is actually happening at this particular location during this particular year.

There is one very curious feature present at WCSST#09. A patch of water, similar in salinity (S~28) to the plume core at WCSST#08 but warmer (T~19.5°C), is seen offshore centered at approximately 124.80°W. From these characteristics, it seems this might consist of a 'tongue' or 'eddy' of the plume that separated from the main body of the plume, possibly travelling south then turning north, mixing and warming somewhat over time. Investigations of temperature and salinity of waters at WCSST#10 (off Washington's Olympic Peninsula; figure 3.2.1.2) reveal no possible water source which could contribute to this feature from the north. This anomaly will be discussed further and will here on be referred to as the secondary plume.

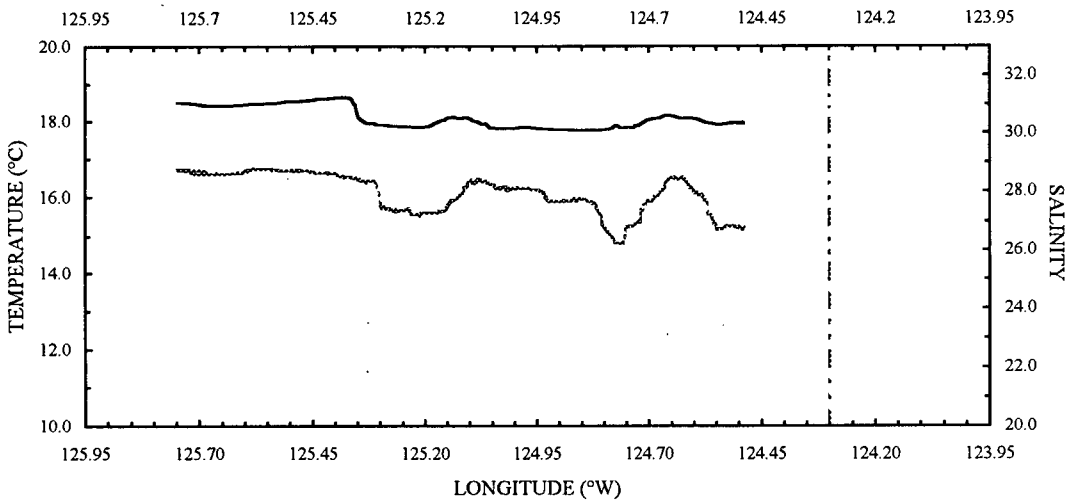

Figure 3.2.1.2 Temperature and salinity data for WCSST#10. (Legend: Solid line = Salinity; Broken line = Temperature; Dashed line = Coastline).

3.2.2 Nutrients and Chlorophyll a

Silicic acid, which results from the weathering of rock, is an impressive tracer of the Columbia River plume (figure 3.2.2.1). Maximum concentrations (~41μM) are observed in the core of the plume at WCSST#09. Silicic acid levels decrease as the plume travels and mixes, becoming quite diffuse by the time it reaches WCSST#07. Similar concentrations for both WCSST#07 and #08 indicate either enhanced mixing at WCSST#08 with the underlying silicic acid-poor oceanic waters or an additional source of silicic acid at WCSST#07. Since the water just below the plume is thought to be CCS surface water characterized by low nutrients, the former explanation is more likely.

Lack of silicic acid data in the center of the secondary plume prevents an accurate estimate of this water's age or origin by comparison with the main plumes in the other transects. Values on either side of the salinity minimum however imply a slight rise indicating this is possibly a older feature whose silicic acid content has been considerably depleted by biological activity.

Slightly elevated levels of nitrate up to 3μM are detected only in the freshest river water (figure 3.2.2.1). Rivers, unless they are heavily impacted by human activity, are not usually strong sources of nitrate. In fact, the nitrate signature observed in the Columbia River plume is more likely the result of river-induced upwelling (entrainment) of nutrient-rich shelf bottom waters in the low reaches of the estuary. What little nitrate that is present is rapidly mixed and/or consumed beyond detection at WCSST#07 & #08 and in the secondary plume at WCSST#09.

Close to shore at WCSST#08, a high salinity low temperature water mass containing high nitrate (~13μM) and silicic acid (~16μM) confirms upwelling of shelf bottom waters at the time of sampling. This upwelling event was probably already a few days old as chlorophyll a (figure 3.2.2.2) was detectable (~3μg/L); more details will be provided in chapter 4.

At WCSST#09, the continuous source of nutrients supplies and maintains a larger bloom. From the absence of chlorophyll a in the secondary plume, either nitrate-limitation prevented a bloom from taking place or else one had already come and gone by the time the samples were collected.

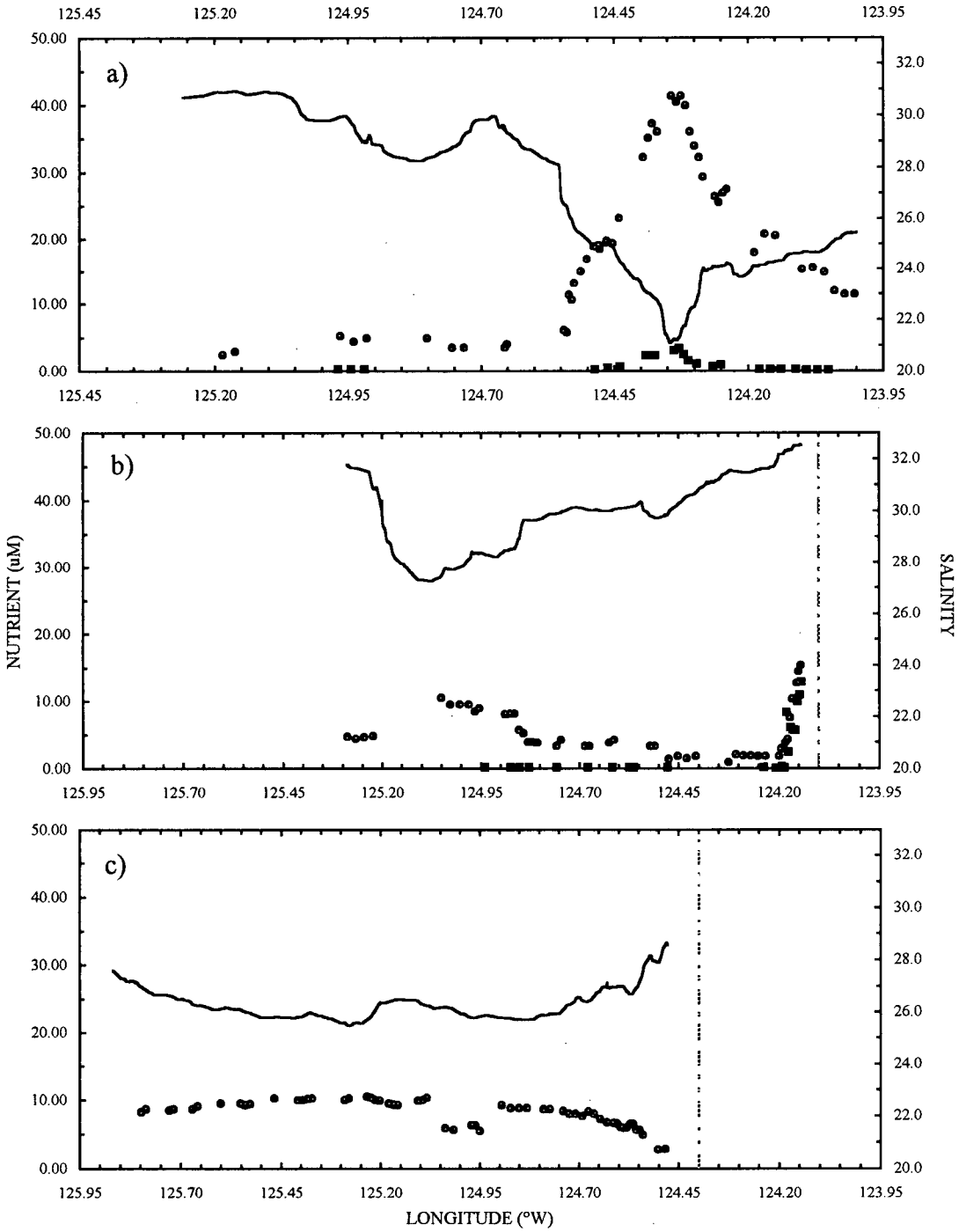

Figure 3.2.2.1 Nutrient data for a) WCSST#09 b) #08 and c) #07. (Legend: Solid line = Salinity; Dashed line = Coastline; ▪ = Nitrate; • = Silicic acid). No flowthrough data available for nitrate at WCSST#07.

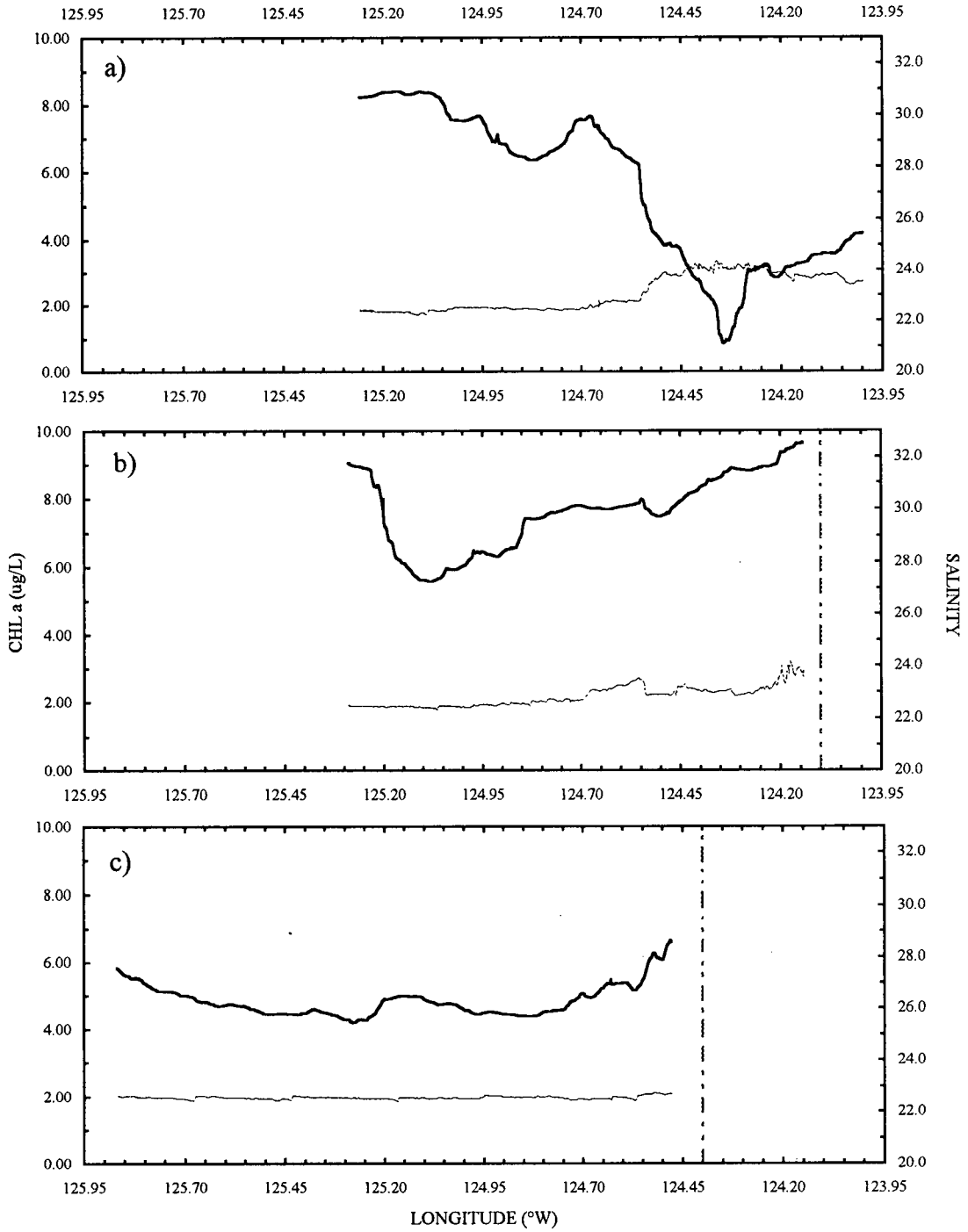

Figure 3.2.2.2 Chlorophyll a data for a) WCSST#09 b) #08 and c) #07. (Legend: Solid line = Salinity; Dashed line = Coastline; - = Chl a).

3.2.3 Trace Metals

Although the data for In is presented, it will not be discussed in great detail since it is suspected of being highly contaminated by tin. Suffice to say that the distributions of In/Sn (figure 3.2.3.1) show very little variability even though the environment sampled is known to be undergoing major changes in temperature and salinity. Either In and Sn are both featureless in a coastal regime influenced by a river or else as one is increasing, the other is counteracting the effect by decreasing. Both cases are quite unlikely as Sn is usually delivered to the oceans by way of anthropogenic activity and therefore should show some signature in coastal environments. In summary, the In distributions presented here may not be accurate.

On the other hand, Ga, Zr (figure 3.2.3.2) and Hf (figure 3.2.3.3) show similar behavior in all 3 transects. Concentrations are high ([Ga]=49pM; [Zr]=86pM; [Hf]=6pM) in the freshest plume water (WCSST#09). Maxima are also observed for Ga and Zr (72pM and 65pM, respectively) in the secondary plume. For Ga, this maximum exceeds that of the main plume. In contrast, Hf is quite low in the secondary plume (<1pM).

At WCSST#08, concentrations of Ga and Zr are once again highest in the center of the plume but approximately 50% lower in comparison to WCSST#09. Towards the coast, Ga remains constant whereas Zr increases steadily to a maximum (53pM) closest to shore in the upwelling region. Hf values have dropped considerably and are fairly constant across the entire transect except for 2 unusually high measurements (2.9pM) which will be discussed shortly.

At WCSST#07, both Ga and Zr are quite uniform across the entire transect (~30 and ~50pM, respectively), although Ga decreases slightly towards the coast (18pM). Concentrations for both elements are slightly higher than at WCSST#08. Hf values are similar to WCSST#08 with the exception again of two anomalous points (3.2 and 2.7pM).

High concentrations in the Columbia River plume imply that Ga, Zr and Hf are supplied to the waters off the coast of Washington and Oregon via the Columbia River. As the plume travels south and mixes, it retains its Ga and Zr signature as far as southern Oregon (WCSST#07) while the Hf signature seems to have been lost between WCSST#09 and #08. Because of the inconsistencies in the WCSST#07 and #08 Hf distributions however, it is difficult to make any definite conclusions. The 4 high Hf data points (2 in WCSST#07 and 2 in WCSST#08) could be the result of contamination during sampling or sample preparation. But contamination of Hf is usually accompanied by Zr contamination which does not seem to be the case. If, however, in a similar manner to Ga and Zr, approximately 50% of the Hf main plume signal was lost by the time WCSST#08 was reached, the 2 high values at WCSST#08 would make sense. Since Ga and Zr concentrations were slightly higher at WCSST#07 than at WCSST#08, the two Hf

"anomalies" at WCSST#07 would also fall in the expected range. This line of reasoning would imply that the remaining data points at WCSST#07 and #08 (16 values in total) would be wrong: a questionable assumption. Looking back to the trace metal results for WCSST#09, the Hf distribution would be identical to Ga and Zr were it not for the minimum in the secondary plume and perhaps the value closest to shore. Yet, it is a major coincidence that these two values are similar in concentrations to all the low Hf values in the other transects and are quite featureless while the questionably high values show some believable oceanographic behavior. Therefore, while the author believes the higher values to be more accurate than the low values, this remains to be seen. In light of the experimental difficulties associated with the analysis of this element (low recoveries, analytical signals limited by blanks and instrumental detection limits despite ~1000-fold concentration factors), any Hf interpretation is highly inconclusive.

The Ga and Zr maxima observed in the secondary plume are a surprise. Hydroxide-dominated elements are known to be quite reactive and sensitive to particle scavenging. Hence, if this low salinity-high temperature feature is indeed an isolated 'tongue' of the main plume, or an older remnant of the plume, one would expect the metal concentrations to be lower in the 'older' secondary plume than in the 'younger' main plume. This might be the case for Zr but not for Ga, thus an additional source of Ga is implied. This said feature could be the result of the mixing of two water masses, namely the Columbia River plume water and another Ga-rich water mass. Orians and Bruland[4,5], who studied Ga extensively in the Northern Pacific, found Ga concentrations in CCS surface waters to be highest away from coasts or productive waters; even then the levels they observed barely reached 20pM. Hence, the only water mass likely to contain these high levels of Ga in the near surroundings is the Columbia River itself. The properties of surface waters immediately seaward of the mouths of large rivers are subject to rapid change in response to natural variations in river discharge and river water quality. For the Columbia River, these variations may be seasonal as a result of melting snows in the high headwaters or they may be short-term as brought about by brief periods of high rainfall and runoff separated by drier periods. Consequently, it should not be surprising that the secondary plume may be a remnant of an earlier plume of considerably different composition.

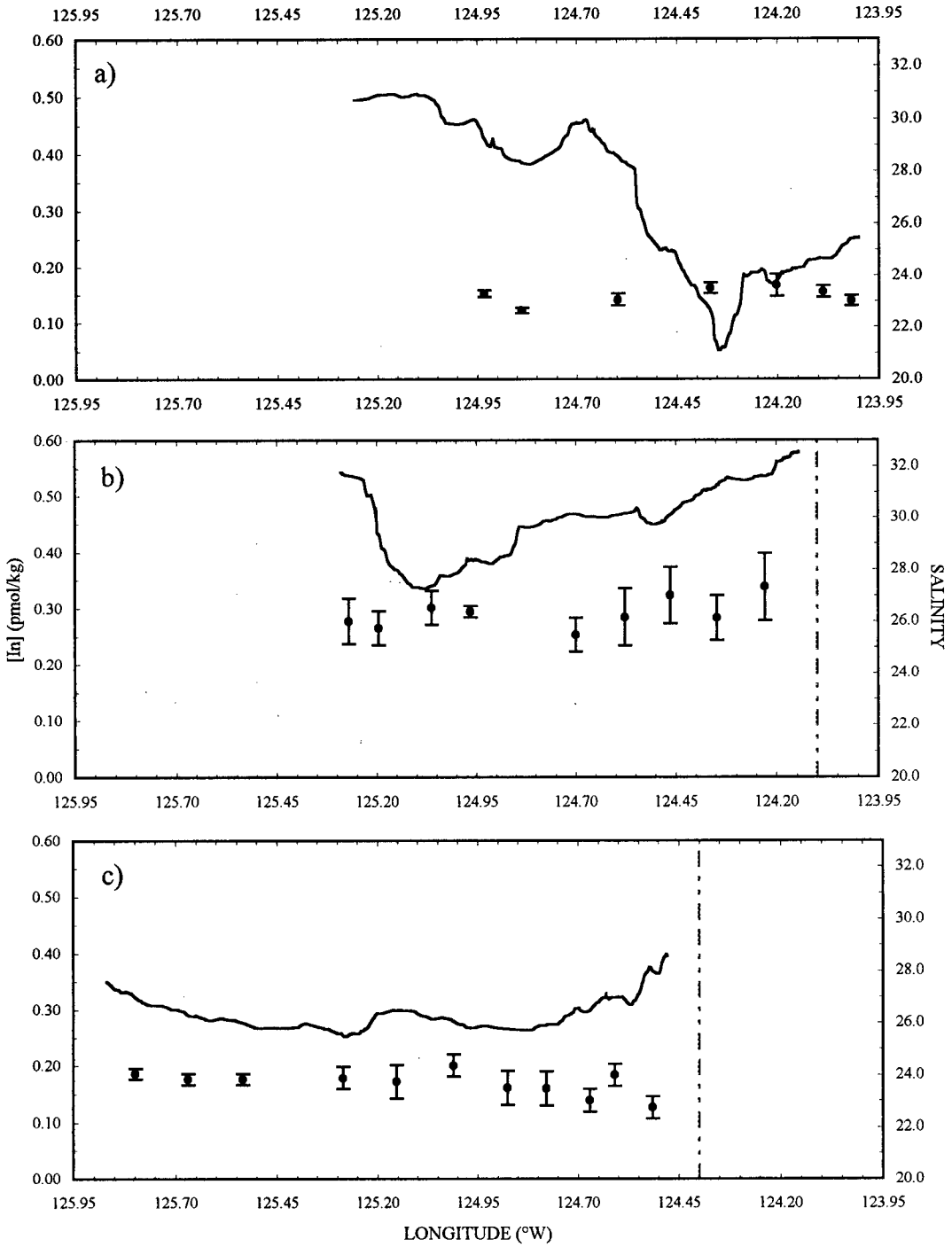

Figure 3.2.3.1 In data for a) WCSST#09 b) #08 and c)#07. (Legend: Solid line = Salinity; Dashed line = Coastline; ● = In).

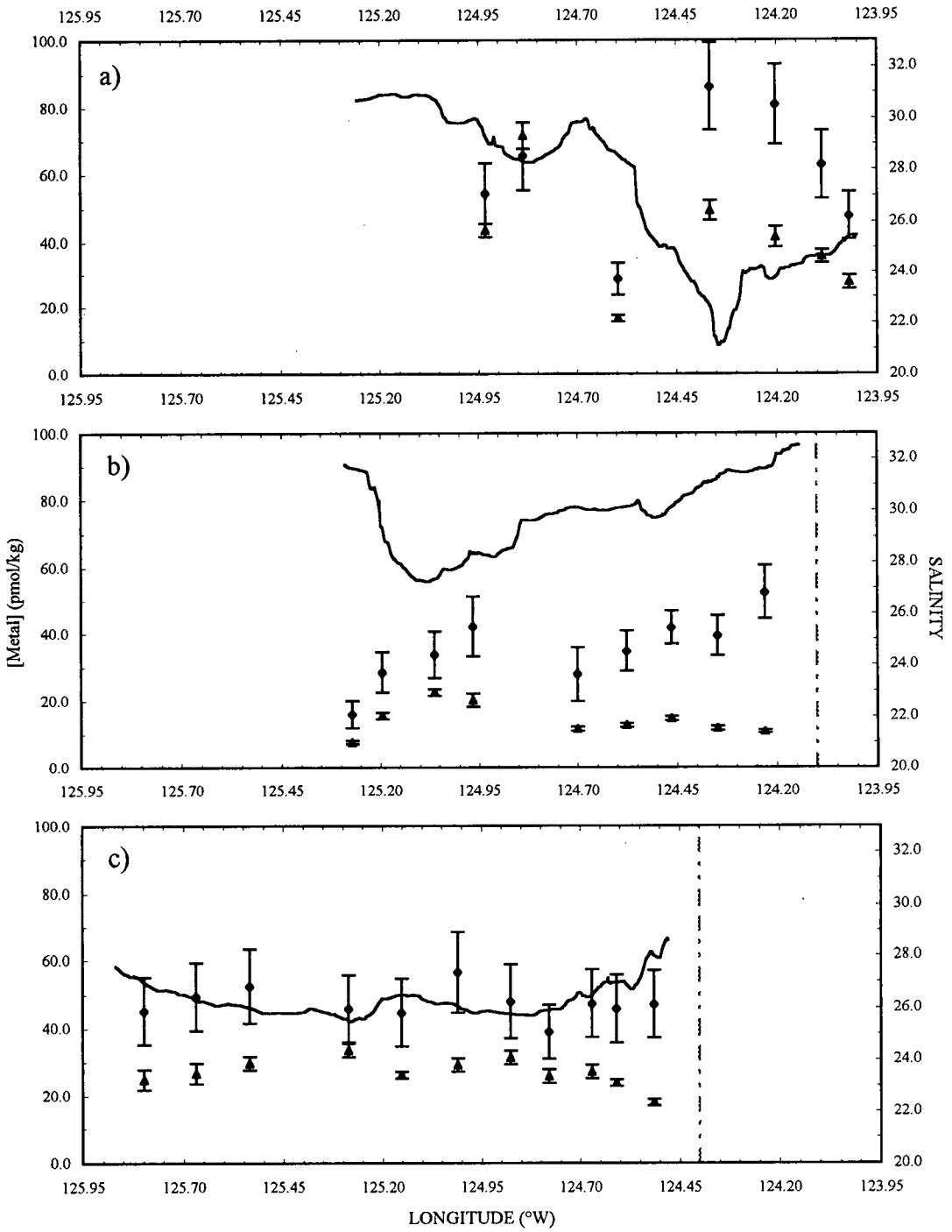

Figure 3.2.3.2 Ga and Zr data for a) WCSST#09 b) #08 and c) #07. (Legend: Solid line = Salinity; Dashed line = Coastline; ▲ = Ga; ◆ = Zr).

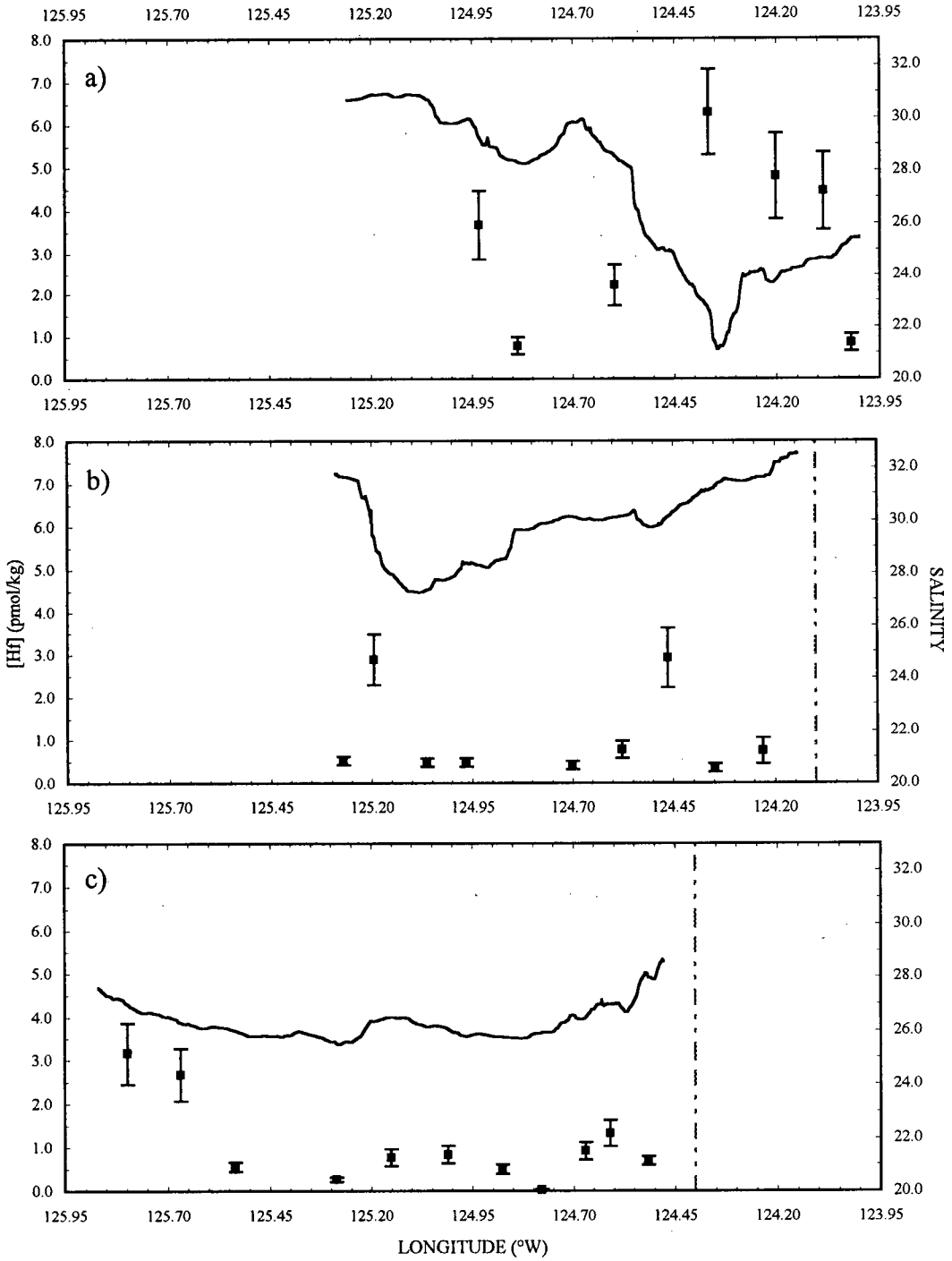

Figure 3.2.3.3 Hf data for a) WCSST#09 b) #08 and c) #07. (Legend: Solid line = Salinity; Dashed line = Coastline; ■ = Hf).

3.2.4 Metal/Salinity Diagrams

Metal/salinity diagrams for silicic acid, Ga and Zr were constructed using the data from transects WCSST#07, #08 and #09. The data from the upwelled waters near the coast of WCSST#08 were not used as they would violate the two dimensional model by introducing a third end-member.

Silicic acid has been shown to display conservative behavior in many estuaries[6-8]. The results from this study (figure 3.2.4.1) demonstrate that in waters of salinity below 24, silicic acid seems to be mixing conservatively, whereas removal is observed above 24. In some earlier works on silicic acid behavior in estuaries, apparent non-conservative behavioral mixing was later attributed to the presence of a third end-member[6]. When the proper end-members were chosen, conservative behavior was observed instead. The data shown below may also suggest two conservative mixing lines (one from S=21 to S=26, the other from S=26 to S=31), with a third end-member at S=26. Although this is theoretically possible, with the exception of the silicic acid-rich upwelled waters which were not even included in this plot, it is unlikely that any other source of silicic acid exists in this regime and the observed removal is true. In any case, non-conservative mixing is expected in continental shelf waters and certainly in the area studied here, where the time scale of mixing is likely to be slower than the rate of removal.

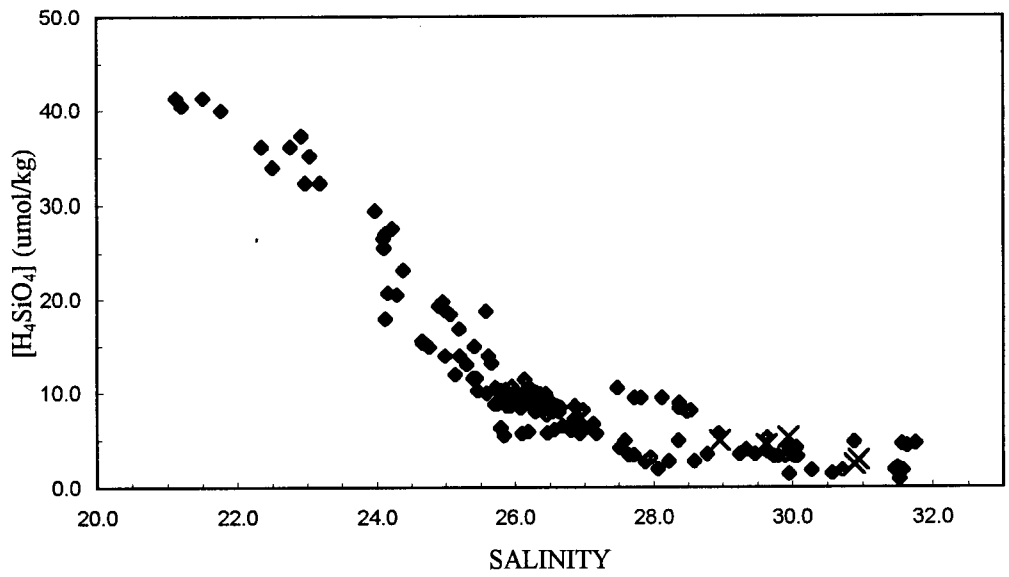

Figure 3.2.4.1 Silicic acid vs. salinity plot for transects WCSST#09, #08 and #07. "X" symbols represent secondary plume data. Data from the upwelling region near shore at WCSST#08 are not included.

Removal is also occurring for Ga and Zr (figure 3.2.4.2), although to a lesser extent than silicic acid. There are not enough data points in the river end-member to determine if removal is happening throughout the entire salinity range studied or simply above 24, as seen for silicic acid. In any case, removal may occur via two processes: particle scavenging and/or biological uptake.

Particle scavenging is often intensified in highly productive regions such as coastal waters. The large particulate fluxes generated by phytoplankton blooms provide adsorption sites for particle-reactive species. This has been demonstrated for ^{234}Th by Coale and Bruland[9]. In the productive waters of the CCS, the scavenging rate of this hydroxide-dominated element was found to be directly correlated with primary productivity. Ga and Zr, like ^{234}Th, are also prone to scavenging. In fact, Orians and Bruland[5] have previously observed that Ga removal was intensified in the productive coastal waters of the CCS, probably as a result of scavenging onto biogenic particles. Hence, it is quite possible that following the onset of a bloom, Ga and Zr are passively adsorbed onto biogenic particles.

Ga is also suspected of partaking somewhat in biological activity. There is some evidence to suggest that Ga may be competing with Fe for iron-binding siderophores. Studies by Emery and Hoffer[10] have revealed that Ga(III) is easily incorporated into the Fe(III) transport system of both mammals and microorganisms. Although this has never been verified for marine phytoplankton, Orians and Bruland[4,5] considered active biological uptake as a possible means of explaining persistent mid-depth Ga maxima observed throughout the North Pacific. They attributed these features to the regeneration at shallow depths of Ga from a solid phase, possibly in association with biological soft tissue.

The vertical distribution of Zr, in its similarity to silicic acid, has occasionally resulted in its categorization as a nutrient-type element. The lack of a nutrient-type Zr interocean fractionation however leads to the conclusion that even though similarities in the vertical distributions of Zr and silicic acid exist, the processes controlling these distributions are different. Nevertheless, McKelvey[11] observed a linear correlation between Zr and silicic acid in the productive surface waters of the North Pacific, whereas Godfrey et al.[12] detected a even stronger correlation with nitrate in the Northeastern Atlantic.

In sum, both active and passive biological uptake are plausible mechanisms to account for Ga and Zr losses in the Columbia River plume and a combination of the two is not unlikely.

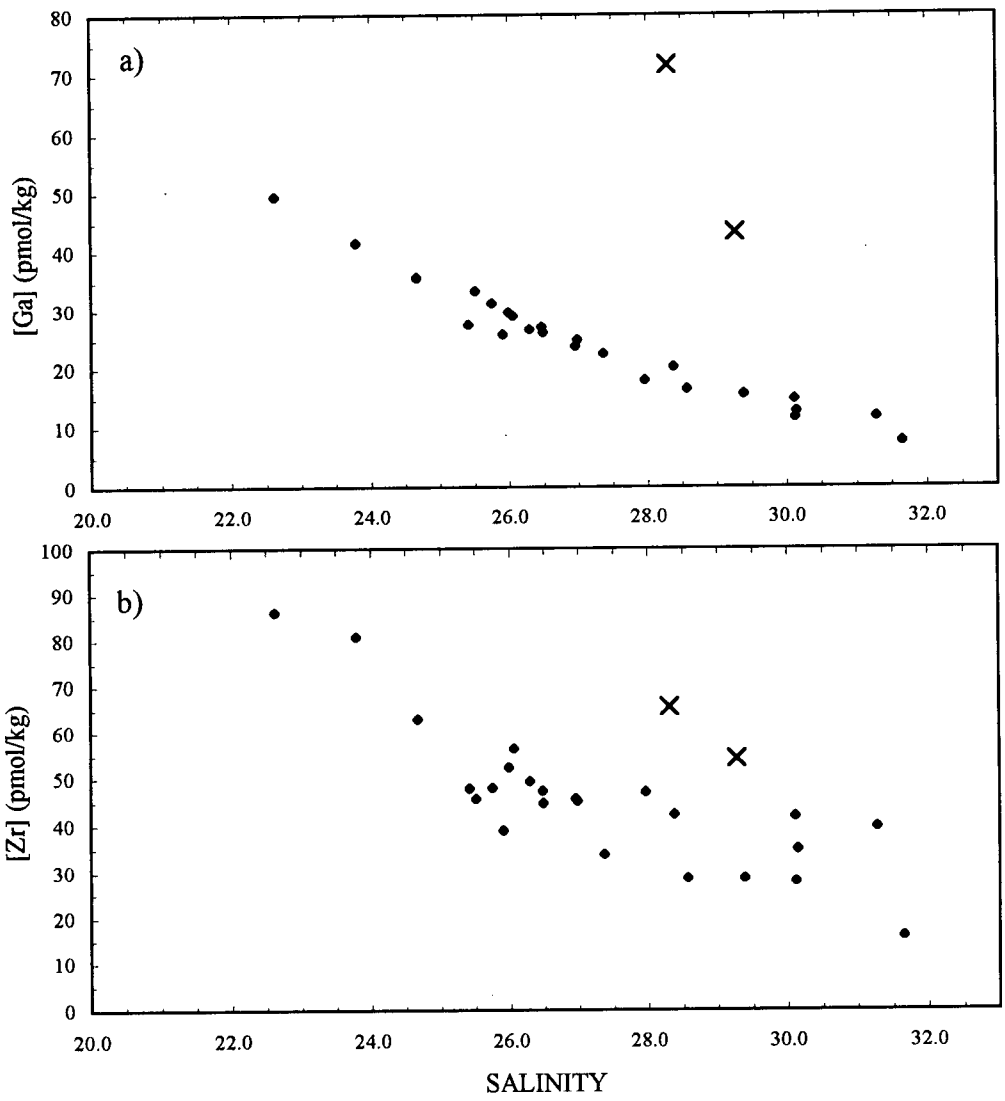

Figure 3.2.4.2 a) Gallium and b) Zirconium vs. salinity plots for transects WCSST#09, #08 and #07. "X" symbols represent secondary plume data. Data from upwelling region near shore at WCSST#08 are not included.

Other often-used informative parameters derived from metal/salinity diagrams are the original river concentration (obtained from extrapolating the conservative mixing line back to zero salinity) and the effective river concentration (obtained from the intersection at zero salinity of the tangent of the metal concentrations at high salinities). This approach for determining the effective river concentration was introduced by Boyle et al.[6] and has since been used frequently to construct realistic mass balances for estuaries as well as to estimate fluxes to the open ocean[13-15].

Original and effective river concentration estimates were determined for silicic acid (figure 3.2.4.3), Ga (figure 3.2.4.4) and Zr (figure 3.2.4.5). The secondary plume data were not considered in any regression analysis. The conservative mixing lines were obtained by simple linear regressions between river (S<24) and ocean (S>31) end-members. The effective river concentrations were determined by linear regressions of all the data of salinities above 27. Admittedly, these are very simplistic exercises as only a very limited range of salinities is used to characterize the entire river-ocean mixing regime. Still, general conclusions can be formulated and preliminary measurements obtained from the Columbia River to be compared with other rivers.

More data points in the low salinity region would have allowed more accurate mixing lines to be obtained. Nevertheless, original river concentrations for silicic acid, Ga and Zr were found to be 119±4μM, 150±30pM and 240±150pM, respectively, whereas the effective river concentrations were 30±10μM, 100±30pM and 120±140pM (errors represent 95% confidence interval calculated from the standard deviation of the intercept). It would appear as though silicic acid is removed much faster that Ga and Zr in the mixing area under study. Only ~27% (effective river concentration divided by the original river concentration) of the silicic acid from the original plume core at WCSST#09 remains in the mixed waters, in contrast to ~70% and ~50% for Ga and Zr, respectively. Whereas 30% removal for Ga is probably a reasonable estimate, this is not necessarily the case for Zr as the data show more scatter, thus generating greater uncertainty. Consequently, although it may seem as if Zr is removed faster than Ga, the difference in removal between the two elements is insignificant considering the uncertainties associated with these estimates.

Estimates of river water concentrations based on extrapolation of metal-salinity relations to zero salinity using limited salinity ranges (S~30-35) were conducted in other coastal regimes[13,16,17] although in these cases the metal/salinity relationships were conservative. Because of the limited amount of data in this study along with the non-conservative behavior of silicic acid, Ga and Zr, the extrapolated river water concentrations at zero salinity are very rough

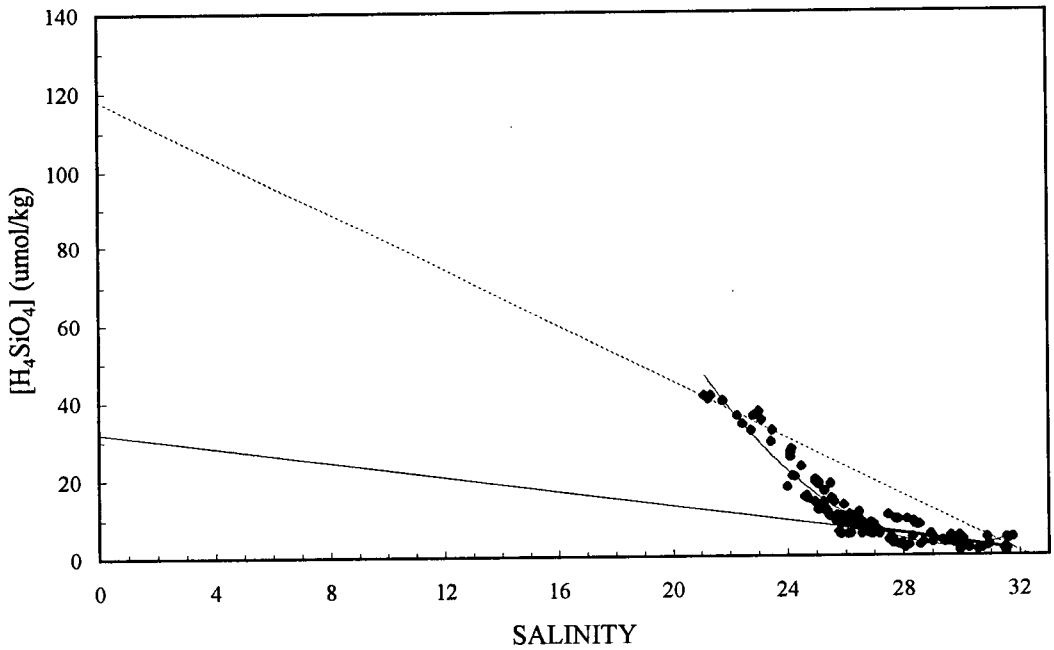

Figure 3.2.4.3 Silicic acid vs. salinity plot of data from transects WCSST#09, #08 and #07 used to extrapolate the original and effective silicic acid river concentrations of the Columbia River. The original river concentration is obtained from extrapolation of the conservative mixing line back to zero salinity. The conservative mixing line (dashed line) is obtained by a simple linear regression between river (S<24) and ocean (S>31) end-members. The effective river concentration is obtained from the intersection at zero salinity of the tangent of the metal (solid line) concentrations at high salinities, which reciprocally is obtained by linear regression of all the data of salinities above 27. Curved line is a second order polynomial best fit (R^2=0.9121) of all data except those from the secondary plume (not shown).

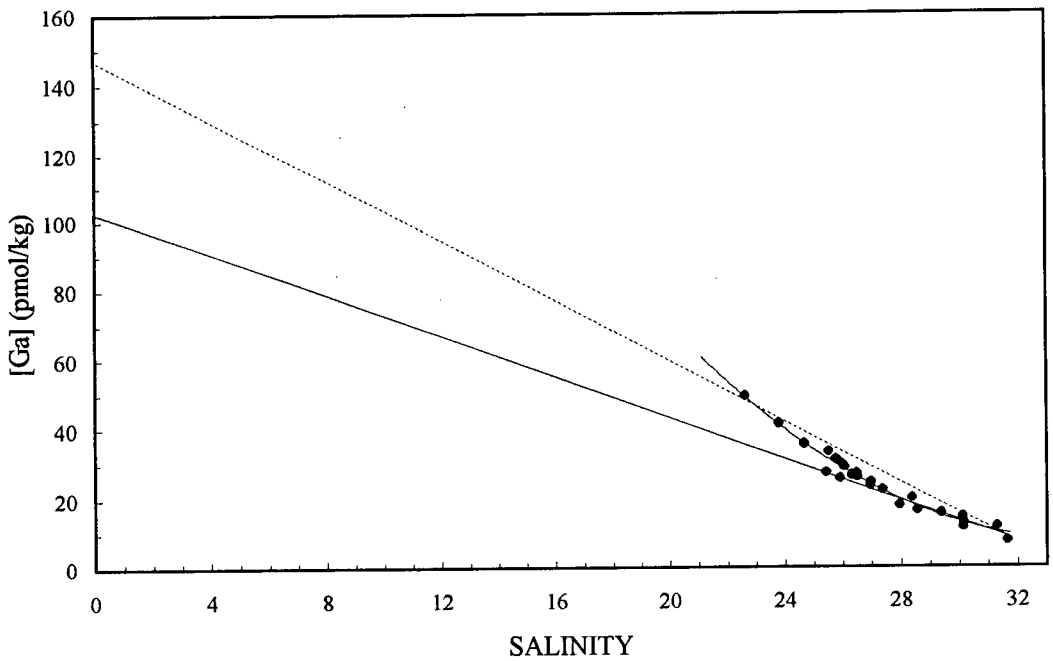

Figure 3.2.4.4 Gallium vs. salinity plot of data from transects WCSST#09, #08 and #07 used to extrapolate the original and effective silicic acid river concentrations of the Columbia River. The original river concentration is obtained from extrapolation of the conservative mixing line back to zero salinity. The conservative mixing line (dashed line) is obtained by a simple linear regression between river (S<24) and ocean (S>31) end-members. The effective river concentration is obtained from the intersection at zero salinity of the tangent (solid line) of the metal concentrations at high salinities which reciprocally is obtained by linear regression of all the data of salinities above 27. Curved line is a second order polynomial best fit (R^2=0.9743) of all data except those from the secondary plume (not shown).

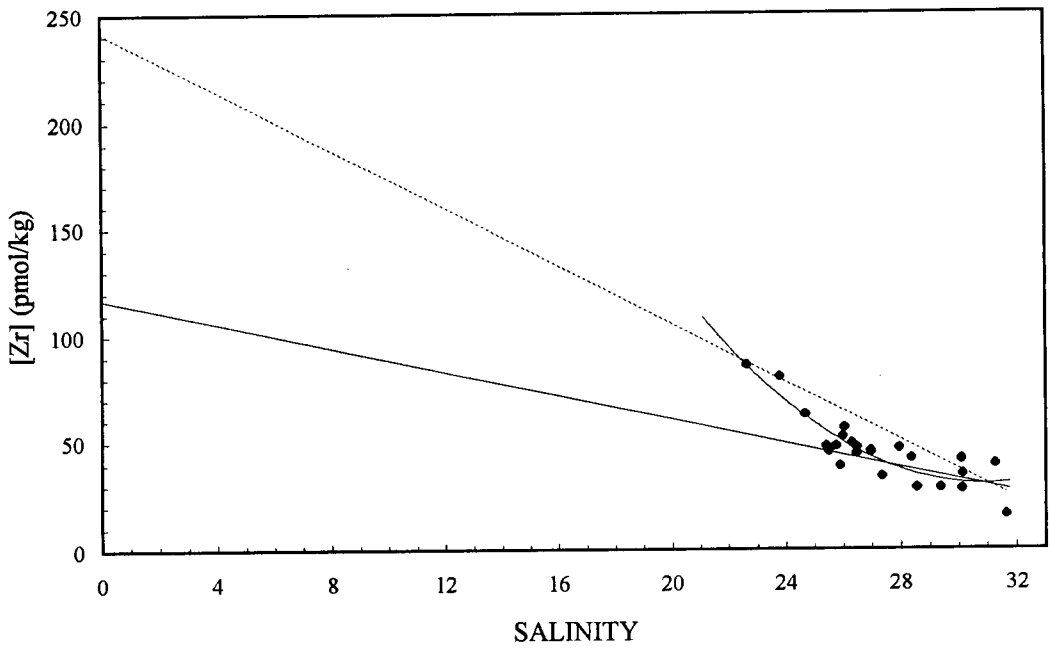

Figure 3.2.4.5 Zirconium vs. salinity plot of data from transects WCSST#09, #08 and #07 used to extrapolate the original and effective silicic acid river concentrations of the Columbia River. The original river concentration is obtained from extrapolation of the conservative mixing line back to zero salinity. The conservative mixing line (dashed line) is obtained by a simple linear regression between river (S<24) and ocean (S>31) end-members. The effective river concentration is obtained from the intersection at zero salinity of the tangent (solid line) of the metal concentrations at high salinities which reciprocally is obtained by linear regression of all the data of salinities above 27. Curved line is a second order polynomial best fit (R^2=0.7975) of all data except those from the secondary plume (not shown).

estimates. Indeed for Ga it seems as though the waters used to estimate the river end-member could themselves be undergoing removal, in which case the conservative mixing line would be largely underestimated. For Zr, the river end-member values seem to mix conservatively although with only 2 data points this is not definitive. For silicic acid, it is clear that the river plume is mixing conservatively up to salinities of 23-24 therefore the interpolated river concentrations are probably more accurate. Using an annual river discharge of $7300 m^3/s$, this works out to $(2.6\text{-}2.8)\times10^{10}$ mol/yr of silicic acid. This is in reasonable agreement with annual Columbia River silicic acid fluxes for five different time periods between 1966 and 1981 which averaged $\sim4.2\times10^{10}$mol [ref.18].

For Ga and Zr, it is more likely that the extrapolated river concentrations are a minimum estimate of the concentration delivered by the Columbia River. This Ga estimate of 150±30pM is similar to Ga values from 5 eastern American rivers reported by Shiller[19] (68 to 250pM). Zr levels in the Columbia River according to these data are at least 240±150pM. Godfrey et al.[12], found Zr levels in 8 major rivers to range from 300pM to as high as 1834pM. The estimate of minimum Zr concentration obtained for the Columbia, 240pM, is not very far from their lowest value and overlaps this range when the error is considered.

One must be very careful when applying this type of model. One of the limits of these plots which often leads to erroneous conclusions is that variations in fluvial concentrations over the time scale of the dilution process can lead to curved property-salinity plots even when the estuarine behavior is conservative[20]. Thus for the standard model to be valid, temporal variations of constituent concentrations in end-members (river and ocean) need to be smaller than the estuary's flushing time (defined as the time required for river flow to replace the existing fresh water in the estuary.) It is not unusual for industrialized rivers, or any other river for that matter, to have constituent concentrations that are quite variable. Since the basin we are monitoring is much larger than any typical estuary, it is very possible the flushing time may be longer than the temporal variability of the river end-member. In fact, the secondary plume has already revealed how variable in composition the river outflow may be. Thus, the relationships observed for Ga and Zr vs. salinity could be due to variations in the river end-member rather than removal with actual conservative behavior occurring in the mixing zone. Without knowledge of the variability of river properties and flow, flushing time of the studied area and changes in ocean end-member properties, definitive conclusions are not possible. Yet, the reasonable agreement between the silicic acid flux estimate in this study and that previously reported lends some credibility to the models presented here.

3.3 The San Francisco Bay Effluent

The Sacramento-San Joaquin River system in central California constitutes another potential source of freshwater to coastal waters of North America's west coast. In contrast to the Columbia River, these rivers do not empty directly into the ocean, but in the largest estuarine system in the Northeast Pacific: San Francisco Bay. The Bay's shallow bathymetry (~5m) combined with a tidal prism of ~24% of the Bay volume and a tidal excursion of ~10km result in a well-mixed vertical water column over most of the estuary. For this reason, effluent from San Francisco Bay is much saltier the Columbia River effluent. It is also a heavily impacted environment, with billions of liters of waste waters from municipal waste treatment plants and industrial facilities released in the estuary on a daily basis. Between 4500 and 36000 metric tons of toxic pollutants enter the estuary with these discharges[21]. Thus the effluent is not only saltier in comparison to the Columbia, it is also considerably different in chemical composition. Trace metal studies of the Bay and adjacent coastal waters have focused mainly on Cu, Cd, Ni, Zn[8,17,22] and Se[23].

A look at temperature and salinity data (figure 3.3.1a) from WCSST#3 (~30-60km south-southwest of the Golden Gate bridge) reveal 5 distinct regimes. Regimes #1 (nearshore-122.55°W), #3 (122.70°-122.95°W) and #5 (123.13°W-offshore) with their high salinities (>33) and low temperatures (~10.5-11.5°C) indicate probable upwelling events which will be discussed in the next chapter. Regimes #2 (122.55°-122.70°W) and #4 (122.95°-123.13°W) with their higher temperatures and moderate salinities (T~13-14°C; S~32.7-32.9) could be either San Francisco Bay effluent or CCS surface water; it is impossible to make the distinction between the two from temperature and salinity alone. It will become clear in the next paragraph dealing with nutrients that regime #2 is indeed outflow from San Francisco Bay while #4 is normal CCS surface water.

Although it is hard to discern next to the nutrient-rich upwelled waters closest to shore, there are definitely nitrate and silicic acid signals in regime#2 (figure 3.3.1b) confirming San Francisco Bay as the source of these waters. Nitrate (~20μM) in this regime is much higher than in the Columbia River; this is not unexpected coming from such an urbanized estuary which undoubtedly receives tons of fertilizers. Silicic acid (~32μM) is also considerably higher than Columbia River waters of comparable salinities, probably the result of an additional sedimentary input of biogenic silica[24]. Due to the availability of nutrients, a bloom was currently underway in the effluent at the time of sampling (figure 3.3.1c). In regime#4, the lack of either nitrate or silicic acid establishes this water mass as simply CCS surface water.

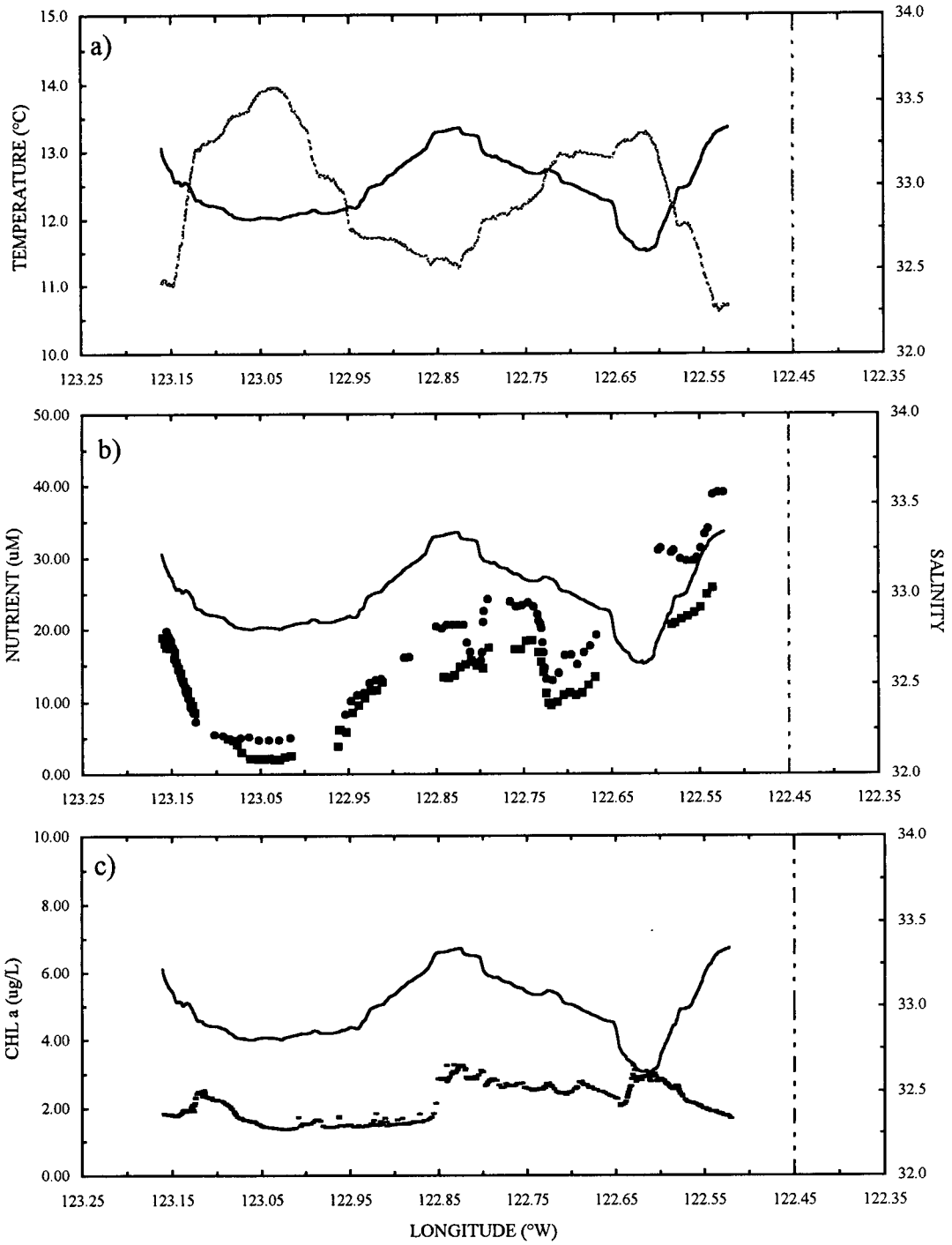

Figure 3.3.1 a) Temperature and salinity b) nutrient and c) chlorophyll a data for WCSST#03. (Legend: Solid line = Salinity; Broken line = Temperature; ▪ = Nitrate; • = Silicic acid; - = Chl a).

Ga (figure 3.3.2a) is the only trace metal of the 4 investigated that undoubtedly shows an effluent signal. The highest concentration of the entire transect (14pM) was measured in regime#2, while the lowest (~6pM) were from regime#4, confirming once more the identity of this water as normal CCS surface water. Indium (figure 3.3.2c) might also have small maxima in both regimes although whether this is an In or a Sn signal is not known. A tin signature would make sense though as it is a common pollutant.

Surprisingly, Zr (figure 3.3.2b) is quite featureless across the entire transect except for the slight increases in upwelled waters close to and farther offshore. Although there are no data points coinciding with the lowest salinity waters, the trends in the rest of the Zr data do not imply maximum values in regimes #2 and #4. A Hf (figure 3.3.3c) signal is absent from the Bay's effluent but the erratic outliers in the remainder of the transect create doubt as to the legitimacy of these measurements.

The similarities between Ga and Zr distributions in the Columbia River plume and the differences between them in the Bay effluent indicate the sources of these elements in the 2 regimes are different. Ga could have an anthropogenic source stemming from the semi-conductor industry or it could be released from the Bay's sediments. Alternatively, Zr may be preferentially or more rapidly removed from the surface layer by scavenging. This would comply with the Columbia River plume, where Zr was removed faster (or to a greater extent) than Ga.

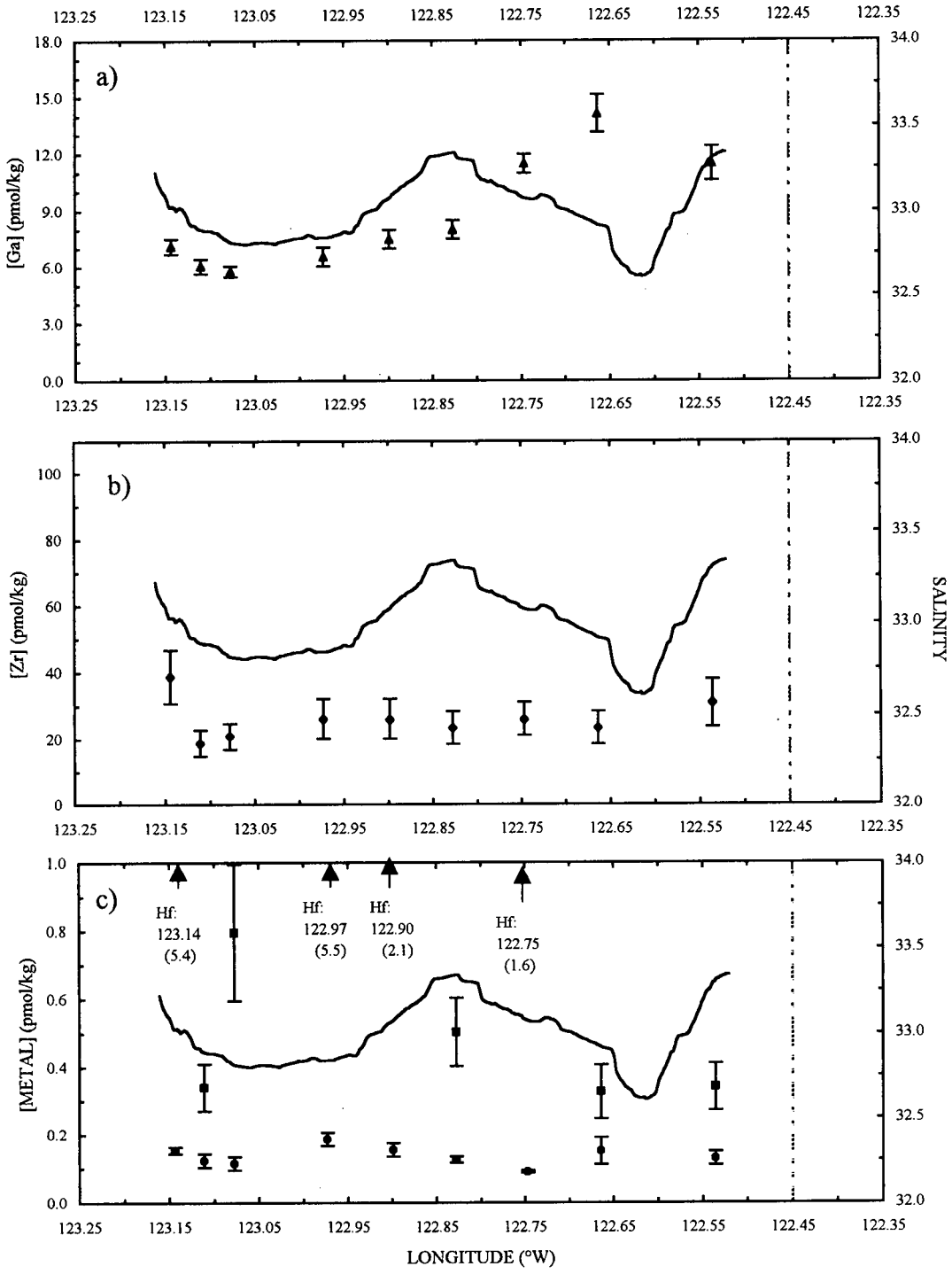

Figure 3.3.2 a) Ga b) Zr and c) In and Hf data for WCSST#03. (Legend: Solid line = Salinity; Dashed line = Coastline; ▲ = Ga; ◆ = Zr; ● = In; ■ = Hf).

3.4 Summary

The area investigated by the northernmost transects is clearly dominated by effluent from the Columbia River. With the exception of In, high levels of trace metals are supplied to coastal waters of Washington and Oregon via this effluent, with maximum values coinciding with the plume's core (S~21; [Ga]=49pM; [Zr]=86pM; [Hf]=6pM). Silicic acid, Ga and Zr act as tracers of the effluent, decreasing progressively as the plume travels southward and mixes under the influence of winds. Ga and Zr could even be detected in effluent-influenced waters of salinities of up to 30 (~12 and ~35pM, respectively).

Metal/salinity plots reveal that despite the presence of phytoplankton blooms in waters of salinities below 24, silicic acid demonstrates conservative mixing whereas above 24, non-conservative behavior implies active biological uptake. Ga and Zr are also removed as the plume mixes, although it is less obvious for Zr due to scatter in the data. Removal of these elements however is not unexpected, as both Ga and Zr have previously been linked to active and/or passive biological uptake mechanisms.

Extrapolation of a conservative mixing line between the two chosen end-members (S<24 and S>31) provided river concentration estimates to be compared with other rivers. The Ga content of 5 eastern American rivers ranged from 68 to 250pM while Zr from 8 major rivers varied between 300 and 1834pM. Minimum estimates for Ga concentrations (150±30pM) in the Columbia River were comparable with the other rivers whereas Zr concentrations (240±150pM) were at the low end of the reported range. Similar calculations for silicic acid yielded river concentration estimates of approximately 120μM which can be converted to an annual flux of ~2.8×10^{10}mol, a reasonable estimate when compared to previously reported values of 4.2×10^{10}mol.

Extrapolation to effective river concentrations from the metal/salinity plots provide preliminary estimates of removal rates of silicic acid, Ga and Zr. According to this study, silicic acid is removed the fastest (with only 27% of that originally present in the core remaining at WCSST#07), followed by Zr and Ga (with ~50-70% remaining).

One of the southern transects also intersected outflow from the San Francisco Bay. The effluent from this estuary, which is heavily impacted by anthropogenic activity, is expected to differ in composition to the Columbia River effluent. Of the four elements investigated, only Ga was observed in the Bay's effluent, indicating that sources and sinks of Ga and Zr in these two estuarine environments are different.

3.5 References

1) E.R. Sholkovitz (1978) The flocculation of dissolved Fe, Mn, Al, Cu, Ni, Co and Cd during estuarine mixing, *Earth and Planetary Science Letters*, **41**, 77-86.

2) A.T Pruter and D.L. Alverson (1972) The Columbia River estuary and adjacent ocean waters, University of Washington Press, Seattle, 868 pages.

3) C.A. Barnes, A.C. Duxbury, B-A. Morse, Circulation and selected properties of the Columbia river effluent at sea. In *The Columbia River estuary and adjacent ocean waters*, University of Washington Press, Seattle, 868 pages.

4) K.J. Orians, K.W. Bruland (1988) Dissolved gallium in the open ocean, *Nature*, **332**, 717-719.

5) K.J. Orians, K.W. Bruland (1988) The marine geochemistry of dissolved gallium: A comparison with dissolved aluminum, *Geochimica et Cosmochimica Acta*, **52**, 2955-2962.

6) E. Boyle, R. Collier, A.T. Dengler, J.M. Edmond, A.C. Ng, R.F. Stallard (1974) On the chemical mass-balance in estuaries, *Geochimica et Cosmochimica Acta*, **38**, 1719-1728.

7) A.M. Shiller, E.A. Boyle (1991) Trace elements in the Mississippi river delta outflow region: behavior at high discharge, *Geochimica et Cosmochimica Acta*, **55**, 3241-3251.

8) A.R. Flegal, G.J. Smith, G.A. Gill, S. Sañudo-Wilhelmy, L.C.D. Anderson (1991) Dissolved trace elements in the San Francisco Bay estuary, *Marine Chemistry*, **36**, 329-363.

9) K.H. Coale, K.W. Bruland (1985) ^{234}Th:^{238}U disequilibria within the California Current, *Limnology and Oceanography*, **30**, 22-33.

10) T. Emery, P.B. Hoffer (1980) Siderophore-meidated mechanism of gallium uptake demonstrated in the microorganism *Ustilago sphaerogena*, *Journal of Nuclear Medicine*, **21**, 935-939.

11) B.A. McKelvey (1993) The marine geochemistry of zirconium and hafnium, Ph.D. Thesis, University of British Columbia.

12) L.V. Godfrey, W.M. White, V.J.M. Salters (1996) Dissolved zirconium and hafnium distributions across a shelf break in the northeastern Atlantic ocean, *Geochimica et Cosmochimica Acta*, **60**, 3995-4006.

13) K.W. Bruland, R.P. Franks (1983) Mn, Ni, Cu, Zn and Cd in the western north Atlantic. *In Trace elements in seawater*, Plenum Press, New York, 920 pages.

14) E.A. Boyle, D.F. Reid, S.S. Huested, J. Herring (1984) Trace metals and radium in the Gulf of Mexico: an evaluation of river and continental shelf sources, *Earth and Planetary Science Letters*, **69**, 69-87.

15) P.A. Yeats (1993) Input of metals to the north Atlantic from two large canadian estuaries, *Marine Chemistry*, **43**, 201-209.

16) K. Kremling (1985) The distribution of cadmium, copper, nickel, manganese, and aluminum in surface waters of the open Atlantic and european shelf waters, *Deep-Sea Research*, **32**, 531-555.

17) A. Van Geen, S.N. Luoma (1993) Trace metals (Cd, Cu, Ni, and Zn) and nutrients in coastal waters adjacent to San Francisco Bay, California, *Estuaries*, **16**, 559-566.

18) R. Carpenter (1987) Has man altered the cycling of nutrients and organic carbon on the Washington continental shelf and slope? *Deep Sea Research*, **34**, 881-896.

19) A.M. Shiller (1988) Enrichment of dissolved gallium relative to aluminum in natural waters, *Geochimica et Cosmochimica Acta*, **52**, 1879-1882.

20) T.C. Loder, R.P. Reichard (1981) The dynamics of conservative mixing in estuaries, *Estuaries*, **4**, 64-69.

21) M.W. Monroe and J. Kelly (1992) State of the estuary: a report on conditions and problems in the San Francisco Bay/ Sacramento- San Joaquin delta estuary, San Francisco Bay estuary project, Oakland, CA, 269 pages.

22) J.S. Kuwabara, C.C.Y. Chang, J.E. Cloern, T.L. Fries, J.A. Davis, S.N. Luoma (1989) Trace metal distribution along a dissolved organic carbon gradient in south San Francisco Bay, *Estuarine Coastal Shelf Science*, **28**, 307-325.

23) G.A. Cutter (1989) The estuarine behavior of selenium in San Francisco Bay, *Estuarine Coastal Shelf Science*, **28**, 13-34.

24) D.E. Hammond, C. Fuller, D. Harmon, B. Hartman, M. Korosec, L.G. Miller, R. Rea, S. Warren, W. Berelson, S.W. Hager (1985) Benthic fluxes in San Francisco Bay, *Hydrobiologia*, **129**, 69-90.

Chapter 4: Upwelling as a Source of Ga, In, Zr and Hf to the California Current System

4.1 Introduction

Coastal upwelling has long been known to occur along the entire west coast of the United States and Baja California. In fact, at the time this cruise took place, intense upwelling events were taking place along the coasts of California (figure 4.1.1) and Oregon and therefore were bound to affect trace metal signals under investigation.

Upwelling defines all processes which cause the upward movement of water from depths of 100 to 300m into the surface layer. Since the temperature of seawater decreases with depth, upwelled water is colder than the surface water it replaces. In addition, its nutrient content (nitrate, phosphate and silicic acid) is higher than that of surface water, which may have been previously depleted by the growth of phytoplankton. Consequently, regions of upwelling are usually regions of high biological productivity. Approximately 90% of the important fisheries of the world are found in areas of upwelling which incidentally constitute only a mere 3% of the oceans total area. Although upwelling also occurs in the open ocean along divergence zones, this study is mainly concerned with upwelling that occurs along coasts, more specifically that occurring along the west coast of North America.

Coastal upwelling is induced by winds acting under favorable conditions. When a wind blows parallel to a coastline, an Ekman transport perpendicular to the coast is established. In the Northern Hemisphere, if the coastline is to the left, looking in the direction the wind is blowing, the Ekman transport is directed offshore (in the southern hemisphere, the coastline must be on the right). In any case, near the coast, water can only be supplied to replace this offshore-directed Ekman transport by drawing it from below. As the surface water is swept offshore, an equal volume of colder deeper water wells up to replace it. The magnitude of the Ekman transport directed offshore, computed from the alongshore component of wind stress divided by the Coriolis parameter, is an index of the magnitude of coastal upwelling. Upwelling Indices for the west coast of North America are tabulated by the National Oceanic and Atmospheric Administration (NOAA).

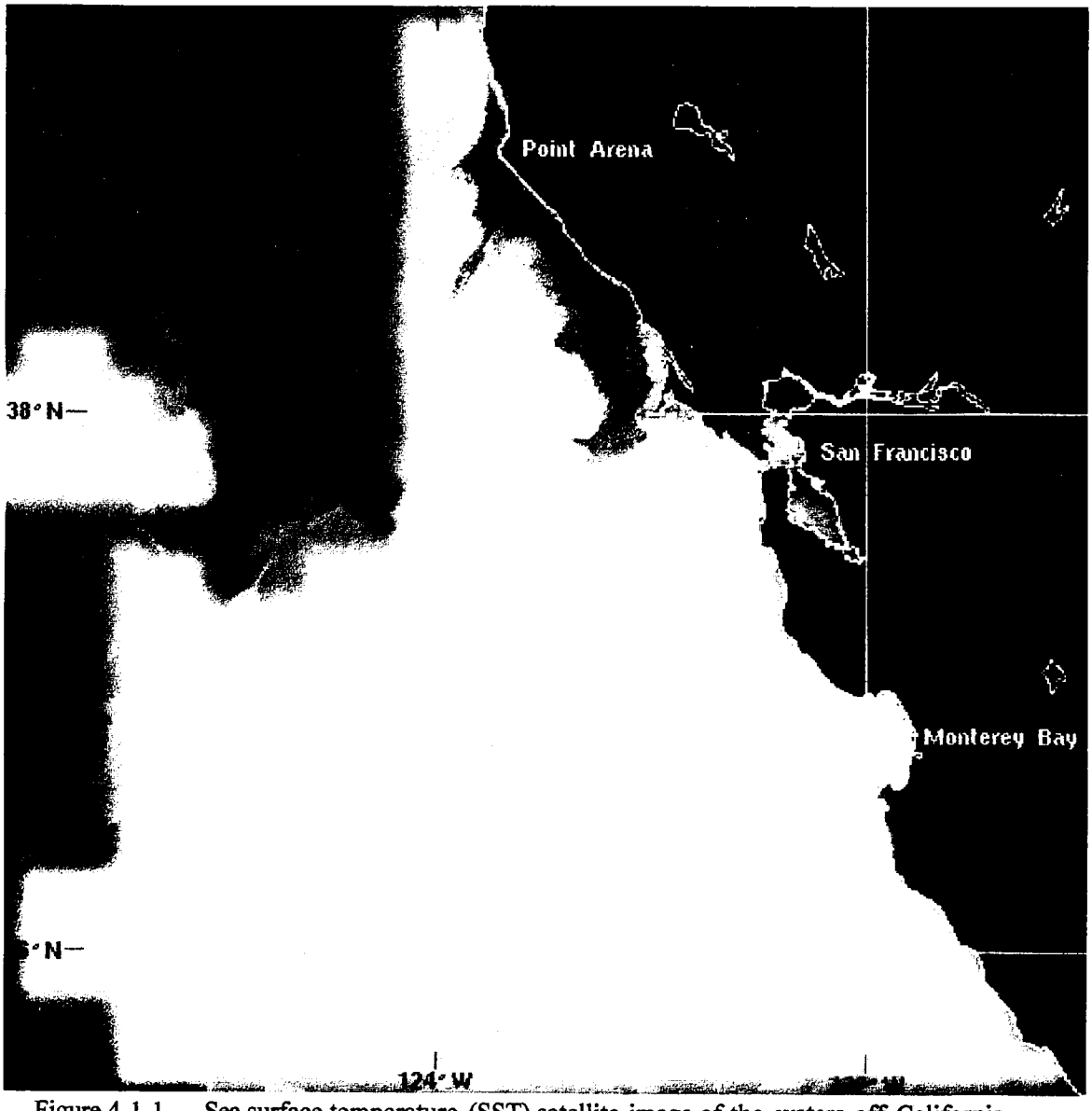

Figure 4.1.1 Sea surface temperature (SST) satellite image of the waters off California on June 23rd, 1997: the same day samples from WCSST#03 were taken. Blue waters indicate colder (8-9°C) upwelled waters while warmer (17-18°C) waters are shown in red.

Most major coastal upwelling regions are located along the eastern boundaries of the oceans, i.e. along the continental west coasts (Peru, Northwest Africa and western North America). When upwelling events occur, predominant winds in these regions are generally blowing parallel to the coast and towards the equator. Along the west coast of North America, the winds which force upwelling are driven by the strength of the pressure gradient between the North Pacific High and the continental thermal low-pressure systems. The gradient is strongest during the summer when the low over California deepens (due to heating) and the North Pacific High moves seaward. Upwelling-favorable northerly winds are thus generated everywhere south of 50°N. In winter, the North Pacific High migrates closer to the continent, the low over the western United States disappears and the Aleutian Low develops over the Central North Pacific. Predominant winds in this case are typically southwesterly off Oregon and Washington and weakly northerly south of 40°N. Hence non-favorable upwelling conditions prevail in wintertime[1].

Observations that provide evidence of coastal upwelling include surveys of sea surface temperatures as well as salinity and nutrient measurements. Upwelled water is obviously colder, but also saltier than the displaced water, which may have been diluted by atmospheric precipitations or riverine discharge. As mentioned previously, its nutrient content is also higher due to the absence of primary production at the depth from which this water originated. Therefore high nutrients, low temperature and high salinity near the coast are good indicators of upwelling events.

Upwelling may also bring to the surface trace metals which are enriched in bottom waters as a result of sediment diagenesis and/or resuspension. This chapter will be devoted to the study of upwelled waters, occurring mainly in the southern transects (figure 4.1.2), as sources of trace metals to coastal waters. Moreover, the width of the continental shelf will be considered since it has already been shown how this parameter determines iron levels in coastal regimes[2,3].

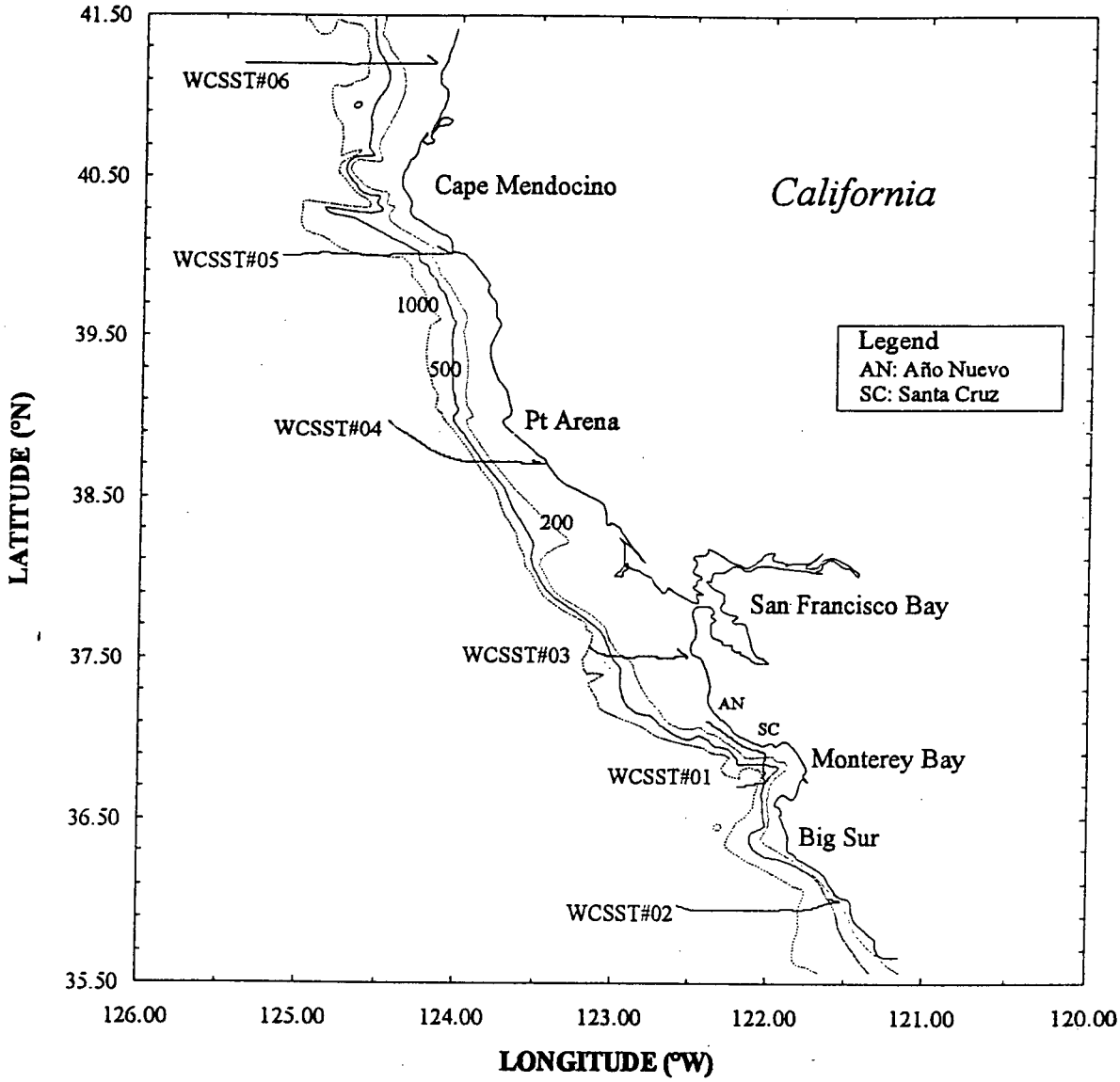

Figure 4.1.2 Study area depicting transects affected by upwelling. Isobaths are in meters. WCSST#08 is not shown here (see figure 3.1.2.1).

4.2 Results and Discussion

4.2.1 Upwelling Events along the West Coast of North America during Summer 1997

Locations, temperature, salinity and trace metal data for transects WCSST#01, #02, #03, #04, #05, #06 and #08 can be found in appendix 1.

Temperature, salinity, nutrient and chlorophyll a plots for these stations are presented in figures 4.2.1.1 through 4.2.1.7. For WCSST#01, only the data from Año Nuevo to Santa Cruz (section alongshore) are plotted; the raw data for the rest of this transect (Santa Cruz to the center of Monterey Bay and then out) can be found in the appendix. Although plots relating to transects WCSST#03 and #08 were already presented in chapter 3, they are reinserted here for clarity. References will occasionally be made to Fe data (measured by K.W. Bruland and colleagues at UCSC) and Mn data (measured by C. Merrin, fellow student) from this same cruise.

The occurrence of upwelling in WCSST#01, #02, #03, #04, #05 and #08 is evidenced by high salinity (>33), low temperature (8.5-11.5°C) water masses containing high nitrate (13-33μM) and high silicic acid (16-46μM). For WCSST#01, where the ship was travelling alongshore from Año Nuevo to Santa Cruz, upwelling seems to be occurring in the northwestern section of this transect. The constant high salinity in the southeastern section suggests upwelling although the increase in temperature as Monterey Bay is approached implies otherwise. Since upwelling at Año Nuevo (north of Monterey Bay) has already been identified as the source of salty surface water frequently seen in the Bay[4], it is likely that this high temperature-high salinity water is older upwelled water which has warmed considerably as it mixed with the shallower waters of Monterey Bay.

WCSST#02 and #03 reveal multiple upwelling regimes within each transect. The constancy of salinity at WCSST#02 is once again a mystery as it suggests upwelling across the entire transect. High nutrients (nearshore-121.65°W and 121.90°-122.25°W), on the other hand, coincide with the low temperature waters, consequently they are better indicators of actual upwelling than salinity at this particular locale.

Three upwelling signals may be discerned at WCSST#03. The signal closest to the coast (up to ~122.55°W) is richer in nutrients than the two further offshore. Since there is generally a lag of a few days between the time nutrients are supplied to surface waters and the time phytoplankton blooms start to develop, high nutrients and the absence of chlorophyll a are usually good indicators of recent upwelling events. Consequently, this near-shore upwelling is probably very recent. In contrast, the two offshore signals (122.70°-122.95°W and 123.10°W-offshore) which contain lower nutrients and detectable chlorophyll a are probably older upwelled waters. These observed signals are probably caused by the southerly advection of waters upwelled further north (see figure 4.1.1). As they traveled south, blooms would have had time to start developing in these waters, thus decreasing their nutrient contents.

The next two transects, WCSST#04 and #05, show single upwelling events occurring closest to shore. For WCSST#06, it is quite uncertain what was happening at the time of sampling. Except for a localized bloom near shore where salinity is highest and temperature is ~12°C, there is little evidence of upwelling having ever taken place. Salinities farther offshore for this transect are lower (31.8-32.4) than non-upwelled oceanic surface waters of the southern transects (~32.8). There could be some freshwater influence from the Rogue River or other southern Oregon rivers. The discharge from southern Oregon rivers in summer however is negligible[5], so it is rather unlikely this northern California transect would feel their effect. In sum, this transect appears to consist mainly of CCS surface water with minor freshwater influences. With the exception of a particularly low-salinity feature at 124.50°-124.75°W, the data from this transect are useful for characterizing the trace metal content of CCS surface water.

Finally, WCSST#08 is the only northern transect where coastal upwelling was observed. The fact that a bloom was underway at the time of sampling indicates this upwelling event was not recent (possibly a few days old).

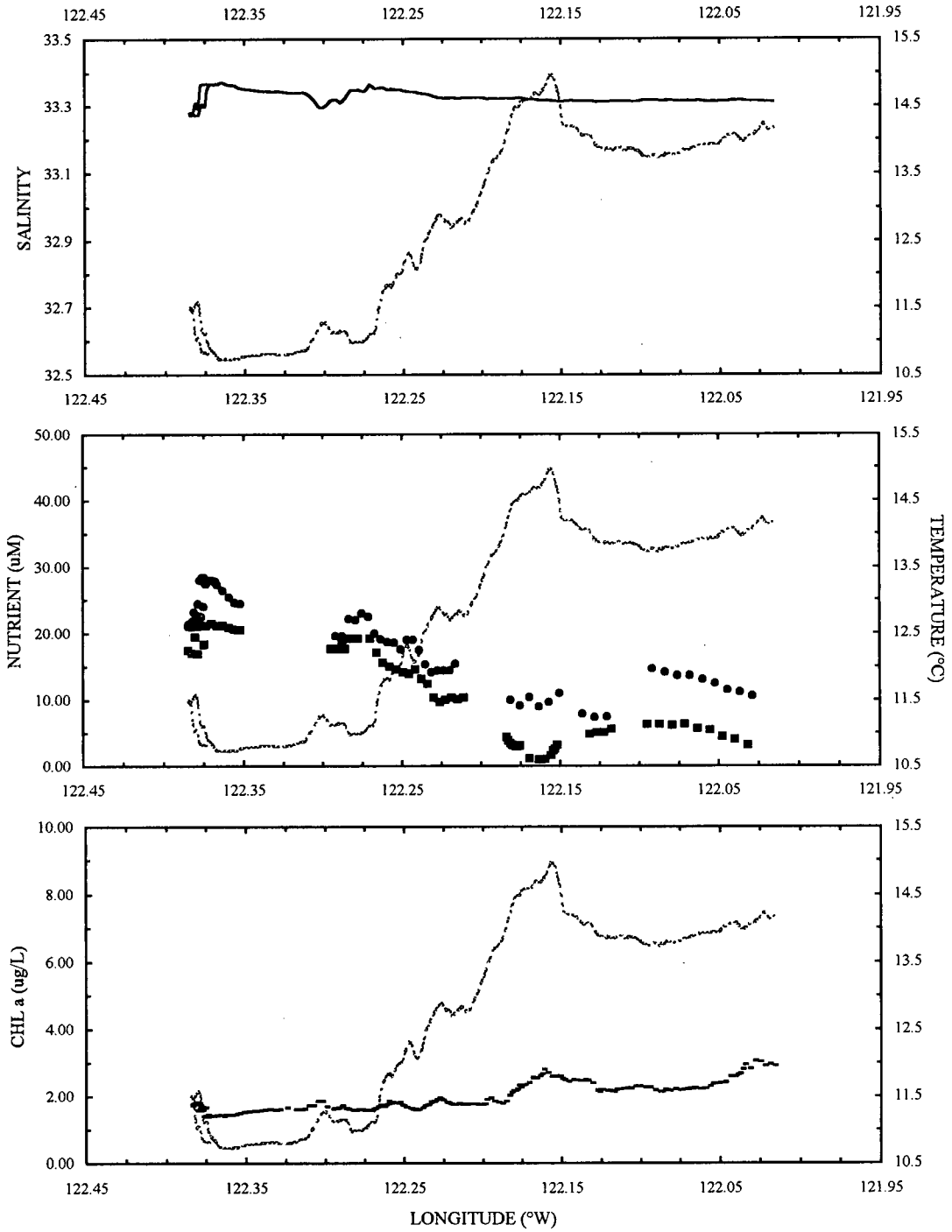

Figure 4.2.1.1 Temperature, salinity, nutrients and chlorophyll a data for WCSST#01. (Legend: Solid line = Salinity; Broken line = Temperature; ▪ = Nitrate; • = Silicic acid; - = Chl a).

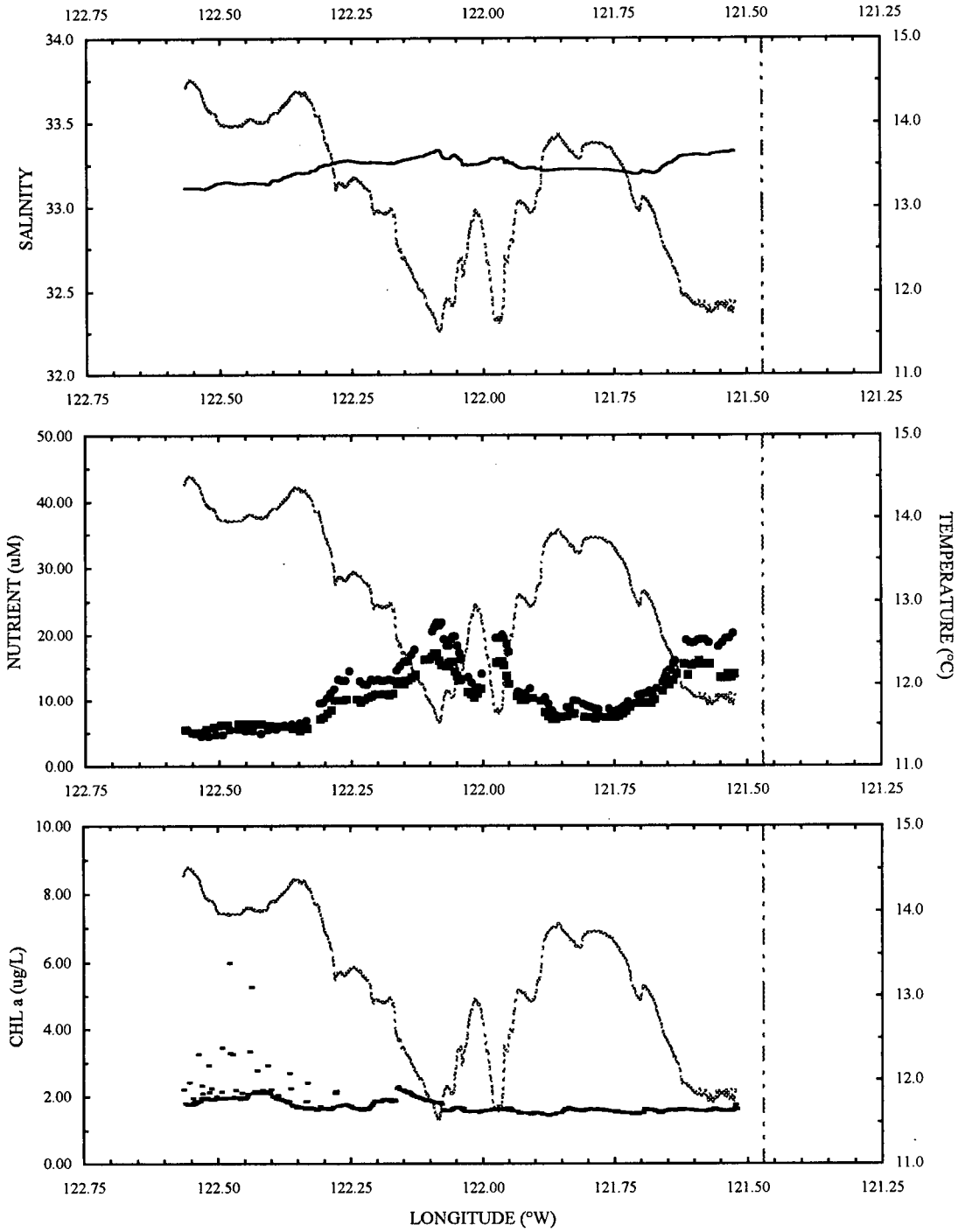

Figure 4.2.1.2 Temperature, salinity, nutrients and chlorophyll a data for WCSST#02. (Legend: Solid line = Salinity; Broken line = Temperature; Dashed line = Coastline; ▪ = Nitrate; • = Silicic acid; - = Chl a).

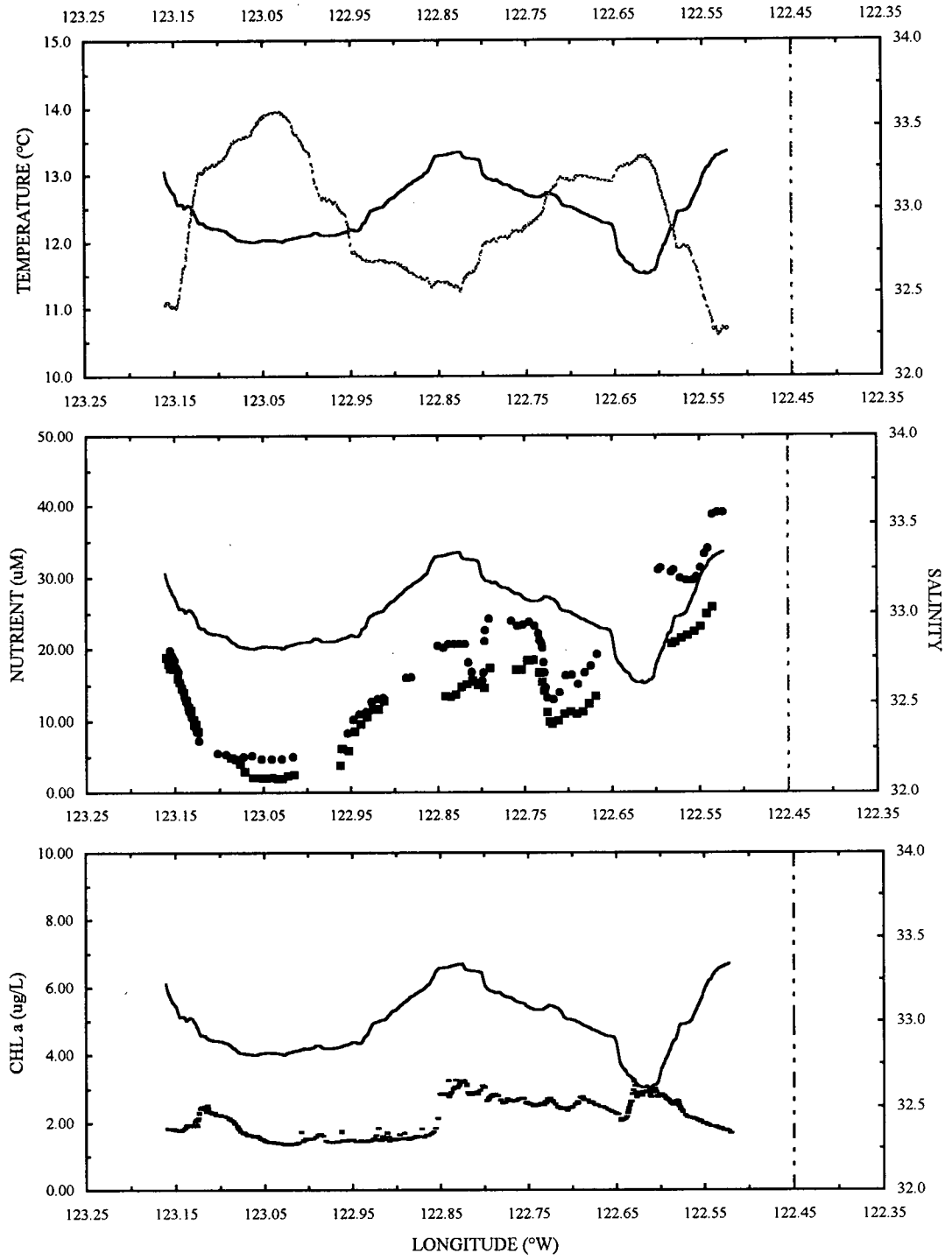

Figure 4.2.1.3 Temperature, salinity, nutrients and chlorophyll a data for WCSST#03. (Legend: Solid line = Salinity; Broken line = Temperature; Dashed line = Coastline; ▪ = Nitrate; • = Silicic acid; - = Chl a).

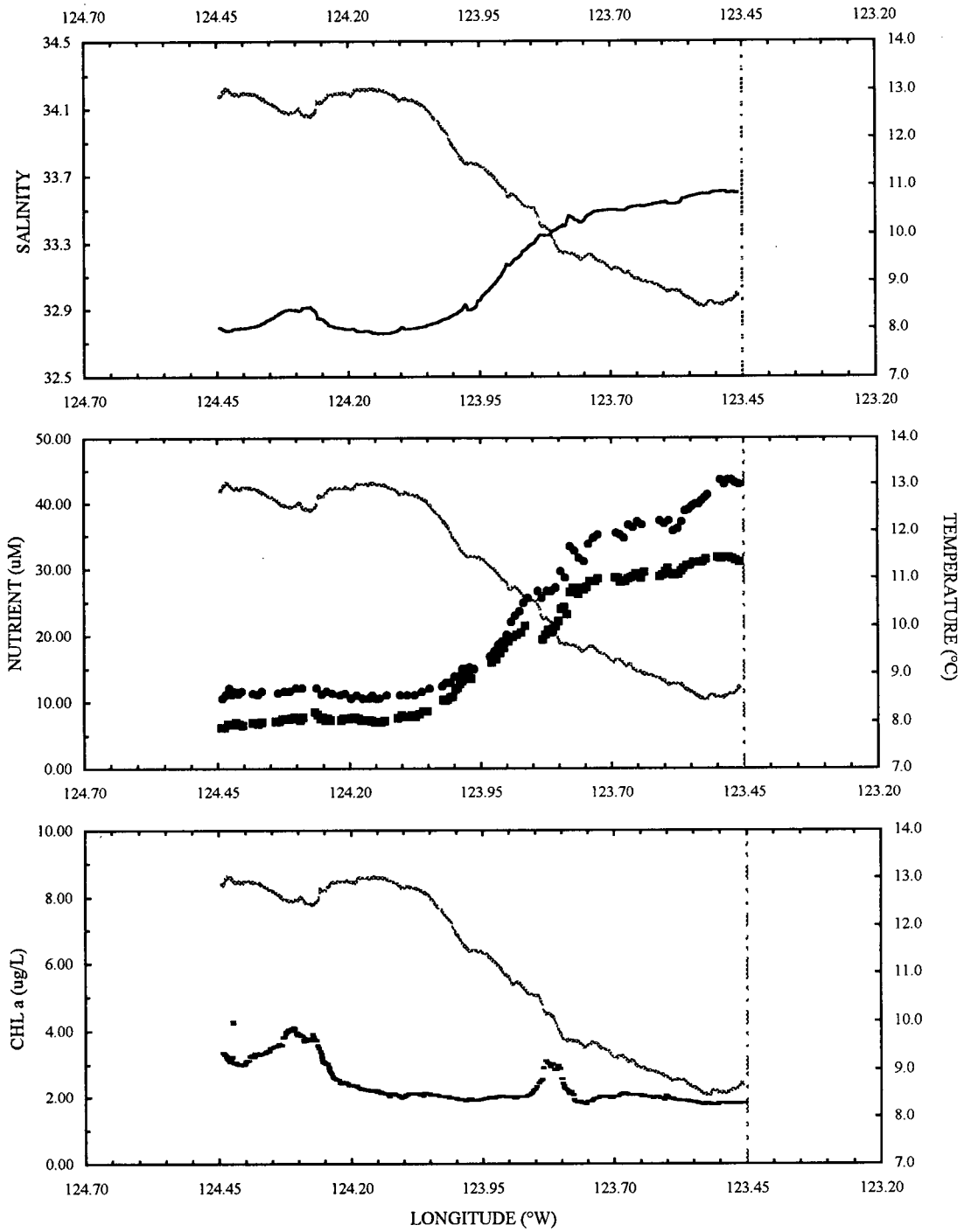

Figure 4.2.1.4 Temperature, salinity, nutrients and chlorophyll a data for WCSST#04. (Legend: Solid line = Salinity; Broken line = Temperature; Dashed Line = Coastline; ▪ = Nitrate; • = Silicic acid; - = Chl a).

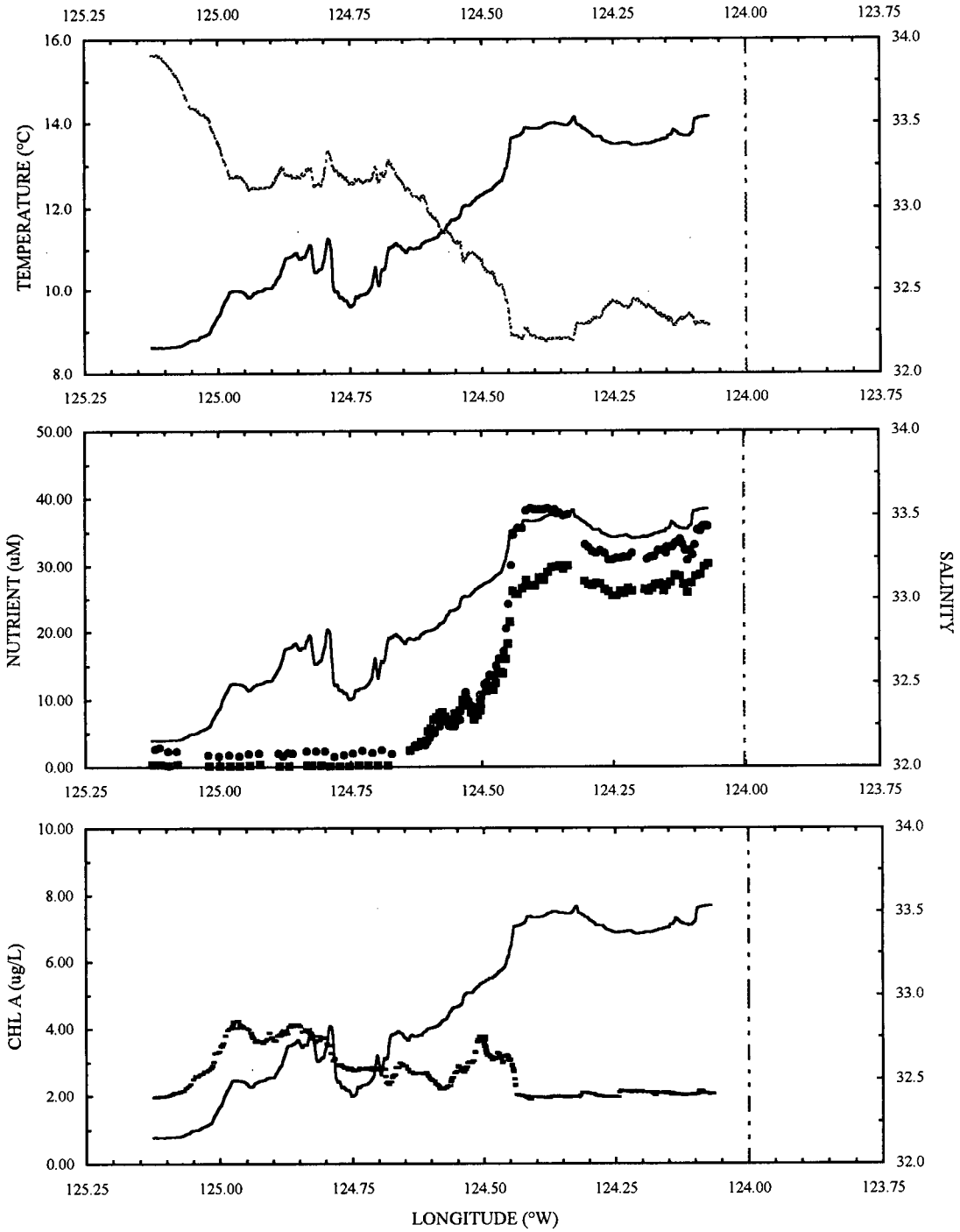

Figure 4.2.1.5 Temperature, salinity, nutrients and chlorophyll a data for WCSST#05. (Legend: Solid line = Salinity; Broken line = Temperature; Dashed line = Coastline; ■ = Nitrate; • = Silicic acid; - = Chl a).

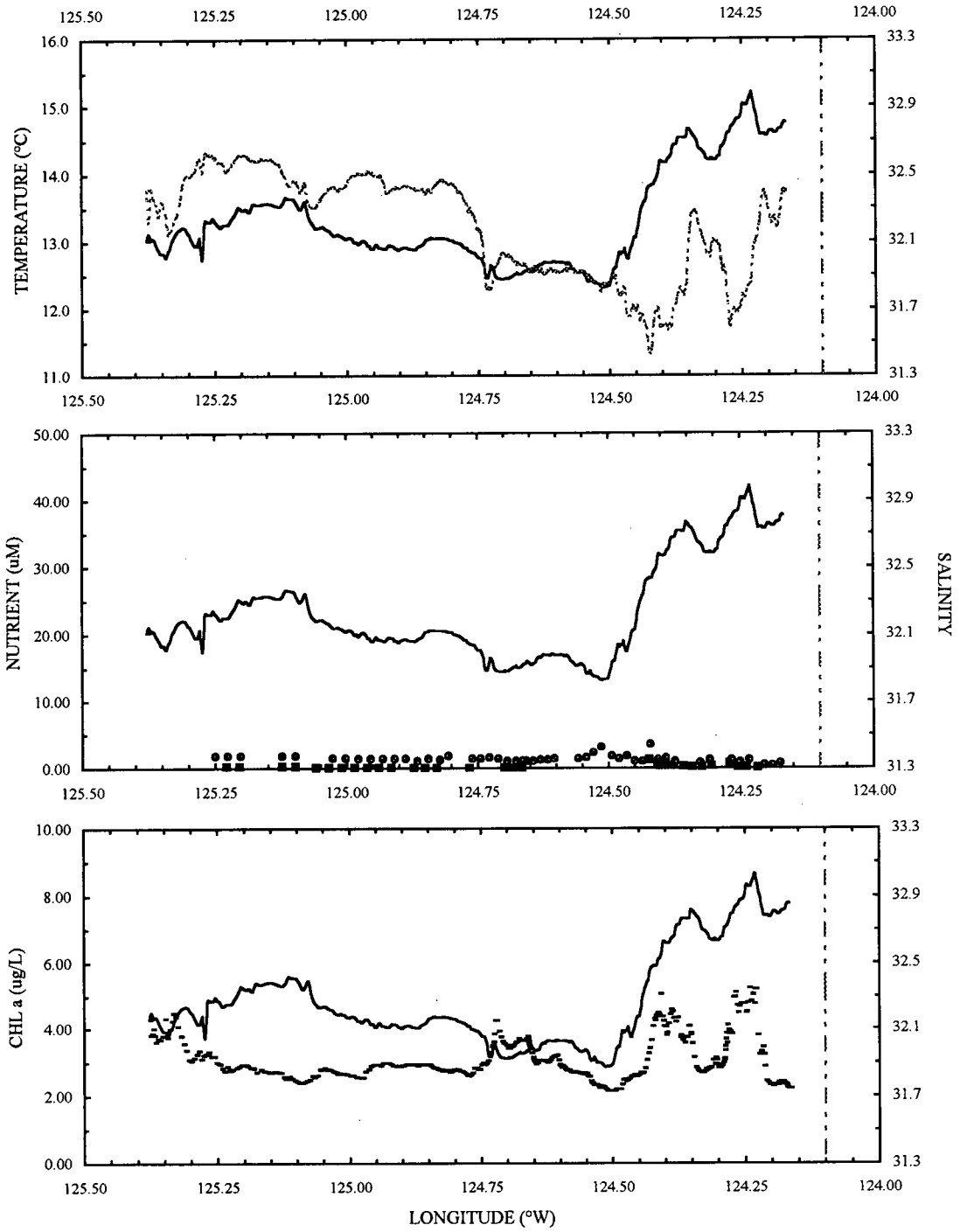

Figure 4.2.1.6 Temperature, salinity, nutrients and chlorophyll a data for WCSST#06. (Legend: Solid line = Salinity; Broken line = Temperature; Dashed line = Coastline; ▪ = Nitrate; • = Silicic acid; - = Chl a).

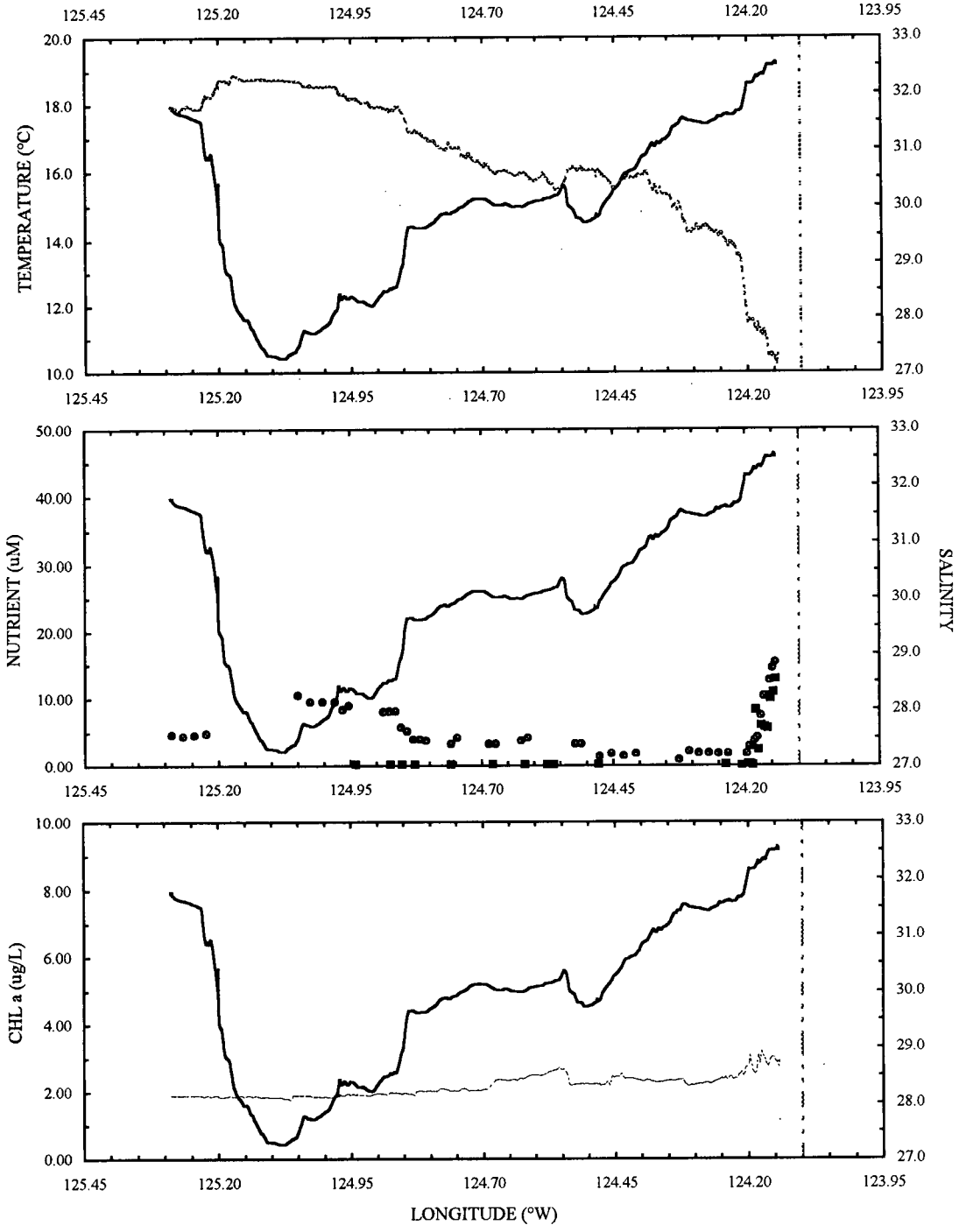

Figure 4.2.1.7 Temperature, salinity, nutrients and chlorophyll a data for WCSST#08. (Legend: Solid line = Salinity; Broken line = Temperature; Dashed line = Coastline; ■ = Nitrate; • = Silicic acid; - = Chl a).

4.2.2 Trace Metal Content of Upwelled Waters vs. Oceanic Waters

Trace metal plots for transects WCSST#01, #02, #03, #04, #05, #06 and #08 are presented in figures 4.2.2.1 through 4.2.2.7.

With the exception of In which shows absolutely no variability whatsoever in any transects where upwelling occurs and may also be questionable due to Sn interferences, all trace metals are enriched in upwelled waters ([Ga]=7-14pM; [Zr]=26-66pM; [Hf]=0.7-1.4pM) compared to CCS surface waters ([Ga]=5-8pM; [Zr]=16-34pM; [Hf]=0.3-0.6pM). The lowest upwelling Ga and Zr values are from the two offshore upwelling features at WCSST#03. The presence of blooms and more importantly the absence of any residual Fe and Mn (K.W. Bruland and C. Merrin, respectively; pers. comm.) in these upwelled waters are indications of their age. Whatever Fe and Mn these waters once contained was completely stripped out by the time they were sampled. In light of their known particle reactivity, it is therefore not surprising to note similar behavior occurring for Ga and Zr.

The CCS surface values for Ga in this study are higher than those previously reported at the same location a few kilometers off the coast of Big Sur (3.5-3.8pM)[6]. In fact, they are closer to those observed on the edge of the North Pacific Central gyre (6.1-10.1pM)[6]. The year 1997 was seeing the beginning of an El Niño event. During these events, relaxation of the Southeast Trade Winds causes tropical mixed-layer water to move eastwards across the Pacific Ocean, even reaching the west coast of North and South America (red water mass on figure 4.1.1). As a result of this climatic anomaly, offshore waters richer in Ga were probably brought in closer to shore, explaining the higher values detected in this work.

In contrast, Zr and Hf levels are lower than those previously observed in the CCS. McKelvey[7] measured Zr (192pM) and Hf (1.55pM) in waters off the Washington Olympic Peninsula (148°N, 126°W) during the fall of 1992. This could be due to a variety of reasons. Since prevailing winds are from the south at this time of the year, it is possible McKelvey was seeing some influence from the Columbia River plume as it was carried northwards. River discharge however is minimal during the fall therefore one would not expect a considerable riverine influence at that time of year. Even if it were, Zr levels measured in the Columbia River in this study were considerably lower than the levels observed by McKelvey but this may once again be a consequence of the river's natural variability.

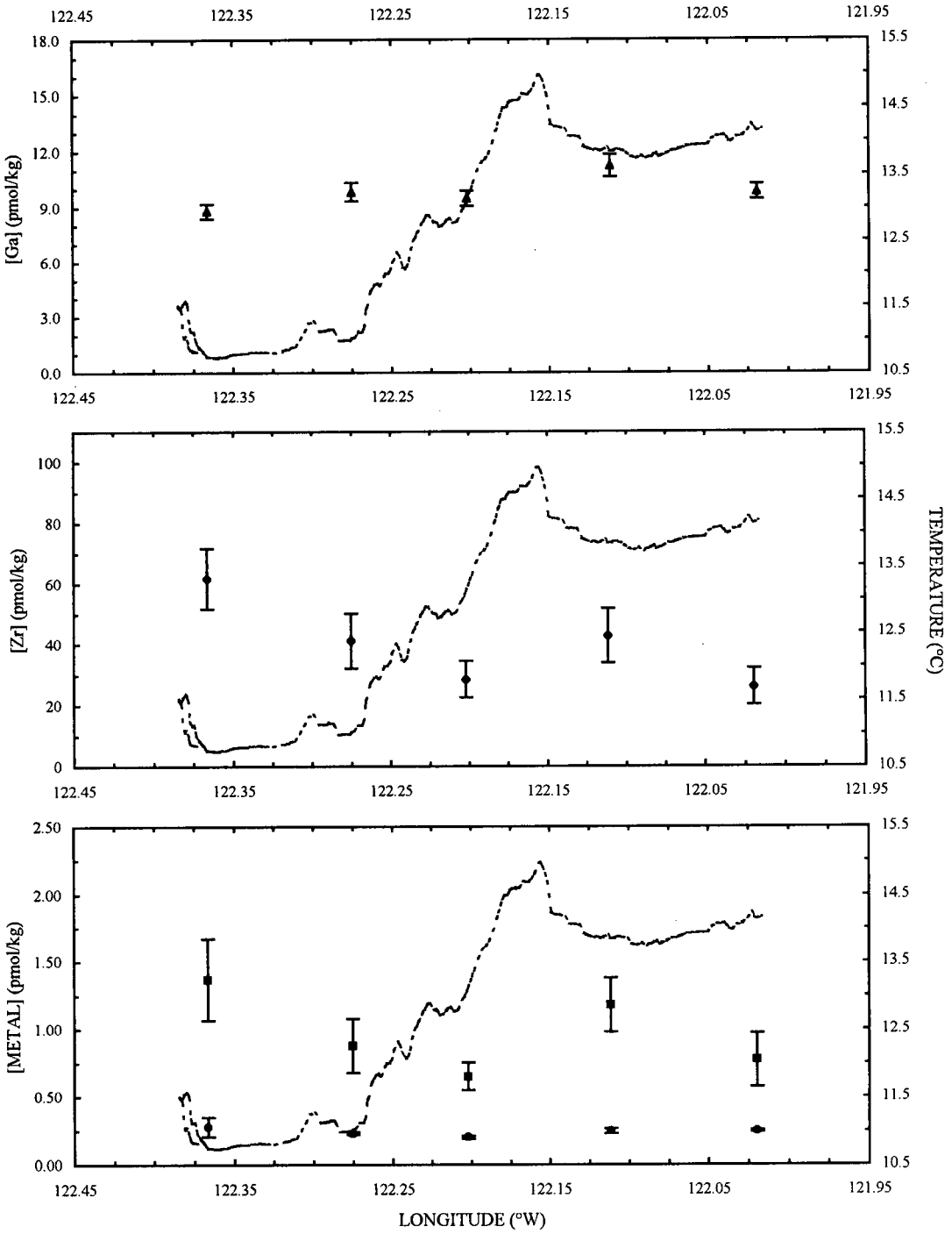

Figure 4.2.2.1 Trace metal data for WCSST#01. (Legend: Broken line = Temperature; Dashed line = Coastline; ▲ = Ga; ◆ = Zr; ● = In; ■ = Hf).

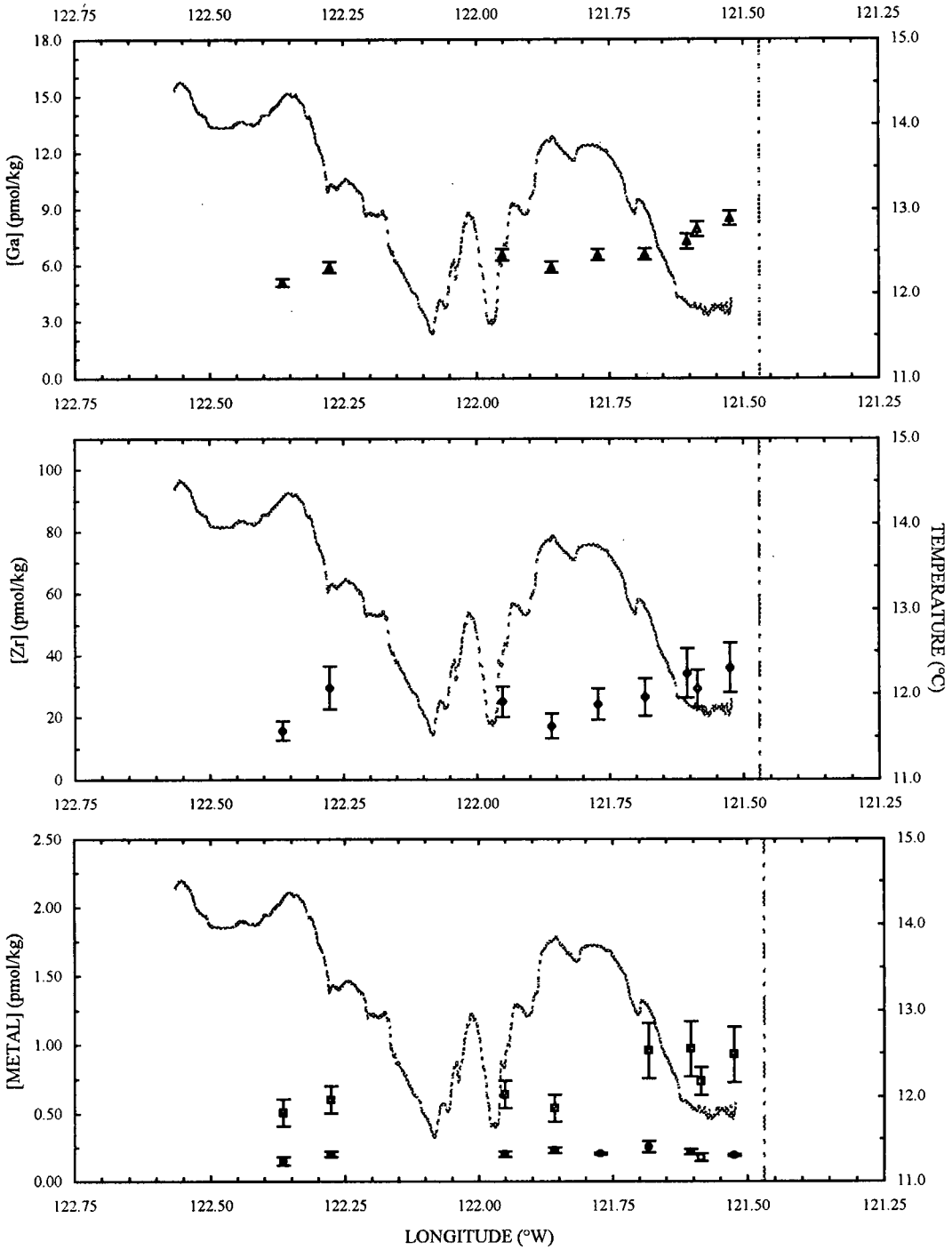

Figure 4.2.2.2 Trace metal data for WCSST#02. (Legend: Solid line = Salinity; Dashed line = Coastline; ▲= Ga; ◆= Zr; ●= In; ■ = Hf). Open symbols represent 'Dog Leg' data.

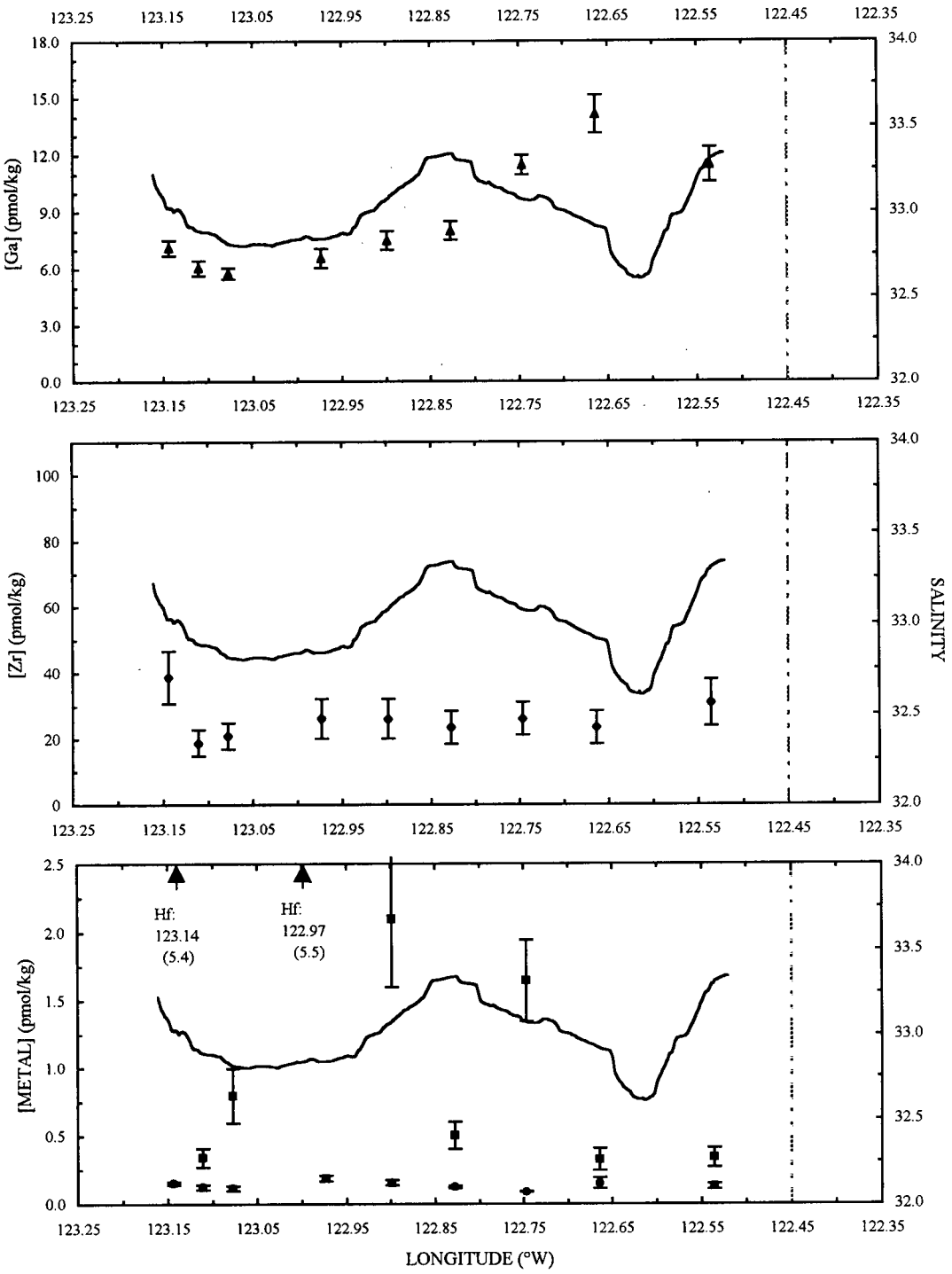

Figure 4.2.2.3 Trace metal data for WCSST#03. (Legend: Solid line = Salinity; Dashed line = Coastline; ▲= Ga; ◆= Zr; ●= In; ■= Hf).

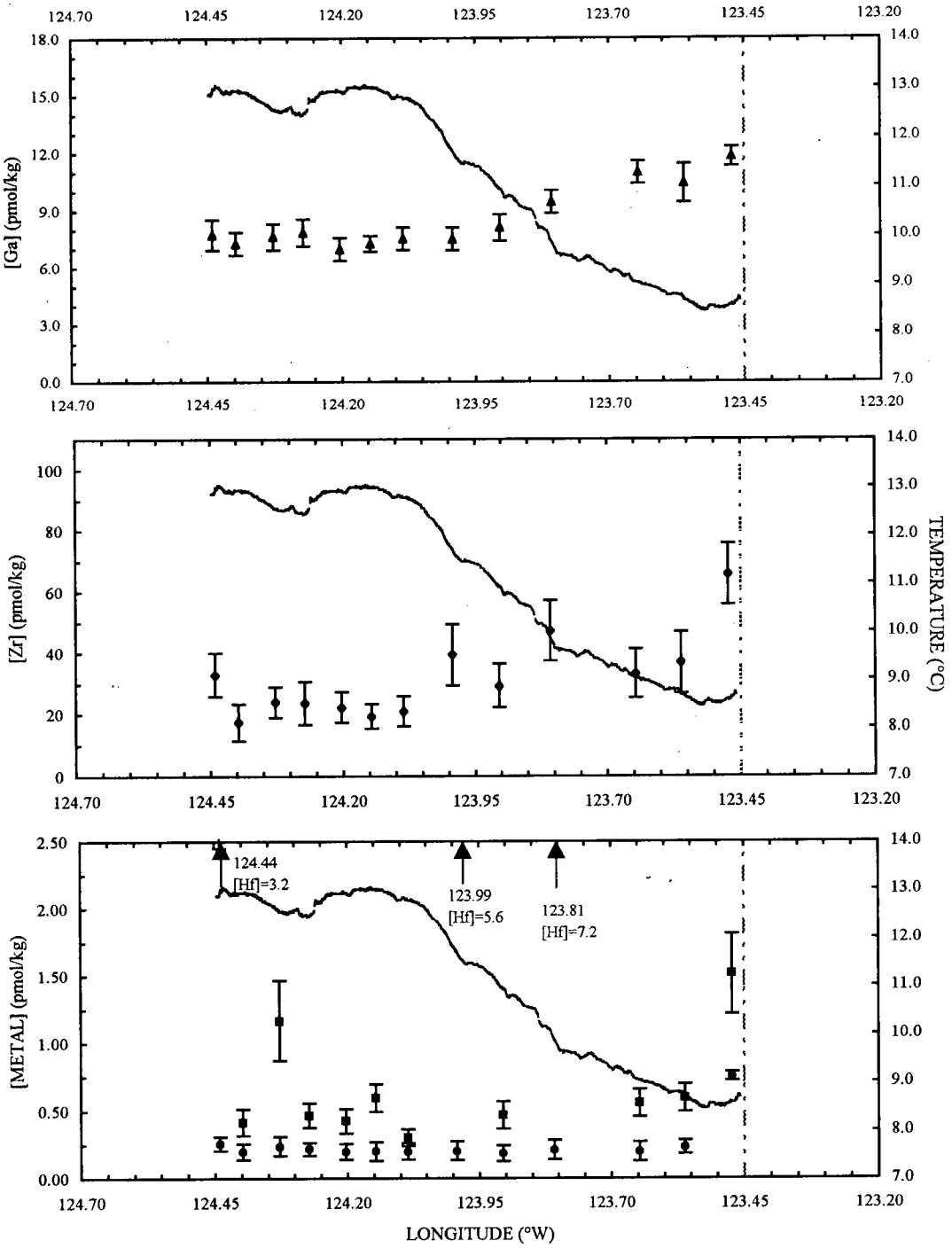

Figure 4.2.2.4 Trace metal data for WCSST#04. (Legend: Solid line = Salinity; Dashed line = Coastline; ▲= Ga; ◆= Zr; ●= In; ■= Hf).

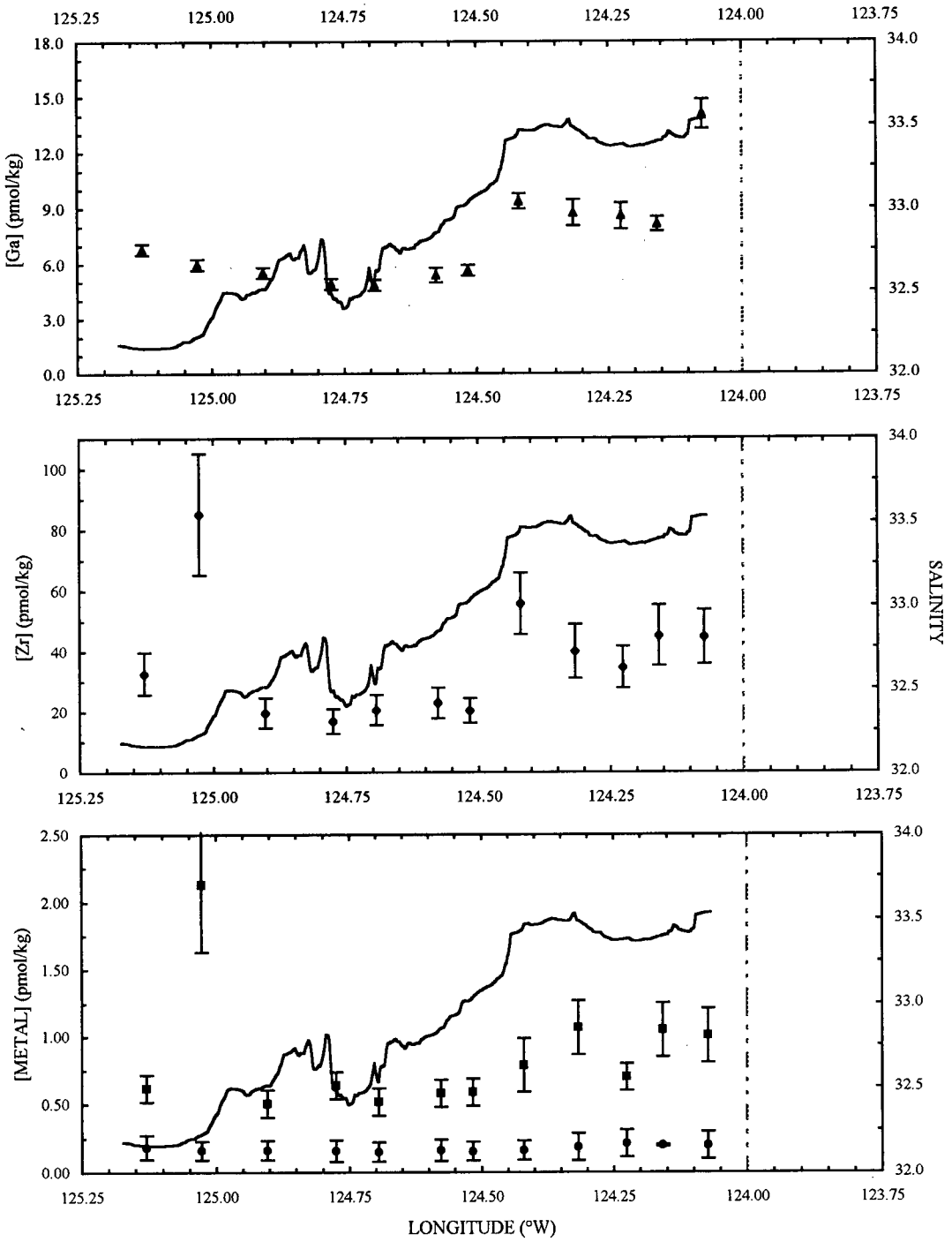

Figure 4.2.2.5 Trace metal data for WCSST#05. (Legend: Solid line = Salinity; Dashed line = Coastline; ▲= Ga; ◆= Zr; ●= In; ■= Hf).

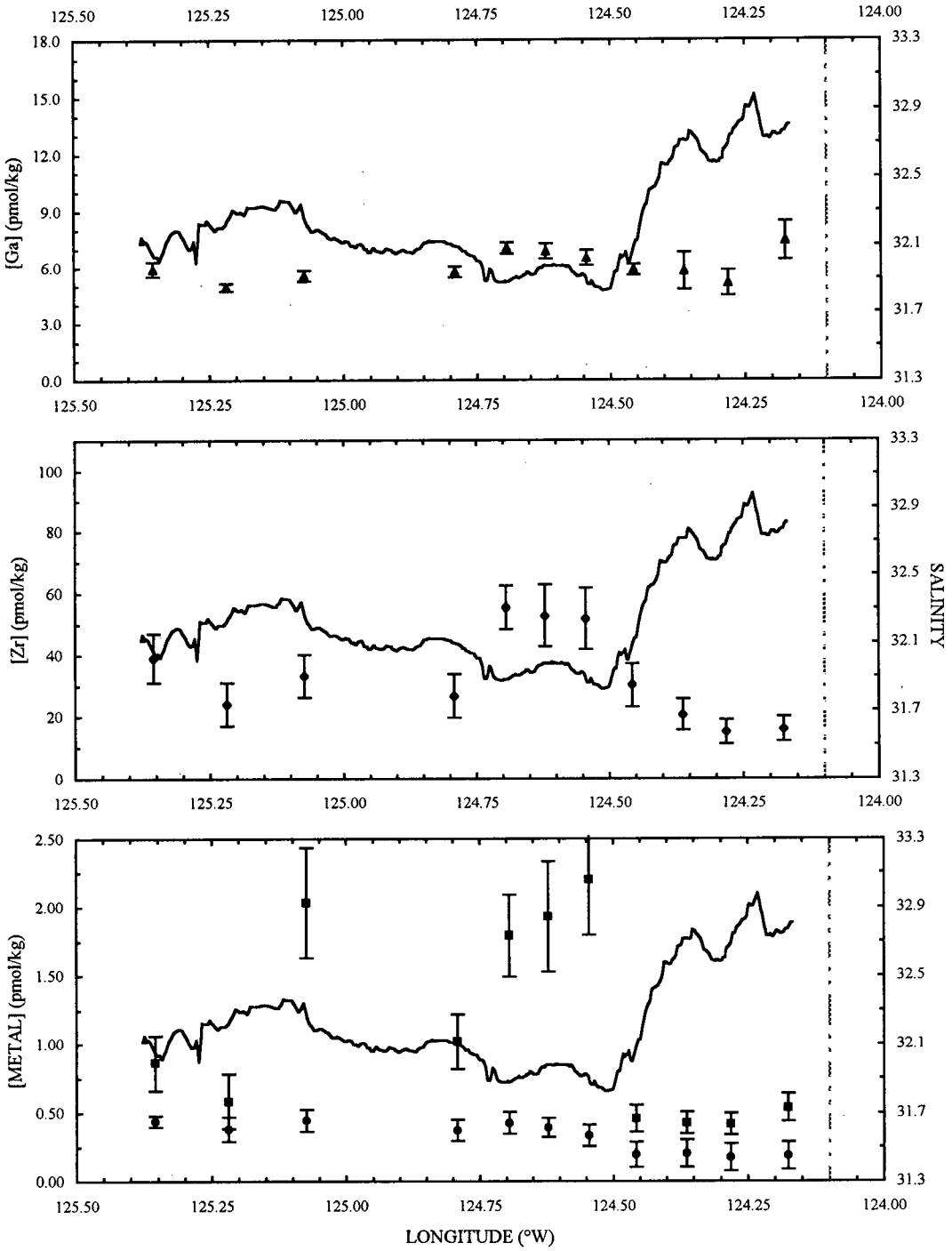

Figure 4.2.2.6 Trace metal data for WCSST#06. (Legend: Solid line = Salinity; Dashed line = Coastline; ▲= Ga; ◆= Zr; ●= In; ■= Hf).

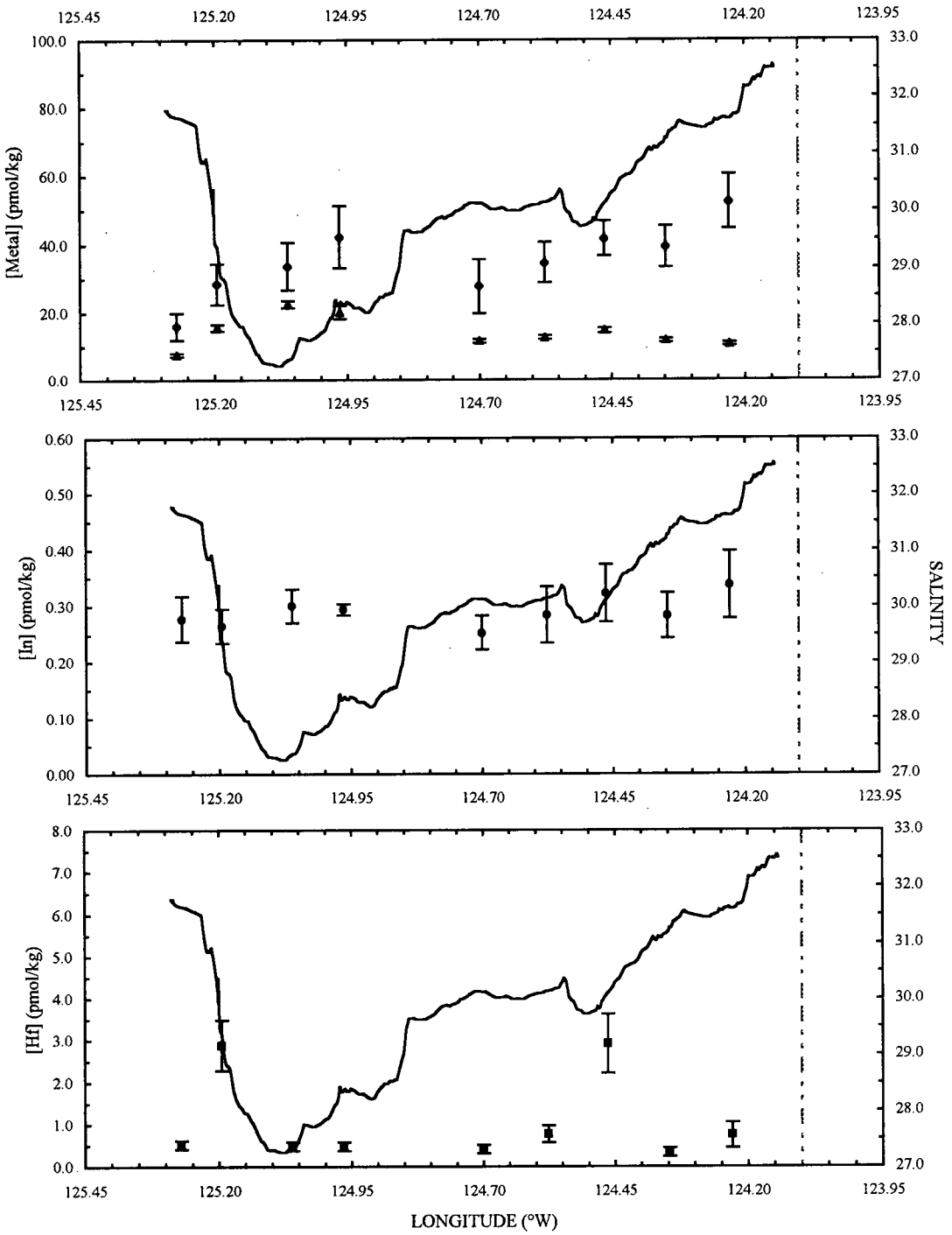

Figure 4.2.2.7 Trace metal data for WCSST#08. (Legend: Solid line = Salinity; Dashed line = Coastline; ▲= Ga; ◆= Zr; ●= In; ■= Hf).

The argument used to explain the higher Ga, i.e. the El Niño effect, could also apply to Zr and Hf. Opposite to Ga, Zr and Hf concentrations decrease farther away from the coast[7]. Hence, if El Niño was causing central Pacific oceanic water to move in closer to shore, low Zr (13-25pM) and Hf (not available) would be expected[7].

Alternatively, it may simply be that adsorption to bottle walls and the problems encountered with the low recoveries of these two elements result in values that are considerably underestimated. There is however one additional source which may account for the differences in concentrations encountered between these two studies: the sediments of the continental shelf.

4.2.3 The Continental Shelf and Sediments

Most substances delivered to the oceans, with the exception of elements lost in hydrothermal vents, are ultimately removed to the sediments. Although often thought of as sinks, sediments (and especially organic-rich sediments such as those present in coastal areas) can be important sources of remobilized trace metals due to their large trace metal enrichments and the lability of organic matter. Once deposited, sediments do not lie passively on the seabed. They are disturbed by deep-sea animals as they forage for food and some sediments may experience erosion and resuspension by bottom currents before being redeposited and eventually buried and lithified. Turbulence or current shear across the bottom may result in resuspension of fine-grained sediments small enough to pass through 0.45μm filters, or exchange with the truly dissolved metal fraction, both leading to high total 'dissolved' concentrations. Recently, high surface Fe and Cu concentrations in certain coastal environments were attributed to the resuspension of sediments over the continental shelf[3,8].

Once buried, sediments undergo diagenesis. Diagenesis is the term applied to the physical and chemical changes that occur within sediments, through interactions with porewaters, as they become compacted after burial. Diagenetic remobilization is said to occur when trace metals, scavenged to the sediments by biogenic detritus, clay minerals and hydrogenous precipitates, are resolubilized *in situ* and diffuse across the sediment surface-seawater interface into the overlying bottom water. This resolubilization may result in part from redox conditions that develop in the sediments due to the degradation of organic matter. The relative supplies of organic matter and electron acceptors such as O_2, NO_3^- and SO_4^{-2} control the depth of the oxic/anoxic redox boundary.

Below the oxic/anoxic boundary, Fe and Mn oxyhydroxides are reduced to Fe^{+2} and Mn^{+2} which are then free to diffuse upwards. Normally in the deep ocean this boundary is deep enough that very little dissolved Fe and Mn are observed diffusing out of sediments; instead they are rapidly re-oxidized and precipitate as oxyhydroxides on contact with oxygen. However, in coastal environments, the rate of organic matter deposition is usually fast enough to cause the redox interface to lie within a few millimeters to a few centimeters of the sediment surface thus allowing some of these elements to escape the sediments before they have a chance to re-oxidize and precipitate[9-11].

Although Ga, In, Zr and Hf are not involved in redox cycles of their own, they do exhibit deep-water regeneration reminiscent of either sediment surface remineralization or sediment diagenesis[6,7,12]. It is possible these metals associate with sinking particles and are subsequently released upon degradation, dissolution or reduction of their carriers following deposition. Copper for example is significantly enriched in coastal waters over continental shelves as a result of diagenetic remobilization in mildly reducing terrigenous sediments[13], even though Cu itself is not mobilized by reduction.

Thus, the continental shelf is a potential source of trace metals via two pathways: either by way of reductive diagenesis or by release from resuspended sediments. Recent studies of upwelled waters off the California Coast show dissolved Fe levels vary according to the width of the shelf[2,3]. In the Big Sur area where the continental shelf is extremely narrow, Fe levels are so low that these waters are as Fe-limited as other HNLC (high nitrate, low chlorophyll) regimes[2]. North of Monterey Bay where the shelf is wider, Fe levels were significantly (~10x) higher. Johnson et al.[3] attributed these higher values to the resuspension of shelf sediments in bottom waters followed by their upwelling to the surface.

The Fe data from this cruise (K.W. Bruland; pers. comm.) complement these earlier observations perfectly. Upwelled Fe concentrations are lowest at WCSST#02 (off Big Sur), intermediate at WCSST#01 and #05, and highest at WCSST#03 and #04 (no data was available for WCSST#08). A look at figure 4.1.2 reveals how the shelf is almost non-existent at WCSST#02, is wider and of comparable width at both WCSST#01 and #05, and is much broader at WCSST#03, #04 and #08. There is one curious occurrence at WCSST#05. Within the upwelled water mass, Fe values closest to shore are almost three times as high as those near the upwelling/CCS surface water front. The higher values are comparable to WCSST#01 (intermediate shelf) while the low values compare to WCSST#2 (narrow shelf). This suggests

Ekman transport is bringing up water that overlies the shelf right near the coast whereas farther offshore water is brought up which isn't in contact with the shelf.

The concentration ranges for Ga, Zr and Hf in the different upwelling regimes are narrow; nonetheless, similar behavioral trends to Fe are observed. Ga mirrors Fe almost perfectly. Lowest concentrations were found at WCSST#02 (7.3-8.5pM) and at WCSST#05 (8.1-9.4pM) where Fe was also low. At WCSST#01, Ga ranges from 8.8 to 11.2pM. Strangely, the lower levels occur in the newer upwelling waters while the higher levels are observed in the older waters (closer to the Bay). There could be an anthropogenic (see section 3.3; p.79)/riverine source of Ga from the Salinas River although the salinity does not show any freshwater influence.

Where the shelf is widest (i.e. WCSST#03, #04 and #08), Ga varies between 10 and 11.8pM. Unfortunately, the sample taken at WCSST#08 does not coincide directly with the upwelling but rather with the boundary between the upwelling and CCS surface waters. Still, even in these boundary waters, the Ga content (10.7pM) is higher than normal CCS surface water therefore Ga levels in the actual upwelled water is likely to be even higher.

The only major difference between Ga and Fe lies in the upwelling that is suspected of occurring over the shelf at WCSST#05. At this location, Ga is an exceptional 14.1pM: the highest concentration seen so far. Although Fe levels were also high in these waters, they were lower than those observed WCSST#03 and #04 where the shelf is considerably wider. Even though this is only one Ga data point, there is no reason to doubt it: the absolute values may not match but the trend between the two elements is identical. In any case, Ga seems to confirm the hypothesis that the upwelled waters along WCSST#05 originate from two different places.

Zr and Hf are not as straightforward as Ga. In fact, Hf interpretation is plagued by frequent outliers, especially at WCSST#03 and #04, which results in questionable data throughout the entire transects. Also, a certain amount of variability within the transects causes overlap in the Zr ranges between the different upwelling regimes. Consequently, definite conclusions are harder to make even though the following observations are noted.

The lowest Zr levels are found at WCSST#02 (29-36pM) and in the older upwelled waters near Monterey Bay at WCSST#01 (26-43pM). The distinct behavioral pattern observed for Fe and Ga in the upwelling at WCSST#05 does not apply to either Zr or Hf. There is no significant increase closest to the coast to differentiate between the two different upwelling regimes suspected of occurring here. Instead, both elements are fairly constant across the entire upwelling feature; Zr is higher (35-56pM) than at WCSST#2 while Hf is comparable (0.7-1.1pM). For the remaining

transects (newer upwelling at WCSST#01; WCSST#04 and #08), Zr levels vary between 33 and 66pM. At WCSST#08, Zr concentrations increase towards the coast, therefore the concentration in the actual upwelled water is expected to be higher than the 53pM in the sampled waters.

The big surprise concerning Zr is the lack of any variability at WCSST#03. This transect intersected three different upwelling regimes, CCS surface water and what is thought to be San Francisco Bay effluent. Yet, levels are very low (<32pM except for one data point in the older upwelled waters) regardless of the fact that fresh upwelling over a wide shelf is occurring near the coast. When Van Geen and Luoma[14] found that dissolved Cd, Cu, Ni and Zn concentrations in nearshore waters at Pillar Point and Moss Beach (south of San Francisco) were comparable to levels in the upper few hundred meters of the California Current, they concluded that shelf sediment diagenesis does not significantly enrich the overlying water in this region. This could account for the absence of Zr in these nearshore upwelled waters but then it would contradict the observed high Fe and Ga signals. The release of Zr from sediments is suspected of originating from the diagenesis of Fe oxides and hydroxides[6], therefore high Zr levels are expected to accompany high Fe levels. Based on shelf width, similar Zr results to those obtained at WCSST#04 and #08 would be expected in the upwelling at this transect.

Thus, unless some unknown process is releasing Fe, Ga and Zr at all transects except WCSST#03, the Zr data for this transect is highly questionable.

4.2.4 Zirconium and Hafnium Fractionation

Because of the lanthanide contraction, Zr and Hf possess virtually identical physical properties despite the increased atomic number, mass and total number of electrons of Hf. Their resulting chemical similarity has led to their intimate association in many minerals. In terrestrial rocks, the Zr/Hf molar ratios show limited variation and a crustal average of 72.

In seawater, however, fractionation between the two elements is known to occur, leading to Zr/Hf molar ratios of less than 10 to more than 350 (section 1.3.4). A few processes where fractionation can occur are chemical weathering of crustal material, sediment diagenesis or scavenging. By measuring the Zr/Hf ratios of the samples collected for this study, it is possible to determine if fractionation takes places during estuarine mixing (seen from Columbia River plume samples) and during sediment diagenesis (seen from upwelling samples). Zr/Hf ratios are

presented in figure 4.2.4.1. There appears to be no significant difference between the Zr/Hf ratios of upwelled waters, oceanic waters or river-influenced waters. The average molar ratio of 44±40, which is well below the average crustal ratio, implies a Hf rather than a Zr enrichment. The validity of the Hf data obtained from this study requires verification before any claims can be made as to whether actual fractionation leading to Hf enrichment is real. Still, regardless of the questionable nature of these ratios, they do seem to indicate that sediment diagenesis in coastal environments, along with riverine mixing are not causing the Zr to Hf enrichments observed previously in other marine environments[6,15].

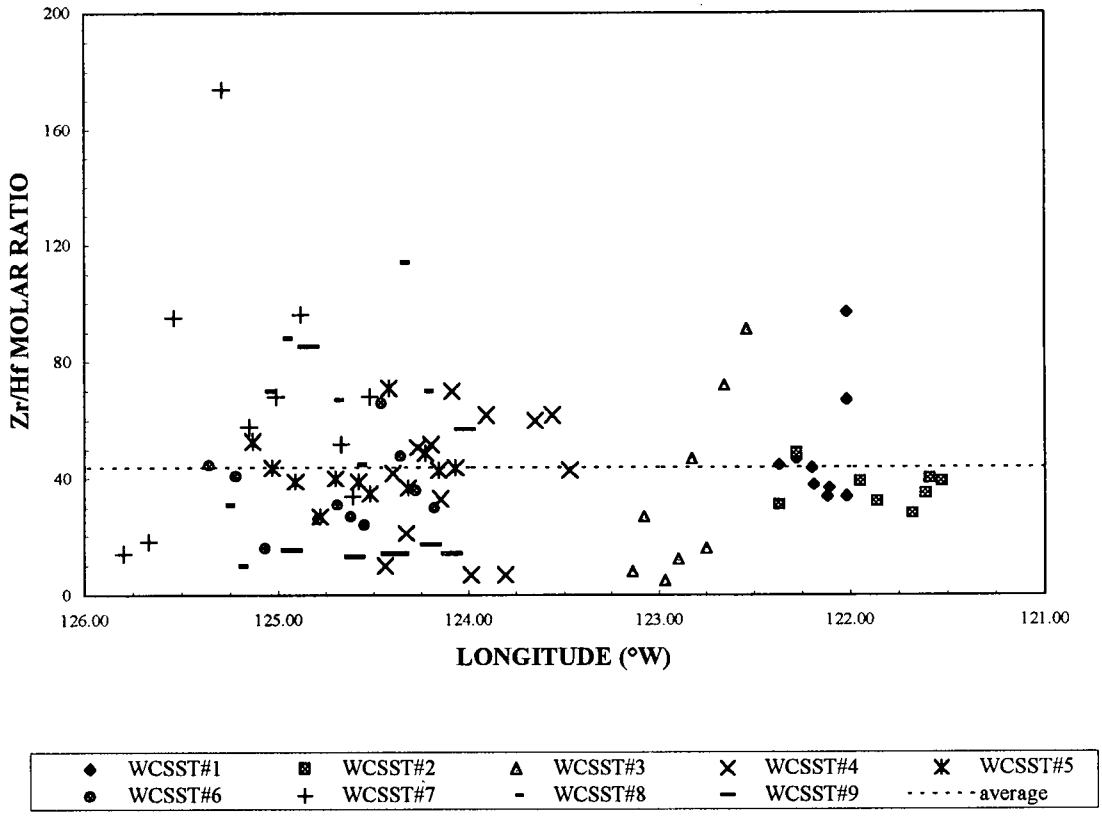

Figure 4.2.4.1 Zr/Hf molar ratios of samples taken from all transects. Dashed line represents average of 44±40.

4.3 Summary

Upwelling regimes along the west coast of the United States of America are identifiable by their high salinity-low temperature-high nutrient signatures. In late June and early July of 1997, a number of upwelling events occurred and were observed along transects WCSST#01-#05 and WCSST#08. These upwelled waters contained higher levels of Ga (7-14pM), Zr (24-65pM) and Hf (0.6-1.5pM) than normal CCS surface water ([Ga]=5-8pM; [Zr]=16-34pM; [Hf]=0.3-0.6pM). Older upwelling events, marked by lower nutrients and production of chlorophyll a, contained lower Ga and Zr concentrations than freshly upwelled waters, most likely the result of active or passive biological uptake. Ga concentrations in CCS surface waters were higher than those previously reported while Zr and Hf were lower. This could be due to the relaxation phenomenon of the Trade Winds brought about by an El Niño event which would result in central North Pacific waters richer in Ga and depleted in Zr being swept in closer to shore. The lower Zr could also result from losses caused by adsorption onto bottle walls during storage which the experimental procedure is unable to account for.

The influence of the continental shelf width on the trace metal content of upwelled waters is best observed for Ga. Where the shelf is narrow, Ga levels are low and where the shelf widens, levels increase. With the exception of one curious featureless transect, Zr shows the same pattern. For Hf, it is impossible to differentiate between narrow and wide shelf regimes due to scatter in the data. Accurate Hf data are difficult to obtain because of low signals which approach instrumental detection limits. Thus as far as Ga and Zr are concerned, these results demonstrate that the continental shelf through its sediments is an important source of metals to the overlying bottom waters. Whether this results from sediment diagenesis or simply sediment resuspension is impossible to tell.

The large uncertainties associated with the Hf data prevent any definite claims from being made as to Zr/Hf fractionation in coastal environments. Nonetheless, with an average crustal molar ratio of 72, the Zr/Hf molar ratios of samples from all transects (average: 44±40) indicate little or no fractionation is taking place during the coastal processes (estuarine mixing, sediment diagenesis/resuspension) studied in this work. Whatever fractionation is observed is in the opposite direction (i.e. implying Hf enrichment) to that observed in oceanic deep waters (molar ratios>100 indicating Zr enrichment).

4.4 References

1) B.M. Hickey (1979) The California current system- hypotheses and facts, *Progress in Oceanography*, **8**, 191-279.

2) D.A. Hutchins, K.W. Bruland (1998) Iron-limited diatom growth and Si:N uptake ratios in a coastal upwelling regime, *Nature*, **393**, 561-564.

3) K.S. Johnson, F.P. Chavez, G.E. Friedrich (1999) Continental-shelf sediment as a primary source of iron for coastal phytoplankton, *Nature*, **398**, 697-700.

4) L.K. Rosenfield, F.B. Schwing, N. Garfield, D.E Tracy (1994) Bifurcated flow from an upwelling center: a cold water source for Monterey Bay, *Continental Shelf Research*, **14**, 931-964.

5) A. Huyer (1983) Coastal upwelling in the California Current System, *Progress in Oceanography*, **12**, 259-284.

6) K.J. Orians, K.W. Bruland (1988) The marine geochemistry of dissolved gallium: A comparison with dissolved aluminum, *Geochimica et Cosmochimica Acta*, **52**, 2955-2962.

7) B.A. McKelvey (1993) The marine geochemistry of zirconium and hafnium, Ph.D. Thesis, University of British Columbia.

8) P.L. Croot, K.A. Hunter (1998) Trace metal distributions across the continental shelf near Otago Peninsula, New Zealand, *Marine Chemistry*, **62**, 185-201.

9) K. Kremling (1983) Trace metal fronts in European shelf waters, *Nature*, **303**, 225-227.

10) C.J. Jones, J.W. Murray (1985) The geochemistry of manganese in the northeast Pacific ocean off Washington, *Limnology and Oceanography*, **30**, 81-92.

11) P.A. Yeats, B. Sundby, J.M. Brewers (1979) Manganese recycling in coastal waters, *Marine Chemistry*, **8**, 43-55.

12) S. Chan (1993) Evaluation of electrothermal vapourization as a method of sample introduction for the ICP-MS and determination of trace levels of titanium, gallium and indium in the Central Pacific gyre, M.Sc. Thesis, University of British Columbia.

13) E.A. Boyle, S.S. Huested, S.P. Jones (1981) On the distribution of copper, nickel, and cadmium in the surface waters of the North Atlantic and North Pacific ocean, *Journal of Geophysical Research*, **86**, 8048-8066.

14) A. Van Geen, S.N. Luoma (1993) Trace metals (Cd, Cu, Ni, and Zn) and nutrients in coastal waters adjacent to San Francisco Bay, California, *Estuaries*, **16**, 559-566.

15) L.V. Godfrey, W.M. White, V.J.M. Salters (1996) Dissolved zirconium and hafnium distributions across a shelf break in the northeastern Atlantic ocean, *Geochimica et Cosmochimica Acta*, **60**, 3995-4006.

Chapter 5: Conclusions

This thesis describes an analytical procedure developed for the simultaneous determination of Ga, In, Zr and Hf in seawater. The said method employs the chelating ion-exchange resin Chelex-100 in column mode as a means of preconcentrating and isolating the trace metals from their salt-water matrix. Pumping flow rates of 0.2mL/min through the resin are necessary to account for slow reaction kinetics between Zr & Hf and Chelex-100. Following the resin extraction, an evaporation step serves to further preconcentrate the metals resulting in an overall concentration factor of ~1000. A Rh internal standard is added and the metals are detected and quantified by flow injection ICP/MS.

The resulting method was found to be quite suitable for the analysis of Ga and In (recoveries: 89% and 97%, respectively) but more problematic for Zr and Hf (recoveries: 38% and 36%, respectively.) Losses for these two metals are thought to occur during the evaporation step, in the form of precipitation caused by matrix interferences. In the future, HF could possibly be added to the eluting acid or during sample reconstitution following evaporation in order to resolubilize and/or help maintain Zr and Hf in solution. This option is only feasible on the condition that spectral interferences generated by the added fluoride are negligible.

Alternatively, the entire evaporation step could be omitted and the USN-MDX introduction system used instead to increase metal detections. Without the evaporation step, more sample (10mL as opposed to 1mL) would be available for instrumental analysis, allowing measurements to be repeated at a later time if necessary. Preliminary results from this study using the USN-MDX system showed Ga, In, Zr and Hf signals could be enhanced by factors of 2 to 16. The uncertainty associated with this optional procedure lies in whether the improvements obtained using the USN-MDX are sufficient to compensate for the loss of the 10-fold concentration factor obtained with the evaporation step.

New resin had to be used for each sample because measurable amounts of Zr and Hf were found to leach slowly from the resin well beyond the first 10mL of eluant. Presumably, HF could have been used to clean the resin of residual Zr and Hf in between samples. This possibility was never investigated although if it had, it might have resulted in significant cost reductions as far as the resin was concerned. Also, the idea of using USN-MDX as an alternative means of increasing sensitivity was regrettably abandoned along with Ti. This might have been a mistake as improvements were observed for the higher mass elements In and Hf. Should the evaporation

difficulties be resolved and adequate recoveries obtained, the use of the USN-MDX system to improve In and Hf signals could allow for smaller samples to be used which would significantly reduce the four-day pumping time. Clearly, further research into these two fields would undoubtedly benefit the existing method.

Nevertheless, the method as it is described in section 2.3.4 was used to obtain the first detailed measurements for Ga, In, Zr and Hf in the western coastal waters of the United States of America. The In data, unfortunately, were discovered to be contaminated by Sn and therefore could not be interpreted. Henceforth, this interference should be accounted for by monitoring a second Sn isotope, possibly Sn-118 (natural abundance: 24.2%), and applying proper corrections to mass 115. Also, Hf analysis was significantly hindered by low counts approaching instrumental detection limits. Consequently, any conclusions concerning Hf are subject to verification. Finally, Zr and Hf levels are most certainly underestimated as this method is not able to account for adsorption that may have occurred onto the bottle walls during sample storage. Yet, despite these shortcomings, the following observations were made.

According to this study, the Columbia River is a considerable, if not the most significant, source of Ga, Zr and Hf to the coastal waters of Washington, Oregon and Northern California. The highest levels of all the transects for all three metals were found closest to the river mouth ([Ga]=49pM; [Zr]=86pM; [Hf]=6pM). During the summer of 1997, meteorological conditions were such that the low salinity waters from the river formed a shallow lens overlying the California Current. Ga and Zr supplied by the river could still be observed in surface waters almost 300km south of the river mouth near Coos Bay, Oregon ([Ga]~30pM; [Zr]~50pM) as well as in measurably diluted waters of salinities up to 30 ([Ga]~12pM; [Zr]~35pM). Thus, Ga and Zr are impressive tracers of the Columbia River effluent.

The behavior of Ga and Zr in the river plume as it travels and mixes with the surrounding waters of the CCS was studied using metal/salinity plots. Discounting possible riverine end-member variability, both elements underwent moderate removal (Ga: 30% and Zr: 50% of the levels observed near the river mouth) by the time the plume reached Coos Bay, as a result of either active biological uptake or particle scavenging. Minimum river concentration estimates for Ga (147±30pM) and Zr (240±150pM) in the Columbia River were comparable to reported values for other rivers. Future work in this area could focus on the actual estuary. Since the estuarine reactivity of Ga, In, Zr and Hf have never been investigated, this could provide an estimate of the riverine input of these metals to coastal waters. Also, a study of the temporal variability of the

Columbia River could shed more light on the mixing behaviors of Ga and Zr out over the continental shelf area.

Coastal upwelling also supplied Ga (7-14pM), Zr (24-65pM) and Hf (0.6-1.5pM) to the surface waters of the CCS (typical background levels: [Ga]=5-8pM; [Zr]=16-34pM; [Hf]=0.3-0.6pM) although to a lesser extent than the Columbia River. Ga levels of upwelled waters were distinctly higher where the upwelling occurred over a wide continental shelf as opposed to where the shelf was narrow. On that basis, the sediments of the western continental shelf of North America, by way of diagenesis or resuspension, are clearly significant sources of Ga to the overlying waters. For Zr and Hf, these conclusions are not as definite although they also seem to apply to these metals.

The Zr/Hf fractionation mystery observed in deep waters of the Atlantic and Pacific oceans (Zr/Hf~100-300) was not resolved. The average crustal Zr/Hf molar ratio is approximately 72. Zr/Hf molar ratios of all samples from this study (which included normal CCS surface waters, Columbia River-influenced oceanic waters and upwelled bottom waters having been in contact with the continental shelf sediments) averaged 44±40 and therefore showed no tendency for Zr enrichment. Consequently, it appears as though Zr/Hf fractionation, or at least Zr enrichment, is not a coastal phenomenon.

Cross-shelf water column profiles and porewater profiles along with analysis of leachable metals from particulate matter would be interesting future directions to explore as they would reveal useful information on the actual source(s) (sediment diagenesis and/or resuspension) of Ga, Zr and Hf to the overlying bottom waters of the continental shelf as well as providing some estimate of dissolved metal fluxes from the sediments.

Appendix 1: Raw Data

WCSST #01

Location		Temperature	Salinity	Concentration (pmol/kg)			
Latitude (°N)	Longitude (°W)	(°C)		[Ga]	[In]	[Zr]	[Hf]
37.094	122.366	10.74	33.369	8.8	0.28	62	1.4
37.035	122.275	11.01	33.345	9.8	0.230	41	0.9
36.986	122.202	13.12	33.326	9.5	0.20	29	0.7
36.94	122.112	13.85	33.314	11.2	0.25	43	1.2
36.916	122.02	14.14	33.314	9.8	0.248	26	0.8
36.859	122.016	13.58	33.313	7.2	0.204	17	0.18
36.771	122.02	12.55	33.303	5.7	0.25	17	0.25
36.711	122.121	13.25	33.102	5.2	0.241	12	0.36
36.706	122.188	13.12	33.105	5.1	0.24	20	0.5

WCSST #02

Location		Temperature	Salinity	Concentration (pmol/kg)			
Latitude (°N)	Longitude (°W)	(°C)		[Ga]	[In]	[Zr]	[Hf]
36.015	121.586	11.62	33.338	7.9	0.18	29	0.7
35.998	121.525	11.79	33.331	8.5	0.191	36	0.9
35.984	121.605	11.88	33.304	7.3	0.22	34	1.0
35.961	121.683	13.03	33.204	6.6	0.25	27	1.0
35.946	121.772	13.75	33.221	6.6	0.204	24	n/a
35.948	121.859	13.84	33.22	5.9	0.23	17	0.5
35.946	121.952	12.36	33.276	6.6	0.20	25	0.6
35.943	122.276	13.26	33.269	5.9	0.20	30	0.6
35.946	122.365	14.3	33.193	5.1	0.15	16	0.5

WCSST #03

Location		Temperature	Salinity	Concentration (pmol/kg)			
Latitude (°N)	Longitude (°W)	(°C)		[Ga]	[In]	[Zr]	[Hf]
37.503	122.536	10.71	33.308	11.5	0.13	31	0.34
37.501	122.664	12.93	32.918	14	0.15	24	0.33
37.503	122.747	12.26	33.074	11.5	0.090	26	1.6
37.503	122.827	11.32	33.34	8.0	0.125	23	0.5
37.497	122.899	11.70	33.076	7.5	0.16	26	2.1
37.505	122.973	12.63	32.84	6.6	0.19	26	6
37.521	123.078	13.53	32.815	5.8	0.11	21	0.80
37.537	123.111	13.13	32.891	6.1	0.12	19	0.34
37.559	123.144	11.20	33.024	7.1	0.15	39	5

WCSST #04

Location		Temperature	Salinity	Concentration (pmol/kg)			
Latitude (°N)	Longitude (°W)	(°C)		[Ga]	[In]	[Zr]	[Hf]
38.700	123.473	8.58	33.596	11.8	0.75	66	1.5
38.704	123.561	8.68	33.562	10	0.24	37	0.6
38.707	123.647	9.03	33.519	11.0	0.20	33	0.6
38.712	123.808	9.86	33.377	9.5	0.21	47	7
38.710	123.905	10.94	33.127	8.1	0.19	29	0.5
38.719	123.993	11.72	32.874	7.5	0.21	39	6
38.746	124.086	12.79	32.780	7.5	0.20	21	0.30
38.773	124.147	13.00	32.757	7.3	0.20	19	0.6
38.802	124.204	12.93	32.780	7.0	0.20	22	0.43
38.848	124.273	12.44	32.915	7.9	0.22	24	0.47
38.881	124.328	12.56	32.884	7.6	0.24	24	1.2
38.925	124.397	12.93	32.789	7.3	0.20	17	0.4
38.966	124.441	12.89	32.786	7.7	0.26	33	3.2

WCSST #05

Location		Temperature	Salinity	Concentration (pmol/kg)			
Latitude (°N)	Longitude (°W)	(°C)		[Ga]	[In]	[Zr]	[Hf]
40.006	124.074	9.16	33.356	14.1	0.2	45	1.0
40.005	124.158	9.33	33.402	8.1	0.199	45	1.1
40.006	124.226	9.57	33.381	8.6	0.2	35	0.7
40.007	124.317	9.19	33.489	8.7	0.2	40	1.1
40.005	124.420	9.06	33.467	9.4	0.16	56	0.8
39.997	124.516	10.93	33.035	5.6	0.16	20	0.6
40.000	124.577	11.45	32.853	5.4	0.16	23	0.6
40.005	124.694	12.64	32.541	4.8	0.15	21	0.5
40.009	124.776	12.88	32.491	4.9	0.16	17	0.6
40.012	124.904	12.49	32.514	5.5	0.16	20	0.5
40.001	125.027	14.20	32.227	6.0	0.16	85	2.1
39.993	125.130	15.63	32.158	6.8	0.18	33	0.6

WCSST #06

Location		Temperature	Salinity	Concentration (pmol/kg)			
Latitude (°N)	Longitude (°W)	(°C)		[Ga]	[In]	[Zr]	[Hf]
41.200	124.176	13.62	32.774	7	0.2	16	0.5
41.198	124.282	12.61	32.689	5.2	0.2	15	0.42
41.203	124.363	12.26	32.716	6	0.2	21	0.43
41.200	124.457	12.03	32.088	5.9	0.19	30	0.5
41.197	124.545	12.49	31.493	6.5	0.33	52	2.2
41.200	124.621	12.53	31.979	6.9	0.39	53	1.9
41.195	124.694	12.80	31.881	7.1	0.43	55	1.8
41.199	124.792	13.80	32.098	5.8	0.37	27	1.0
41.203	125.074	13.62	32.275	5.6	0.44	33	2.0
41.204	125.220	14.11	32.227	4.9	0.38	24	0.6
41.198	125.350	13.37	32.049	5.9	0.44	39	0.9

WCSST #07

Location		Temperature	Salinity	Concentration (pmol/kg)			
Latitude (°N)	Longitude (°W)	(°C)		[Ga]	[In]	[Zr]	[Hf]
42.541	124.520	16.57	27.888	9.0	0.12	45	0.24
42.497	124.515	16.74	27.952	18	0.13	47	0.7
42.499	124.609	17.66	26.953	24	0.18	46	1.3
42.501	124.670	17.89	26.469	27	0.14	47	0.9
42.503	124.779	18.04	25.903	26	0.16	39	0.03
42.502	124.876	18.07	25.751	31	0.16	48	0.5
42.506	125.010	18.38	26.058	29	0.20	57	0.8
42.500	125.152	18.10	26.482	26	0.17	45	0.8
42.499	125.286	18.35	34.789	33	0.18	46	0.26
42.506	125.535	18.28	25.989	30	0.18	52	0.6
42.504	125.669	18.29	26.293	27	0.18	49	2.7
42.503	125.798	18.14	26.98	25	0.19	45	3.2

WCSST #08

Location		Temperature	Salinity	Concentration (pmol/kg)			
Latitude (°N)	Longitude (°W)	(°C)		[Ga]	[In]	[Zr]	[Hf]
44.201	124.229	13.92	31.605	10.7	0.34	53	0.8
44.204	124.347	15.17	31.277	11.8	0.28	39	0.3
44.203	124.464	15.77	30.112	14.7	0.32	42	2.9
44.199	124.577	15.76	30.142	12.7	0.28	35	0.8
44.200	124.700	16.17	30.121	11.6	0.25	28	0.4
44.203	124.965	18.30	28.372	20	0.29	42	0.5
44.202	125.062	18.71	27.364	23	0.30	34	0.5
44.206	125.195	18.73	29.380	16	0.27	29	2.9
44.212	125.271	17.85	31.647	7.5	0.28	16	0.5

WCSST #09

Location		Temperature	Salinity	Concentration (pmol/kg)			
Latitude (°N)	Longitude (°W)	(°C)		[Ga]	[In]	[Zr]	[Hf]
46.000	124.019	16.78	25.413	28	0.139	48	0.8
46.000	124.087	16.55	24.669	36	0.16	63	4.4
46.002	124.202	16.45	23.791	42	0.17	81	4.8
45.996	124.366	16.50	22.624	49	0.16	86	6.0
46.002	124.597	17.90	28.564	16	0.14	29	2.2
45.999	124.837	19.36	28.310	72	0.122	65	0.8
46.001	124.932	18.88	29.277	43	0.152	54	3.7

Appendix 2: CTD Profiles

Columbia River plume at 44.20°N, 124.97°W (WCSST#08).

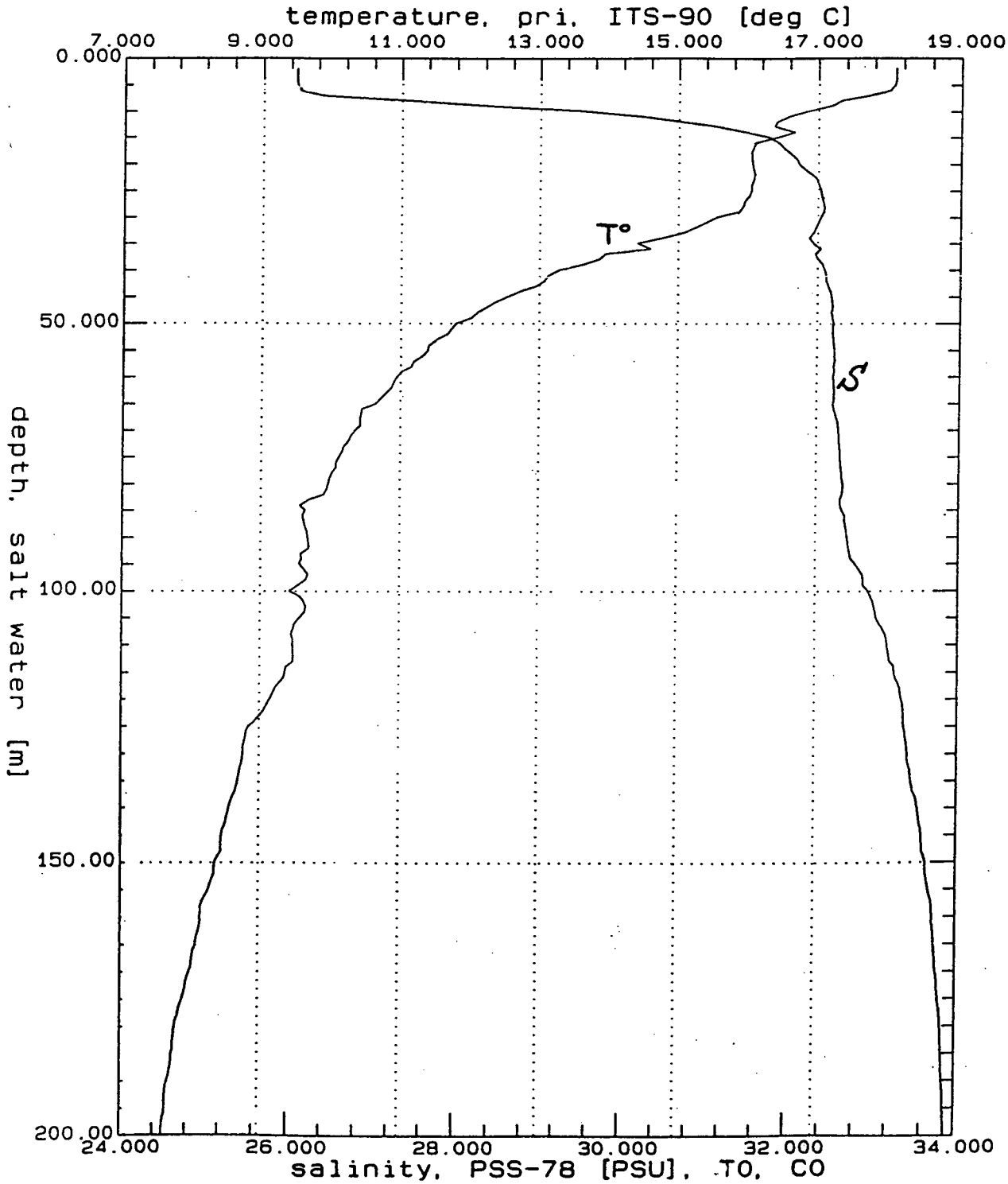

Columbia River plume at 42.50°N, 125.32°W (WCSST #07).